THE UNIVERSITY OF MICHIGAN

COLLEGE OF ENGINEERING

DEPARTMENT OF AEROSPACE ENGINEERING

Satellite-Plasma Interaction Manual

V. C. LIU

National Aeronautics and Space Administration

Grant NsG-660

Administered through: May 1968

OFFICE OF RESEARCH ADMINISTRATION • ANN ARBOR

I. Objectives of the Manual

The orbiting Geophysical observatory (OGO) satellites move in the ionosphere and the magnetosphere of the earth and carry on board various experiments to obtain scientific informations on the geophysical properties of the atmosphere pertaining to the solar-terrestrial relationships. Although the satellites are designed to have booms to carry detectors which extend away from the gasdynamical disturbances generated by the moving satellite, it is not always possible to achieve the goal in view of the various orientations, with respect to the direction of motion, that a satellite must assume during its orbital motion. This is further complicated by the fact that the extent of the disturbed region for a tenuous plasma such as the ionosphere is quite large. It is, therefore, almost unavoidable that a detector or intake orifice happens to situate in a disturbed flow field which is generated by the other parts of the moving satellite. Consequently, it becomes imperative to be aware and understand the disturbed-flow effect on the measurements in order to minimize the error of measurement so incurred.

In determining the field of disturbance around an orbiting OGO, one must make considerable flow analysis for both the neutral and the charged particles of the ambient atmosphere pertaining to various complex geometrical configurations of an OGO. The task can be exasperating and even the presentation of the calculated results of the

flow field becomes intractable as the guidance for its users. To circumvent such difficulty, a practical manual for the users is devised to provide the basic informations of flow fields which can be synthesized for a given geometrical configuration with minimum effort. A manual must satisfy two basic requirements: (1) the informations on field variables, e.g., particle densities, electric field potentials, etc., must be readily available from tables and charts without undue computations on the part of the users; (2) the collections of the basic informations on the field variables of interest must be versatile such that it is possible to synthesize for various geometrical configurations and orientations of the orbiting OGO satellites.

In view of the basic characteristics of restricted zone of action for supersonic flows, such as those of the orbiting satellites, it is found most fruitful to achieve the above-mentioned objectives by presenting the field variables in charts under various ambient conditions for simple geometrical bodies, e.g. sphere, cylinder, disks, etc., of which OGO satellites are composed. The superposition of appropriate basic flow fields with due account of the mutual interference from the proximity of the neighboring elements can be made to estimate the flow field of interest.

II. Preliminary Informations

The qualitative and quantitative nature of the disturbance induced by an orbiting satellite must depend, among other things, upon the ambient atmosphere in which it is moving and the body

parameters characterizing the surface potential, size, and speed, etc., of the moving object in question. Two tables are provided, one of which describes the averaged properties of the upper ionosphere; the other, the properties of typical satellites.

Table I - Gross Mean Properties of the Upper Ionosphere

Distance from surface of the earth	250-400 Km	600-700 Km	~3000 Km
Concentration of neutral particles (no./cm^3)	10^{10} - 10^9	10^7	
Concentration of electrons and ions (no./cm^3)	5×10^5 - 5×10^6	10^5	10^3
Ambient temp. (^oK)	~1000	~2000	~4000
Mean molecular wts. of the particles	~24	~16	~2
Effective Coll. frequency (electrons, ions)	$(1 - 3) \times 10^3$	$(1 - 3) \times 10^2$	10
Mean free path of neutral particles (cm)	$(1 - 7) \times 10^5$	$(1 - 5) \times 10^7$	2×10^{14}
Mean free path of an electron among ions (cm)	$\sim 10^4$	$\sim 10^5$	$\sim 10^6$
Thermal speed of neutral particles and ions (cm/sec)	$\sim 10^5$	$\sim 1.5 \times 10^5$	$\sim 6 \times 10^5$
Thermal speed of electrons (cm/sec)	$\sim 2 \times 10^7$	$\sim 3 \times 10^7$	$\sim 4 \times 10^7$
Larmor radius of electrons (cm)	~3	~4	~10
Larmor radius of ions (cm)	$\sim 5 \times 10^2$	$\sim 8 \times 10^2$	$\sim 10^3$
Debye Length (cm)	~0.5	~0.5	~3

Table II a - Properties of Satellites

Distance from surface of the earth	250-400 Km	600-700 Km	3000 Km
Body velocity (cm/sec)	$(8 - 11) \times 10^5$	$(8 - 11) \times 10^5$	$(8 - 10) \times 10^5$
Speed ratio, body/thermal(ion)	8 - 11	5 - 7	1

Table II b - Accommodation of Particles on a Solid Wall*

Neutral particles accommodated	Air	He	A	He	A	He
Surface	polished Al.	Tungsten wire flashed	T. wire flashed	T. wire not flashed	T. wire not flashed	glass
α	0.87-0.95	0.17	0.82	0.53	1.00	0.31

*S. Flügge(ed) Handbuch der Phys. 8/pt.2 (Mech. of Rarefied Gases), 1963.

III. Neutral Particle Distributions near a Moving Satellite

It can be seen from Table I on the properties of the ionosphere that the mean free path of the ambient particles in question are many orders larger than the characteristic dimension of the satellite. Consequently, the neutral particles, e.g. molecules and neutral atoms, of the atmosphere interact with the satellite according to the theory of the free molecular flow. Reflection of the incident stream to the satellite creates an excess of particles in front of the body where an enhancement region is formed. Behind the body, a rarefaction region develops since the rapidly moving body sweeps the particles, the ambient particles cannot fill the cavity aft the body immediately. The length of the rarefaction wake increases with the velocity (V_o) of the body. An important parameter here is the speed ratio, V_o/v_{th}, where v_{th} is the thermal speed of the ambient molecules that fill the wake. Note that the thermal random motions of the molecules tend to damp out the disturbances generated by the motion of the body.

To determine the flow field around a body which can be decomposed geometrically into simple basic elements of sphere, cylinder and disk, one may use a principle of flow synthesis wherein the flow field of the combined configuration is obtained by patching the component fields and taking the mean values in the overlapped regions.

IIIa. Neutral Particle Distribution in Front of a Moving Body

The concentration (or number density) of the particles in front of a rapidly moving body such as a satellite are contributed from

two sources: (1) the undisturbed ambient particles of concentration n_o prior to their impacts with the body, (2) the particles reflected from the body upon collisions. The density and shape of the cloud of reflected molecules may be of importance in many OGO-experiments. The number density of the reflected particles in this cloud decreases as the square of the distance from the body, due to the essentially spherical nature of the distribution of the reflected particles with respect to the body. The concept of free molecular flow will be applied to the analysis of this cloud.

It is noted that the quantitative description of the cloud of reflected molecules depends critically on the nature of the reflection mechanism at the surface of the body. Although the reflection mechanism for very high speed molecules may not be adequately described by the classical models of specular and diffuse reflection, it is felt, however, for the mean molecular energy of impact on OGO-satellites close approximations are expected with the use of these models and judicious choice of accommodation coefficient (α) which is defined as the fraction of the mean translational energy of the incident molecules which is transferred to the surface. The quantity α is thus a measure of the degree to which the molecules have their mean energy accommodated to what it would be if the molecules were reflected with a Maxwellian distribution corresponding to the surface temperature (T_w). For perfect accommodation $\alpha = 1$, also called diffuse reflection; while for the case of vanishing energy exchange

with the surface, $\alpha = 0$, it is called specular reflection where the molecules reflect as a light beam on a mirror. A statistical approximation of the true reflection which obviously depends on the molecular energy of impact upon the surface and the smoothness of the surface finish among other things. Typical values of α are shown in Table IIb. The approximation for the density of reflected molecules can be made with $n = \alpha\, n(\text{diffuse}) + (1 - \alpha)\, n(\text{sp})$.

(i) Reflection from a Small Surface Element

Consider a stationary surface element making an angle θ with the free stream velocity (V_o). The free stream density (or ambient density) and temperature are n_o and T_o, respectively. The temperature of the surface element is T_w. Let $v_{th} = (2kT/m)^{1/2}$ and $S = V_o/v_{th}$ where k = Boltzmann constant and m = molecular mass. For diffuse reflection ($\alpha = 1$), the number density of reflected molecules at the wall is

$$n_w = \frac{1}{2} n_o (T_o/T_w)^{\frac{1}{2}} \left\{ \exp(-S^2 \sin\theta) + \sqrt{\pi}\, S \sin\theta \,(1 + \operatorname{erf}[S \sin\theta]) \right\}$$

where $\operatorname{erf} x = \frac{2}{\sqrt{\pi}} \int_o^x e^{-u^2} du$.

It is noted that in OGO flight, S is in the order of 10, unless $\sin\theta$ is very small, the following approximation is valid

$$n_w \approx n_o \left(\frac{\pi m}{2kT_w} \right)^{\frac{1}{2}} V_o \sin\theta .$$

When the molecular specular reflection at the surface is assumed, $\alpha = 0$, the angle of reflection is equal to the angle of incidence for any incident molecule. Since available evidence suggests that specular reflection is likely to be of importance only in very high speed flows ($S \gg 1$), the analysis will be restricted to this case. The number density of the reflected molecules at the surface is very nearly equal to (for $\theta > 0$)

$$n_w = n_o .$$

(ii) Reflection from a Flat Plate

Consider a stationary flat plate with the free stream velocity (V_o) normal to the plate (Figures 1 and 2). The shape of the cloud of the reflected molecules as indicated by the contour of constant density $n_w = 10^{-4} n_o$ for either the case of nearly diffuse reflection (Figure 1) or specular reflection (Figure 2) under different speed ratios (S) are shown.

(iii) Reflection from a Cone at Zero Incidence

Consider a stationary cone with a base radius R_o and a semi-vertex angle β exposed to a stream of velocity (V_o) at zero incidence (see Figure 3). With diffuse reflection the number density of the reflected molecules at a point $P(r, \phi)$, where r, ϕ are the polar coordinates with origin at the tip of the cone, is given by

$$n_r = \frac{n_o x}{4\pi \sin\beta} \left(\frac{R_o}{r}\right)^2 \sqrt{\frac{T_o}{T_w}}\, F_1$$

where

$$x = \exp(-S^2 \sin\beta) + \sqrt{\pi}\, S \sin\beta \,[1 + \operatorname{erf}(S \sin\beta)]$$

and

$$F_1 = \cos\phi \sin\beta \left\{\pi - \cos^{-1}(\cot\phi \tan\beta)\right\} + \sin\phi \cos\beta \sin\left\{\pi - \cos^{-1}(\cot\phi \tan\beta)\right\}$$

Noted that S is large (about 10) for OGO, hence, for a cone with $\sin\beta > 0.2$ an approximation for n_r can be used

$$n_r = \frac{n_o}{\pi} \left(\frac{R_o}{r}\right)^2 F_1$$

With specular reflection; the number density of the reflected molecules at $P(r, \phi)$ becomes

$$n_r = \frac{n_o S}{2\sqrt{\pi}} \left(\frac{R_o}{r}\right)^2 (\sin\phi \sin 2\beta)^{-\frac{1}{2}} \exp\left\{-2S^2[1 + \cos(2\beta + \phi)]\right\} x$$

$$\operatorname{erf}\left[S(\sin\phi \sin 2\beta)^{\frac{1}{2}} \left\{\pi - \cos^{-1}(\cot\phi \tan\beta)\right\}\right]$$

Figure 3 presents some results of reflected molecules for both diffuse and specular reflections at the cone.

(iv) Reflection from a Sphere

Consider a sphere of radius R_o which is exposed to a stream of velocity (V_o) as shown in Figure 4. The expression for number density (n_r) of the reflected molecules at a point $P(r, \phi)$ can no longer be given in closed form. With the assumption of $S \gg 1$ which is valid for OGO, the number density of reflected molecules with an assumption of diffuse reflection can be reduced to a simple integral which must be integrated numerically:

$$n_r = \frac{n_o}{\pi} \left(\frac{R_o}{r}\right)^2 \int_o^{\frac{\pi}{2}} \sin 2\xi \, F_2(\phi, \xi) \, d\xi$$

where

$$F_2(\phi, \xi) = \cos\phi \cos\xi \left\{\pi - \cos^{-1}(\cot\phi \cot\xi)\right\} + \sin\phi \sin\xi \sin\left\{\pi - \cos^{-1}(\cot\phi \cot\xi)\right\}$$

With specular reflection, the number density of the reflected molecules at $P(r, \phi)$ is

$$n_r = \frac{n_o S}{2\sqrt{\pi}} \left(\frac{R_o}{r}\right)^2 \int_o^{\frac{\pi}{2}} \left(\frac{\sin 2\xi}{\sin\phi}\right)^{\frac{1}{2}} \exp\left\{-2S^2[1 - \cos(2\xi - \phi)]\right\} x$$

$$\operatorname{erf}\left[S(\sin\phi \sin 2\xi)^{\frac{1}{2}} \left\{\pi - \cos^{-1}(\cot\phi \cot\xi)\right\}\right] d\xi$$

which also must be integrated numerically.

Figure 1 - Iso-concentrations of diffusely reflected molecules ($n_r/n_o = 10^{-4}$) from a flat plate.

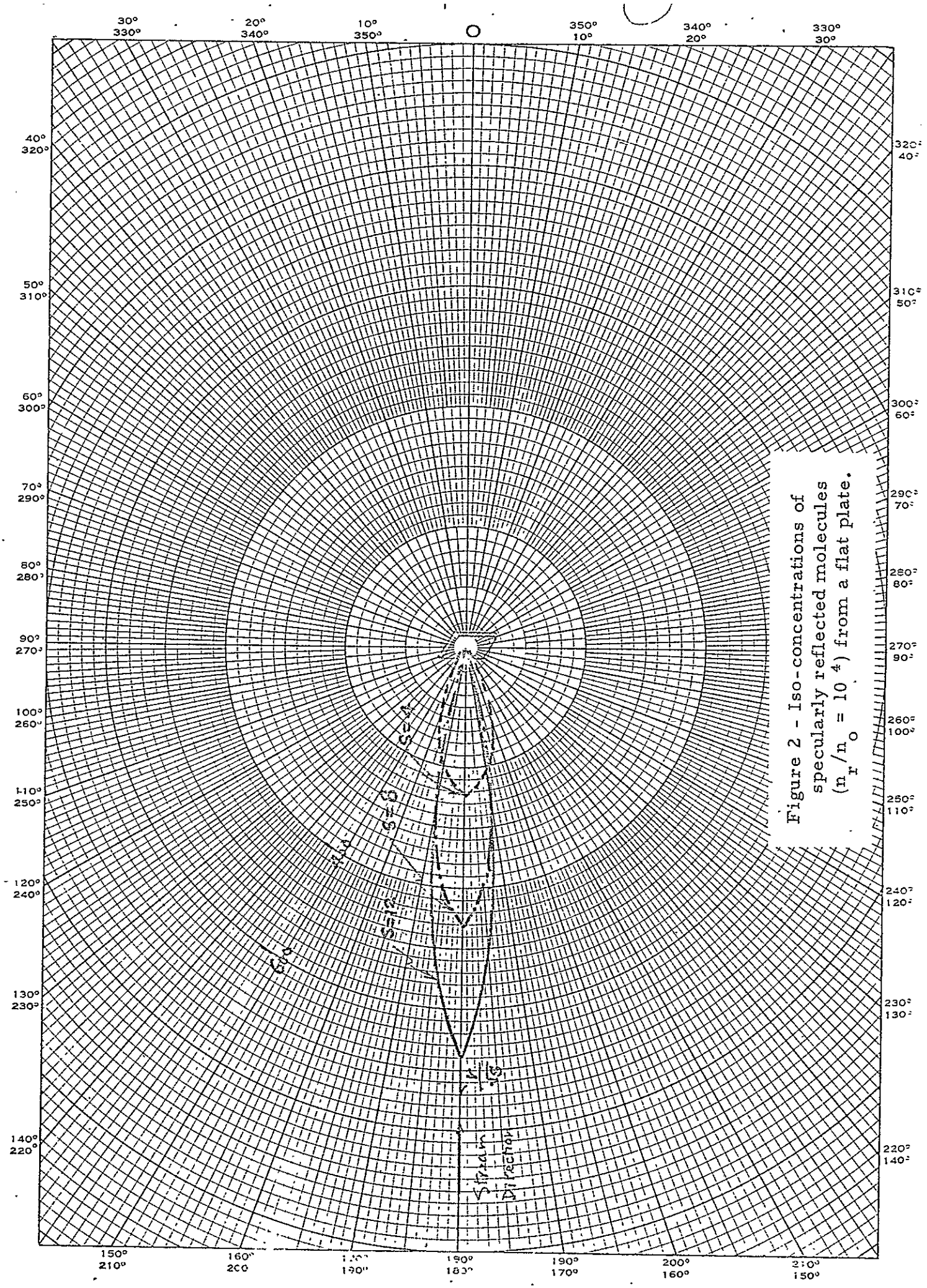

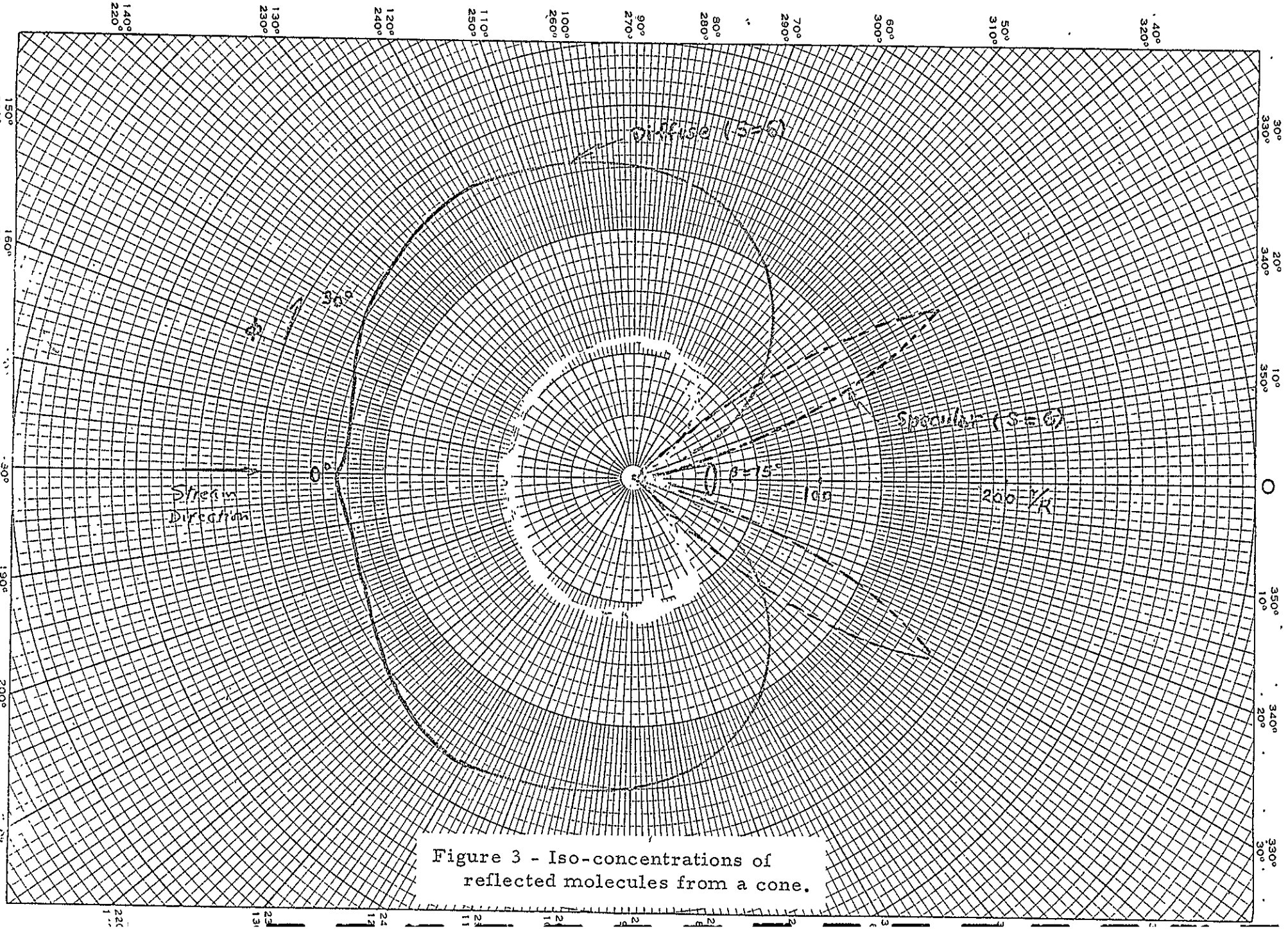

Figure 3 - Iso-concentrations of reflected molecules from a cone.

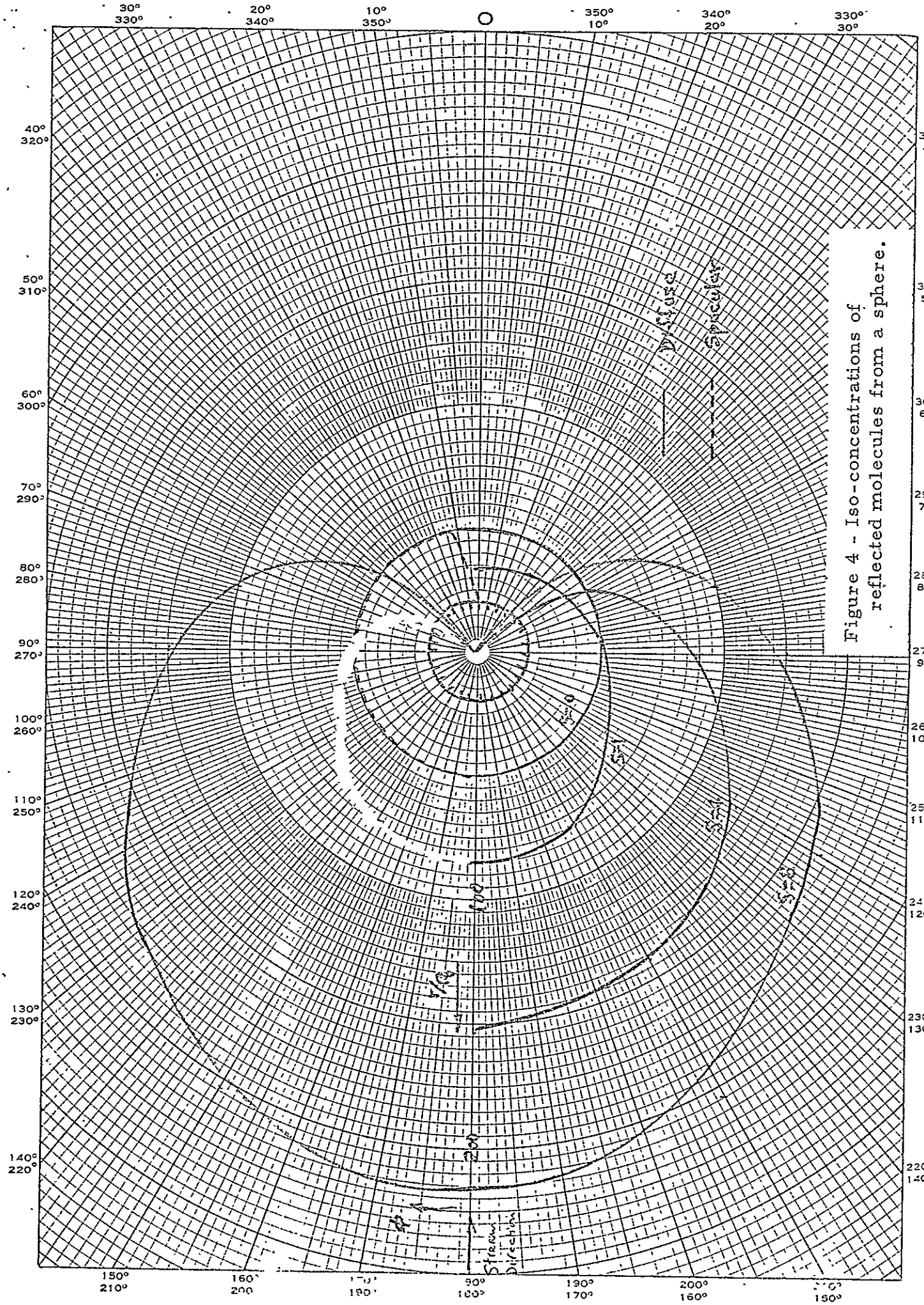

Figure 4 - Iso-concentrations of reflected molecules from a sphere.

Some results of the numerical integration for the number densities of reflected molecules for both diffuse and specular reflection at a sphere are shown in Figure 4.

(v) Reflection from a Circular Cylinder

Consider a cylinder of radius R_o and length h having its axis aligned with a stream of velocity (V_o). The number density of the diffusely reflected molecules from the curved surface at a point $P(r, \phi)$

$$n_r = \frac{n_o R_o h}{2\pi r^2} \sqrt{\frac{T_o}{T_w}} \sin \phi$$

IIIb. Neutral Particle Distributions Behind a Moving Body

The concentration (or number density) of neutral particles behind a moving body is also attributed to two sources: (1) those filling into the cavity behind the rapidly moving body; (2) those reflected from the surface of the body. It is noted, however, that the second source of input decreases as the speed of the body increases. For a moving body, such as OGO, the contribution of the reflected molecules in the wake becomes insignificant except in special situations such as that discussed in section IV of this manual.

(i) Neutral Particle Density in the Wake Behind a Sphere or a Circular Disk

As a sphere moves rapidly in a tenuous atmosphere, it continuously bores out a cylindrical cavity in the medium. The neighboring ambient molecules must move in to fill the cavity which remains, however, underpopulated. Consider a stationary sphere

of radius R_o, the center of which is at the origin of the cylindrical coordinate system (z, ρ, θ) with z aligned with the free stream velocity (V_o), the filling action of the ambient molecules is provided by their random thermal velocities. The wake structure is obviously axisymmetrical, hence, the position-dependency of number density in the wake is two-fold (z, ρ). To simplify the expression, the position coordinates are measured in units of R_o, the radius of the sphere.

The expression for the number density in the wake of a moving sphere must be specified differently for different regions of the wake. Where $\rho < 1$, the number density is given by the following integral which must be integrated numerically:

$$\frac{n(z,\rho)}{n_o} = \frac{1}{2}(1 - \operatorname{erf} S) + (4\pi)^{-1} \int_o^{2\pi} \left\{ A(1 + A^2)^{-\frac{1}{2}} \exp\left[-\frac{S^2}{1 + A^2}\right] \times \left[1 + \operatorname{erf} \frac{AS}{\sqrt{1 + A^2}}\right] \right\} d\phi$$

where

$$A = z(1 - \rho^2)^{-1} \left[(1 - \rho^2 \sin^2 \phi)^{\frac{1}{2}} - \rho \cos \phi\right]$$

$$\operatorname{erf} S = \frac{2}{\sqrt{\pi}} \int_o^S e^{-u^2} du$$

while for $\rho > 1$

$$\frac{n(z,\rho)}{n_o} = 1 + (4\pi)^{-1} \int_{-\arcsin(1/\rho)}^{\arcsin(1/\rho)} \left\{ A(1+A^2)^{-\frac{1}{2}} \exp\left[\frac{-S^2}{1+A^2}\right] \left[1 + \operatorname{erf} \frac{AS}{\sqrt{1+A^2}}\right] - \right.$$

$$\left. B(1+B^2)^{-\frac{1}{2}} \exp\left[-\frac{B^2}{1+B^2}\right] \left[1 + \operatorname{erf} \frac{bS}{\sqrt{1+B^2}}\right] \right\} d\phi$$

where

$$B = - z(1-\rho^2)^{-1} \left[(1 - \rho^2 \sin^2\phi)^{\frac{1}{2}} + \rho \cos\phi\right]$$

It is noted that in the above analysis, the contributions to the concentration of particles in the wake due to those reflected from the surface of the moving body have been ignored in view of $S \gg 1$ for OGO. Consequently, the result is independent of the shape of the body except the contour of its maximum cross section facing the stream. Therefore, the result is identical for either a sphere or circular disk in motion except in the semi-spherical region $r \leq R_o$. Some results of the numerical computation of number densities of neutral particles in the wake behind a sphere (or circular disk) are shown in Figures (5), (6), and (7).

(ii) Neutral Particle Density in the Wake of a Cylinder or a Rectangular Disk

Consider a cylinder of radius R_o and length $2R_x$ with its axis on the x-coordinate and the free stream velocity (V_o) along the z-coordinate. Let the position coordinates be measured in units of R_o; velocities in units of $v_{th} = \sqrt{2kT/m}$. The number density at a point (x, y, z) in the wake of the cylinder is

$$\frac{n}{n_o} = \pi^{-\frac{1}{2}} \int_{-\infty}^{\infty} \exp\left[-(v_z - S)^2\right] \left\{1 - \frac{1}{4}\left[\operatorname{erf} M - \operatorname{erf} N\right]\left[\operatorname{erf} P - \operatorname{erf} Q\right]\right\} dv_z$$

where

$$M = (v_z/z)(x - R_x) \qquad N = (v_z/z)(x + R_x)$$

$$P = (v_z/z)(y - R_o) \qquad Q = (v_z/z)(y + R_o) .$$

As in the case (i), the contribution due to molecules reflected from the surface of the cylinder has been ignored in view of the high speed ratio ($S \gg 1$) of OGO. Consequently, the above expression is also valid for a rectangular disk with the free stream (V_o) normal to the surface of the disk $2R_o \times 2R_x$.

Some results of the neutral particle distributions in the wake behind a cylinder (or disk) are shown in Figures (8), (9), (10), (11), (12), (13), (14), (15), and (16).

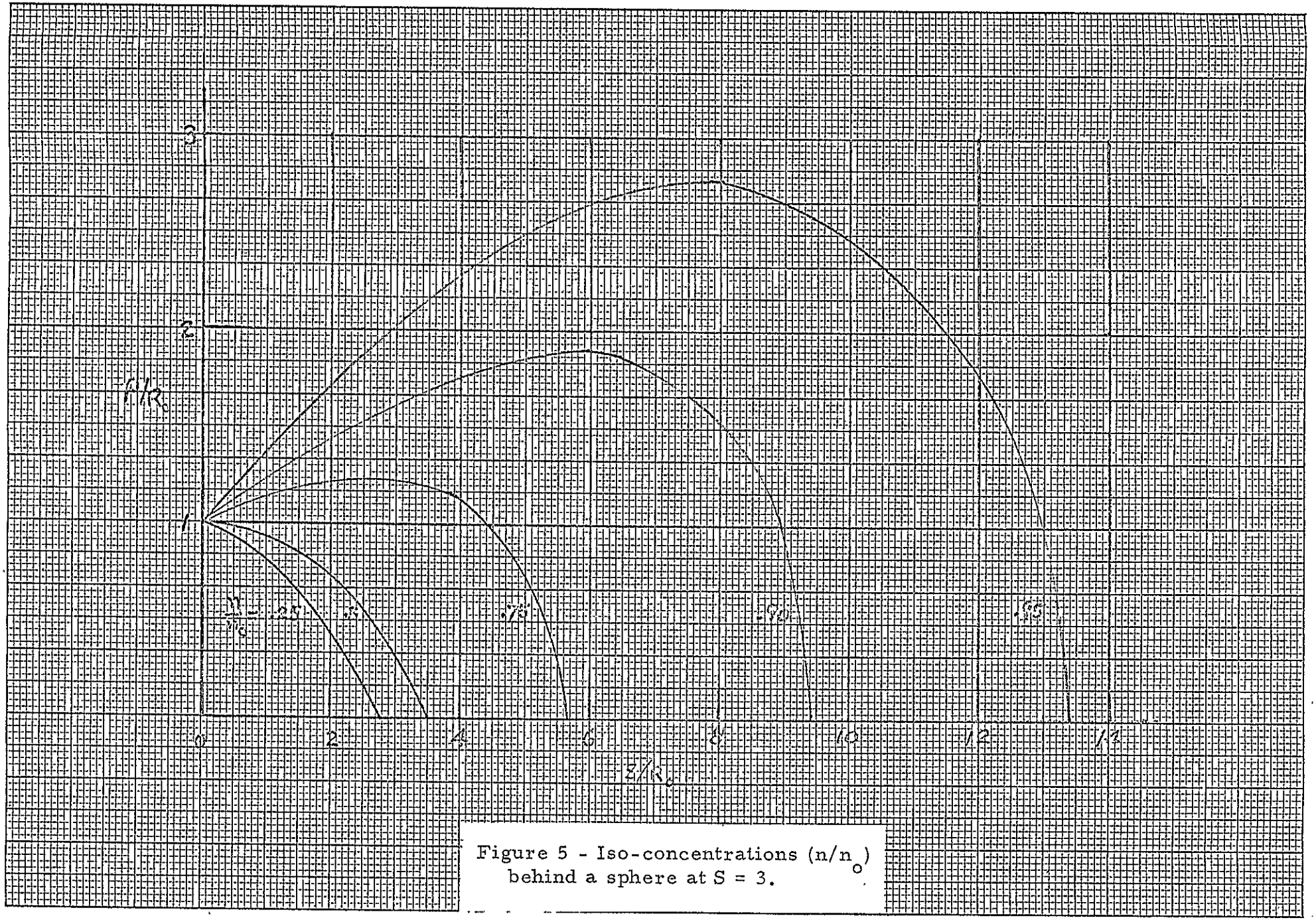

Figure 5 - Iso-concentrations (n/n_o) behind a sphere at S = 3.

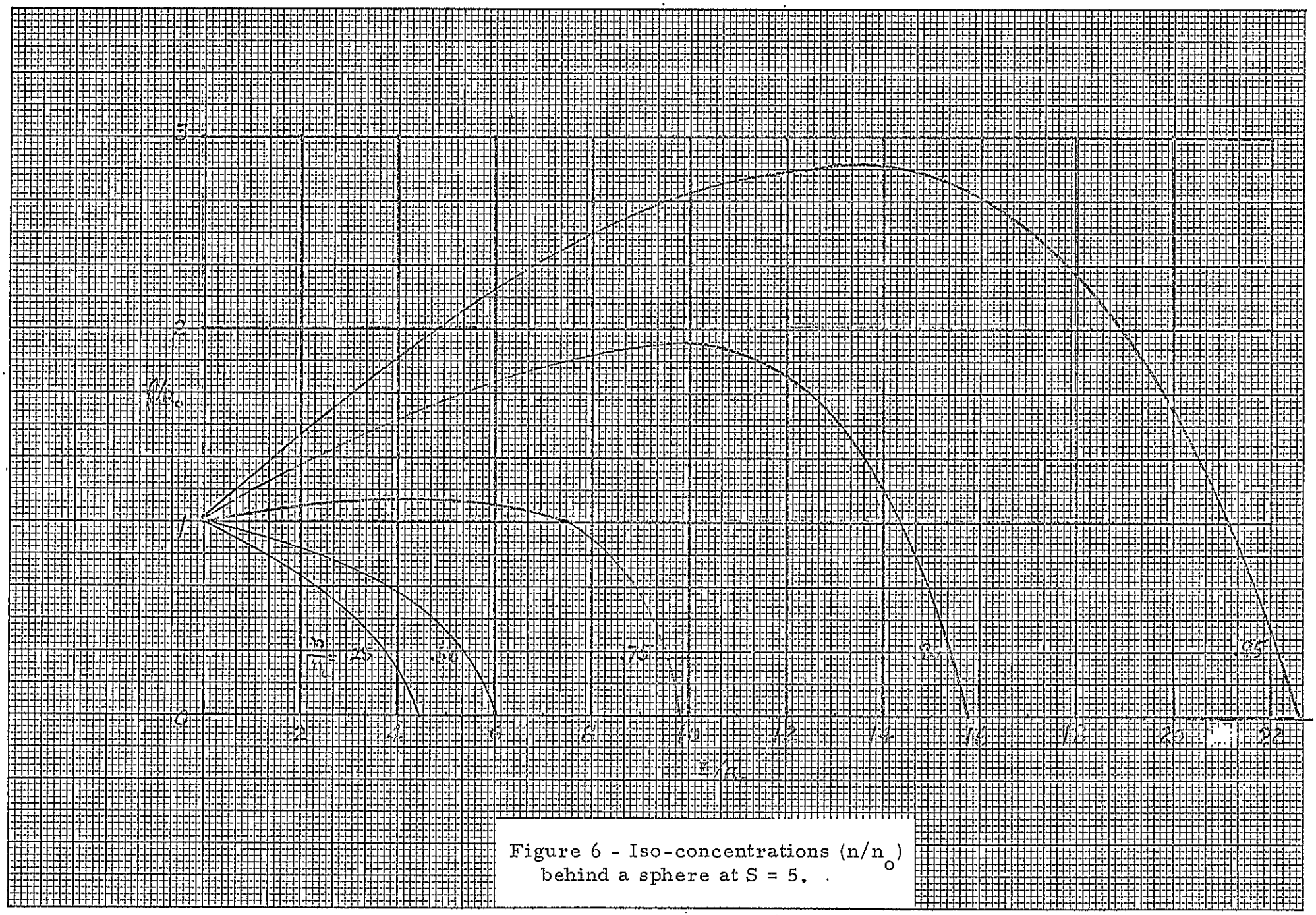

Figure 6 - Iso-concentrations (n/n_o) behind a sphere at S = 5.

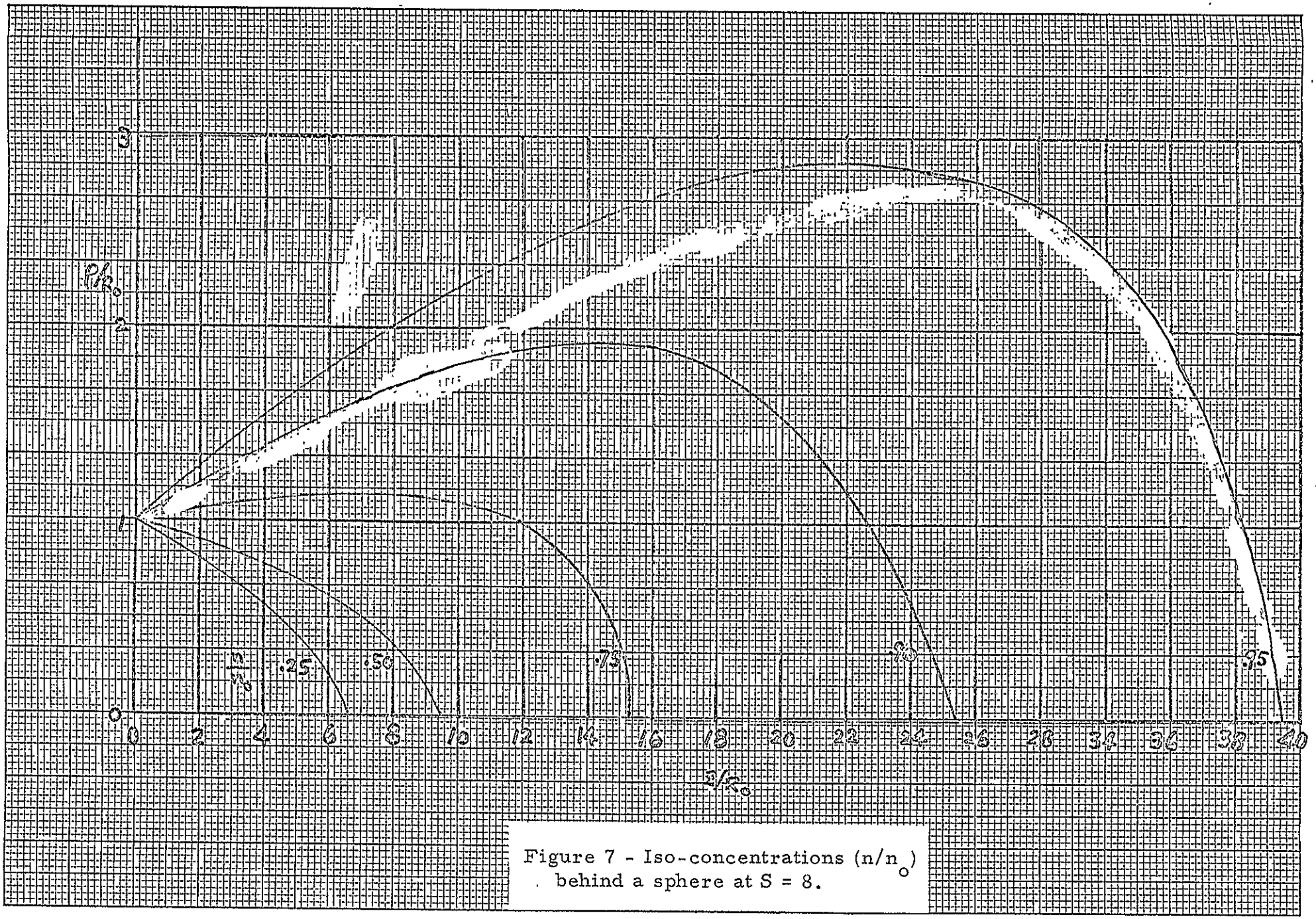

Figure 7 - Iso-concentrations (n/n_o) behind a sphere at S = 8.

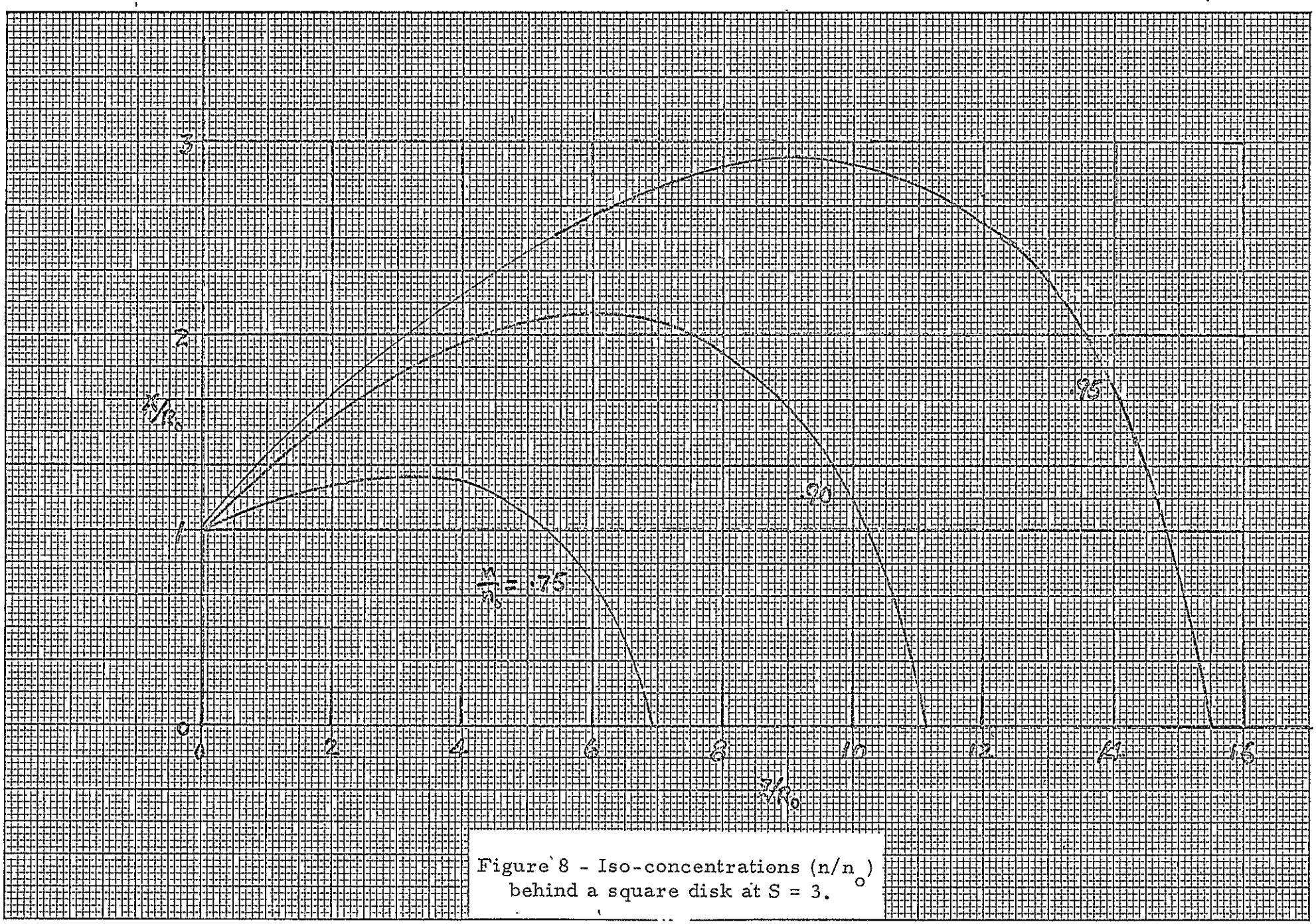

Figure 8 - Iso-concentrations (n/n_o) behind a square disk at S = 3.

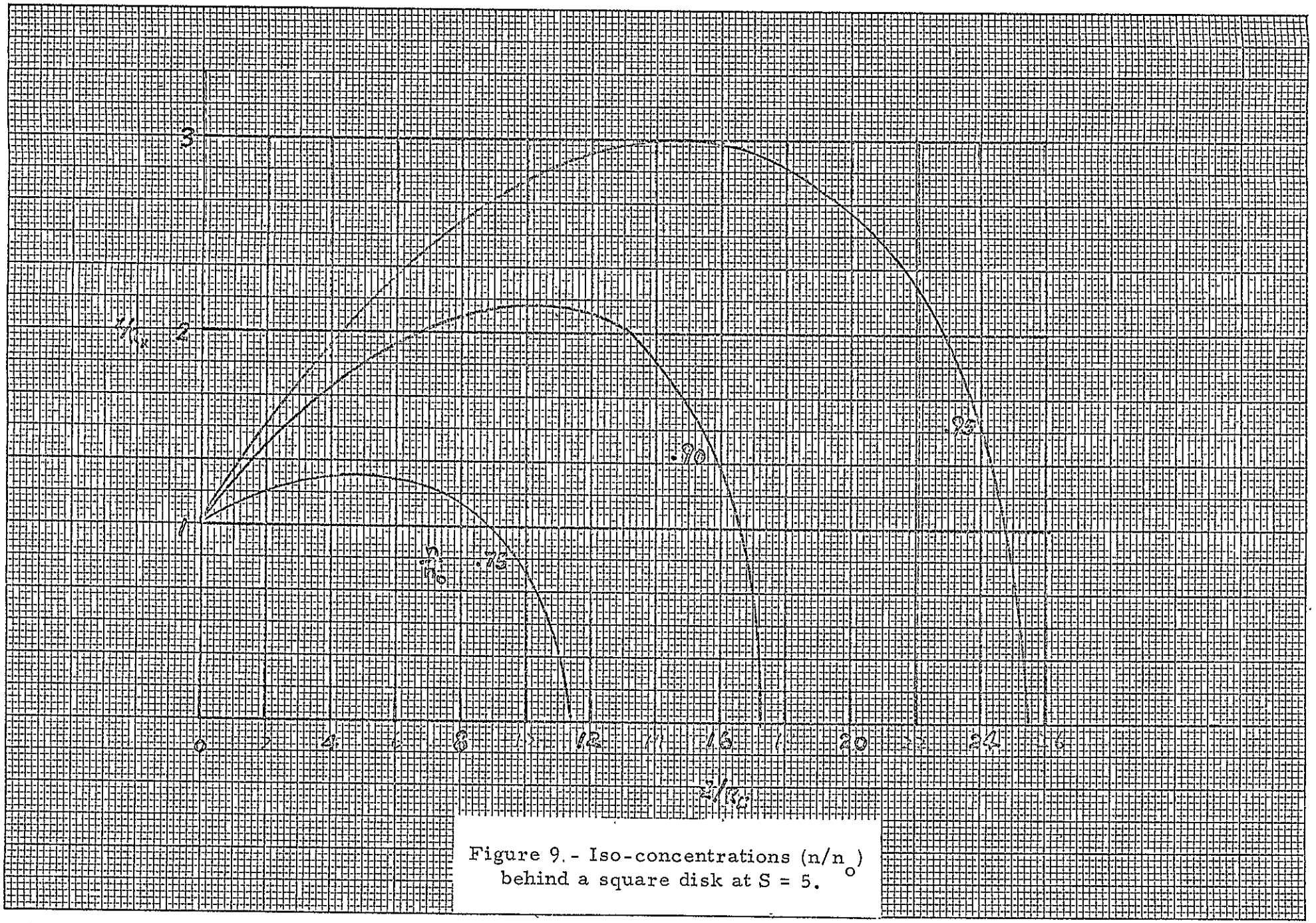

Figure 9.- Iso-concentrations (n/n_o) behind a square disk at S = 5.

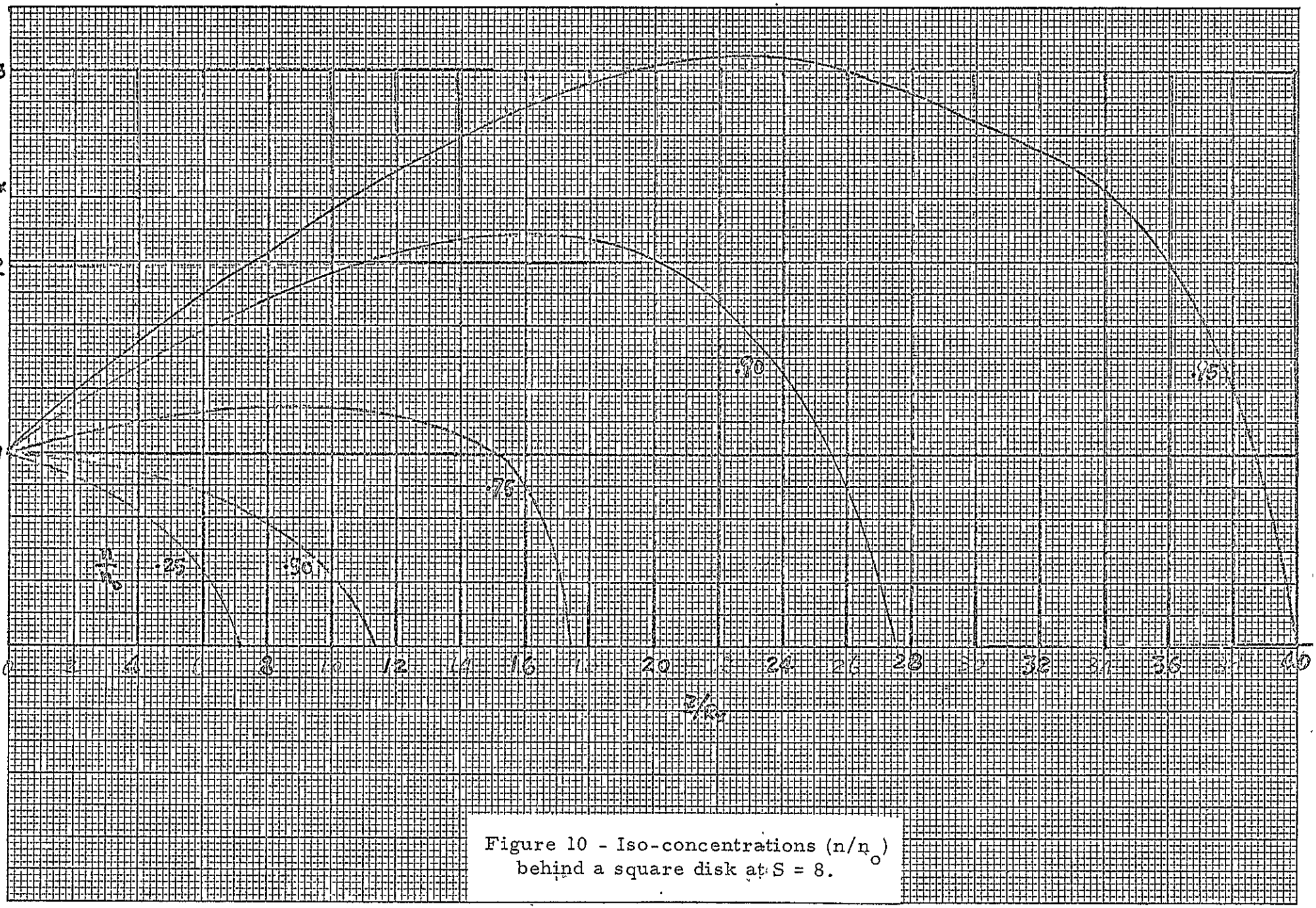

Figure 10 - Iso-concentrations (n/n_o) behind a square disk at S = 8.

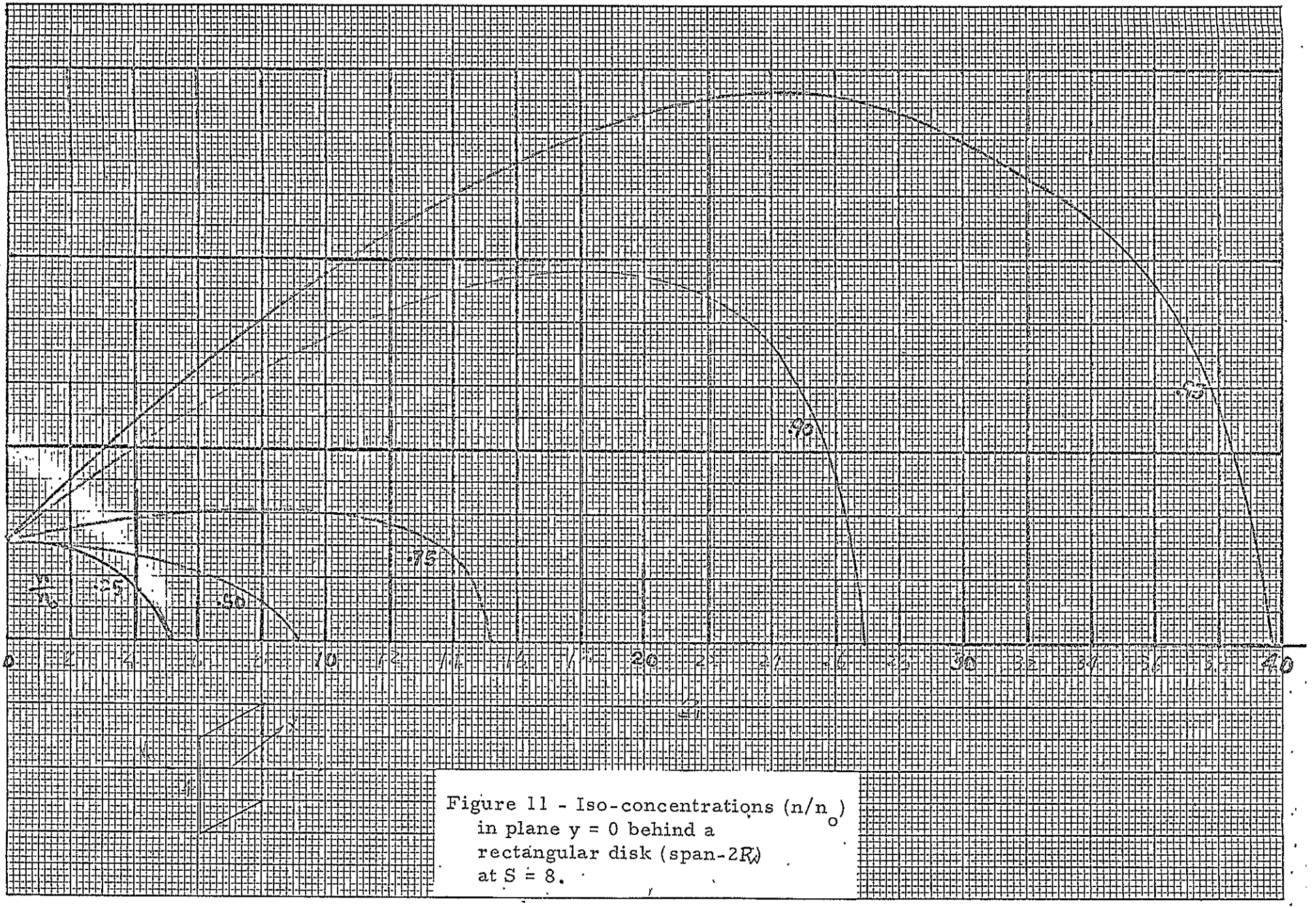

Figure 11 - Iso-concentrations (n/n_o) in plane y = 0 behind a rectangular disk (span-$2R_w$) at S = 8.

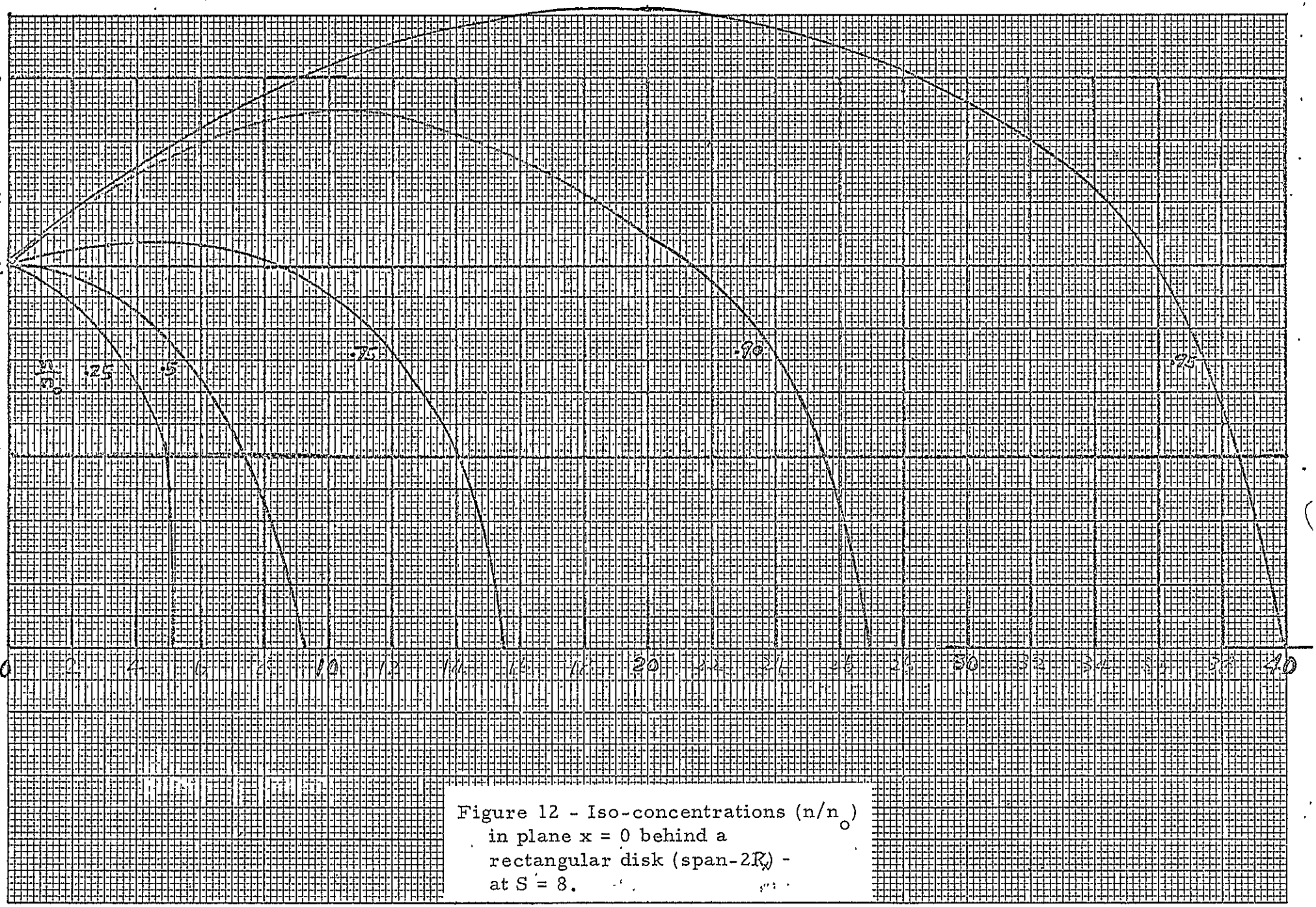

Figure 12 - Iso-concentrations (n/n_o) in plane x = 0 behind a rectangular disk (span-$2R_x$) - at S = 8.

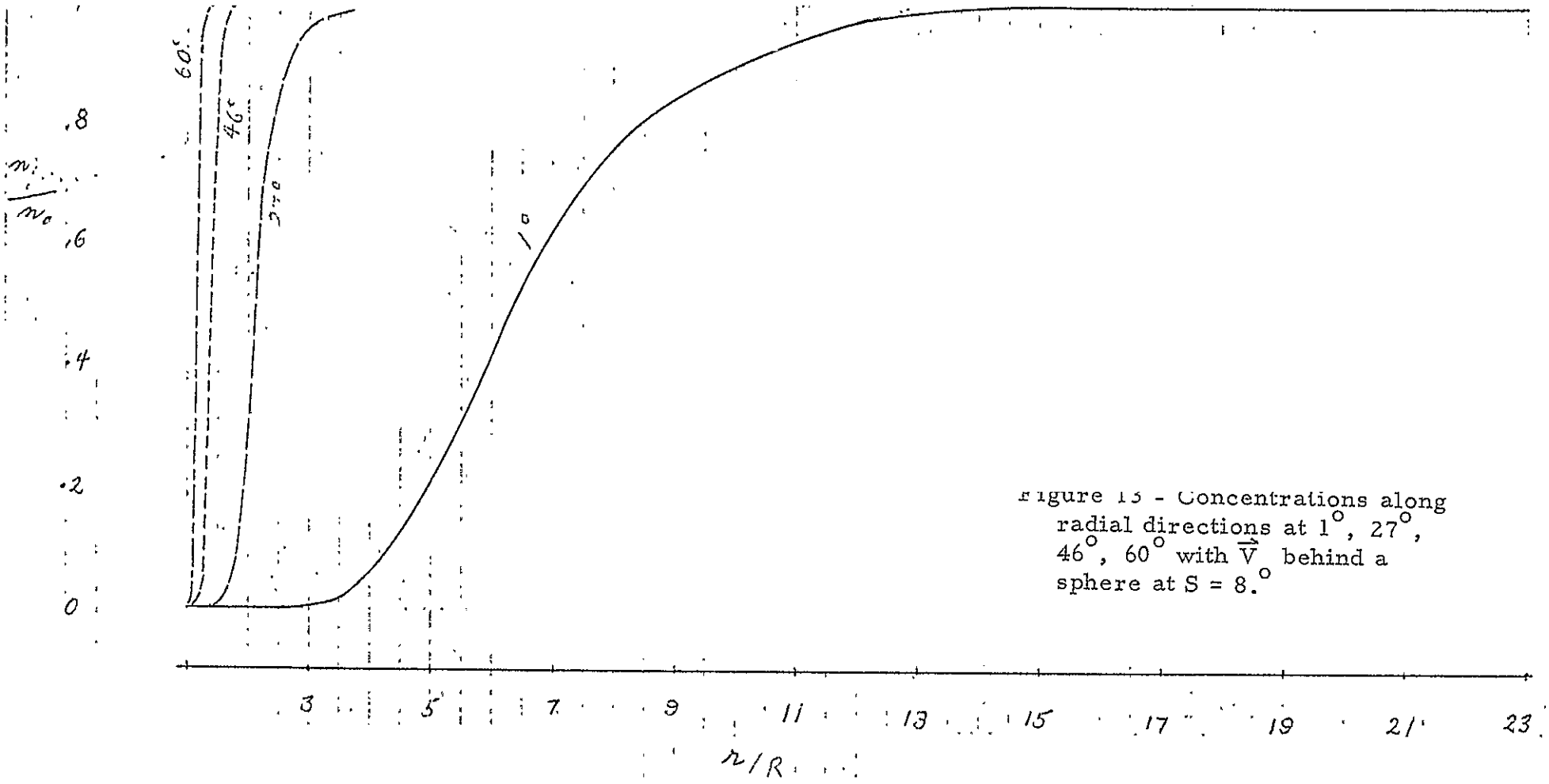

Figure 15 - Concentrations along radial directions at 1°, 27°, 46°, 60° with $\vec{V}$ behind a sphere at $S = 8.^{\circ}$

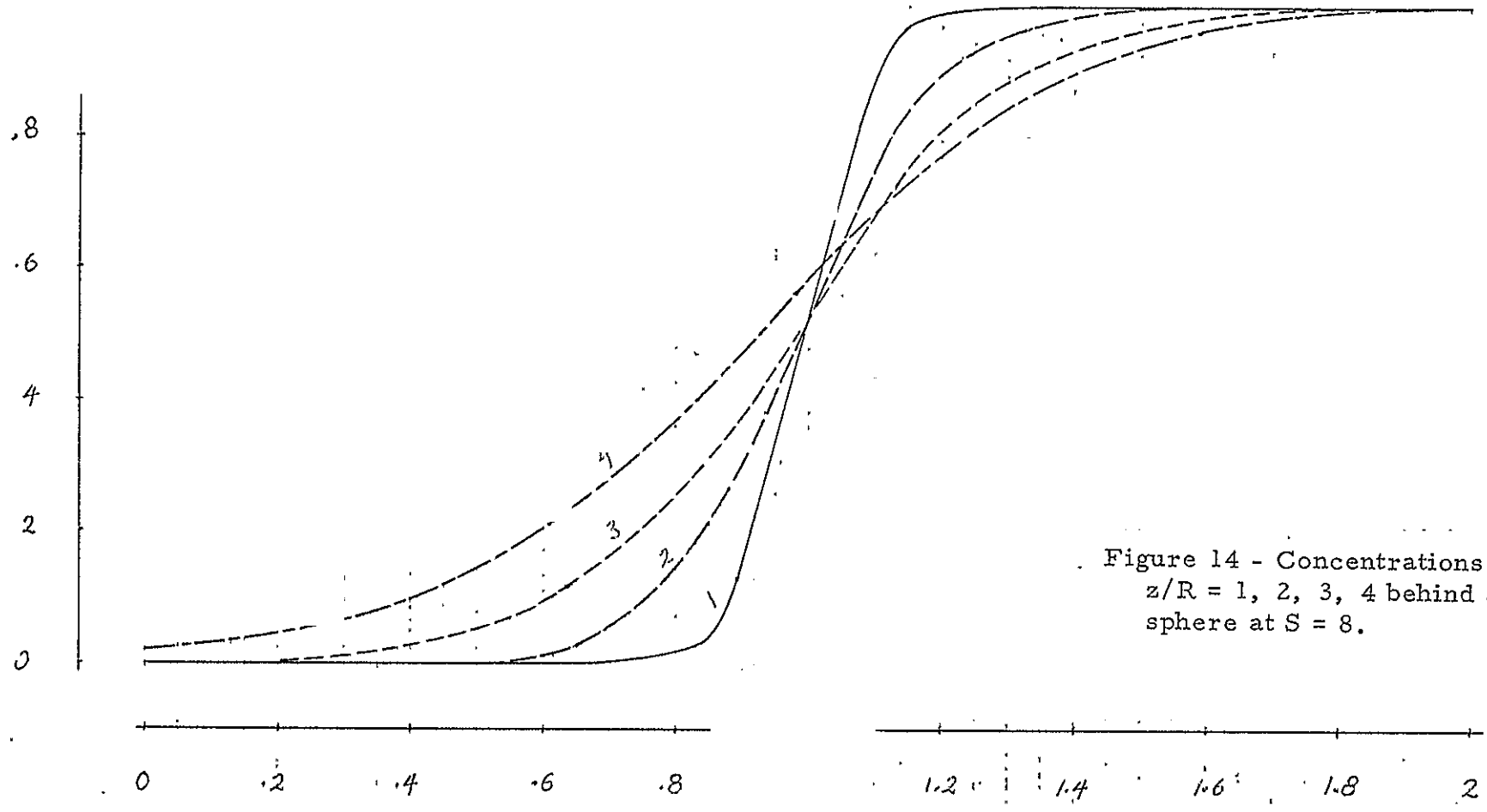

Figure 14 - Concentrations at z/R = 1, 2, 3, 4 behind a sphere at S = 8.

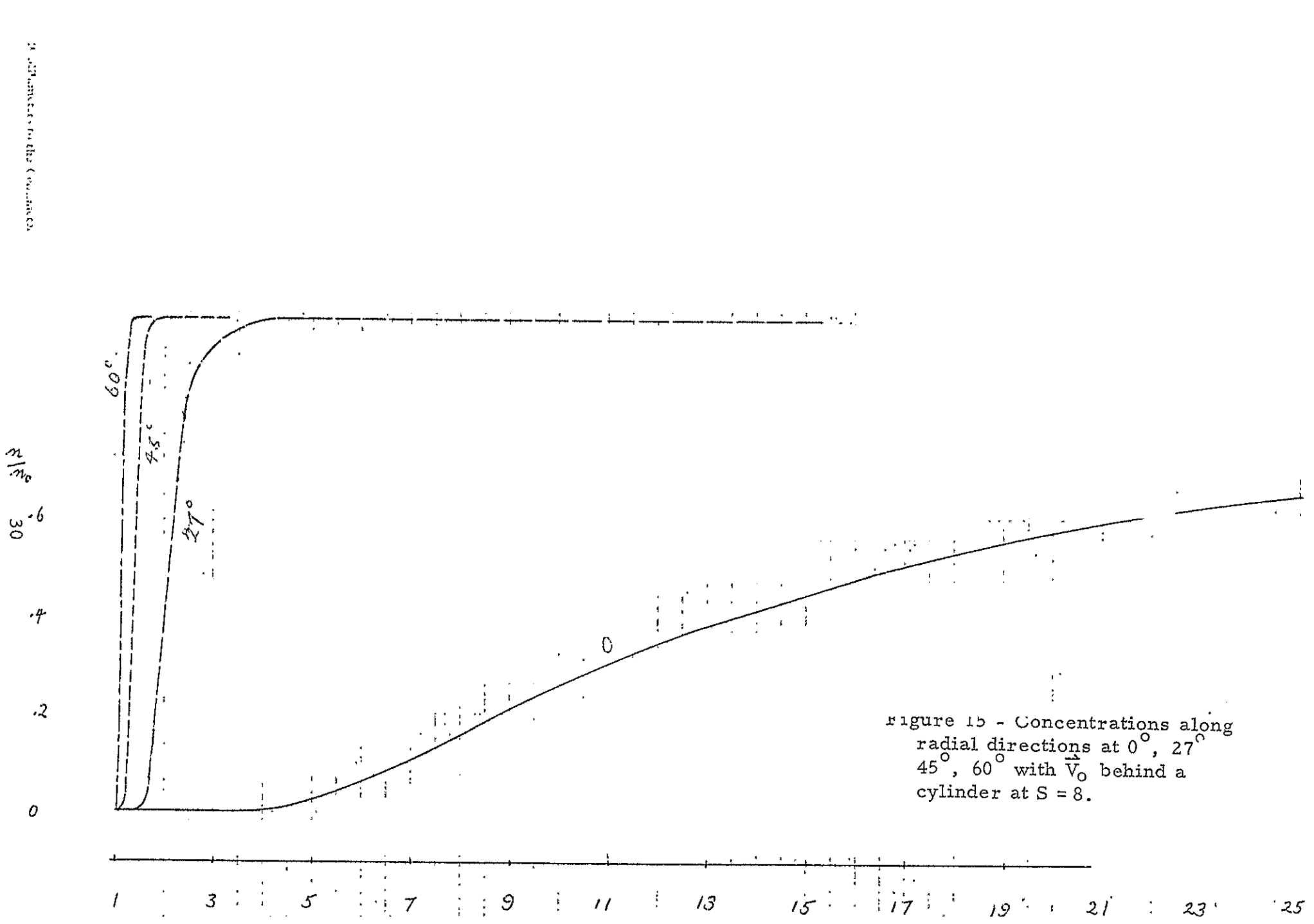

Figure 15 - Concentrations along radial directions at 0°, 27° 45°, 60° with $\vec{V}_o$ behind a cylinder at S = 8.

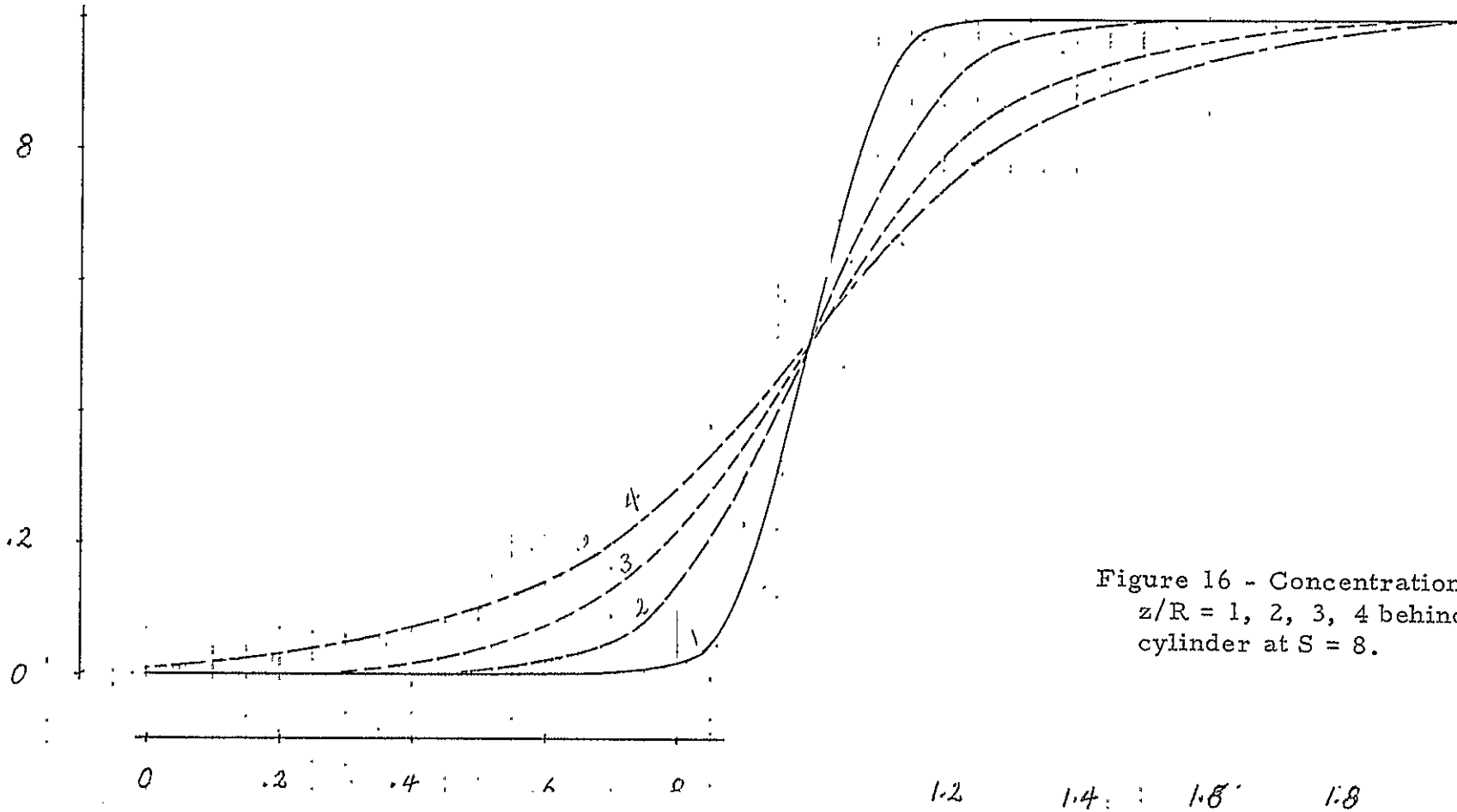

Figure 16 - Concentration at z/R = 1, 2, 3, 4 behind a cylinder at S = 8.

V. Charged Particle and Electric Potential Distributions Near a Moving Satellite

The problem of charged particle distribution in the vicinity of a moving body is much more complicated than that of the neutral particles. The fact that the particles are electrically charged and the satellite in motion is a conducting body means that the latter will become electrically charged even if it is started with zero surface potential. In the near earth environment where the charge input to the satellite by the ambient plasma dominates over that by the photoelectric effect due to solar radiation, the equilibrium surface potential is negative in the order of a few volts. This condition has been assumed in the following discussions of the charged particle distribution near a satellite. Such a condition could become invalid under special circumstances of the OGO flight. This possibility will be studied in a future program.

One of the charged-particle effects is that the particle motion is coupled to the electric potential field which, in turn, depends on the space charge contributed by the moving particles. A solution for the particle distribution in the vicinity of a moving satellite must be self-consistent with the solution for the electric potential distribution of interest. The results presented in the following are self-consistent solutions. In the study of the plasma interaction pertaining to a satellite which moves with a mesothermal speed (much higher than the thermal speed of the ambient ions and yet

much lower than the thermal speed of the ambient electrons) it is convenient for study purpose to divide the region of plasma disturbance into two parts: (1) the sheath which refers to the thin layer lying between the ambient plasma and the frontal surface of a rapidly moving body; (2) the wake which denotes the cloud of particles immediately behind a moving body.

IVa. Plasma Sheath

There are two important characteristics of the sheath associated with a negatively charged body moving at the mesothermal speeds that renders simplifications for its analysis: (1) cold-ion approximation; (2) quasi-one dimensional nature of the sheath structure. These are recognized in the sheath study.

A new concept using the Schrodinger wave equation together with the Poisson equation for the sheath of cold-ion plasma at mesothermal speeds has been proposed and a solution for the sheath of an inclined charged surface of negative potential is obtained. Let the free stream velocity (V_o) impinge on a large conducting plate of potential ϕ_o at an angle θ to its normal which aligns with the x-axis; free stream ion density = electron density = n_o; free stream ion kinetic energy, $E = \frac{1}{2} m V_o^2$, electron temperature, T_e. The electric potential $\phi(x)$ in the sheath is given

$$x - x_o = \int_{\phi_o}^{\phi} (8\pi n_o)^{-\frac{1}{2}} \left\{ 2E\cos^2\theta \left(\sqrt{1 - e\phi/E\cos^2\theta} - 1 \right) - kT_e \left[1 - \exp(e\phi/kT_e) \right]^{-\frac{1}{2}} \right\} d$$

where ϕ_o denotes the potential at $x = x_o$. Some results of the

electric potential and ion density in the sheath along an inclined plate are shown in Figures (17) and (18) where S_x denotes the component speed ratio. (For details see Appendix A).

The extension of the above analysis for a curved surface is feasible. It is noted, however, that the sheath behaves much like the boundary layer in fluid mechanics in that it varies much faster in the direction normal to the surface than along it (the quasi-one dimensional nature). This makes it possible to segment the curved surface into short inclined planes for which the sheath theory is known.

IVb. Distribution of Charged Particles and Field Potential in the Near Wake

With a satellite, e.g. OGO, moving at a mesothermal speed, the nature of the plasma disturbances of the wake differs considerably from that of the sheath in front of the body. When a body moves rapidly through a plasma, a momentary cavity is created behind the body. The ambient ions and electrons rush into the cavity by virtue of their thermal velocities. The ionic thermal velocity, though small compared with the free stream velocity, cannot be ignored in the wake analysis as done in the sheath analysis.

It is the search for the self-consistent solution of the plasma disturbances of the near wake that much of our efforts have been directed at.

To cope with the complex geometrical configuration of an OGO, we again consider the satellite as composed of simple geometrical

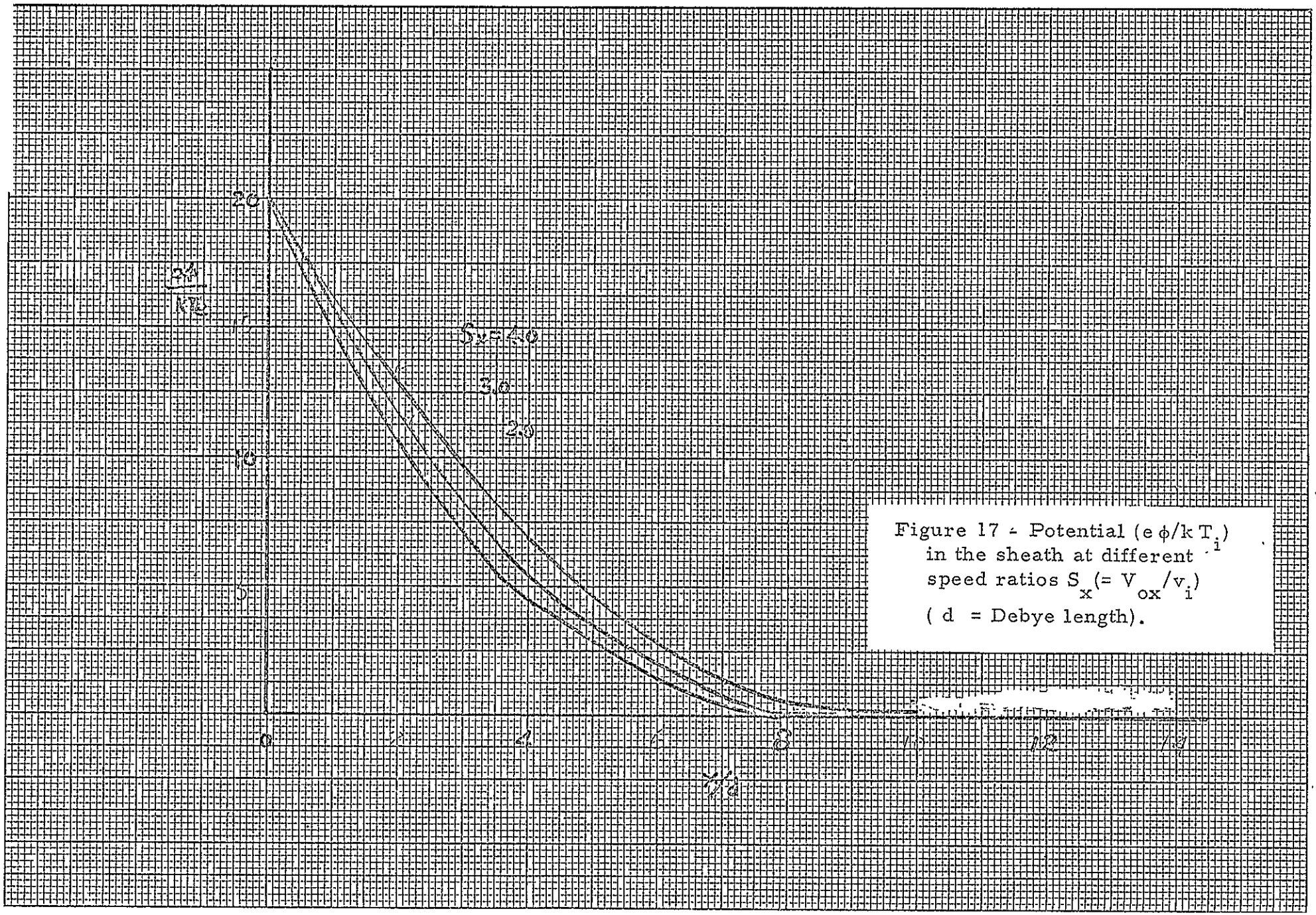

Figure 17 - Potential ($e\phi/kT_i$) in the sheath at different speed ratios $S_x (= V_{ox}/v_i)$ (d = Debye length).

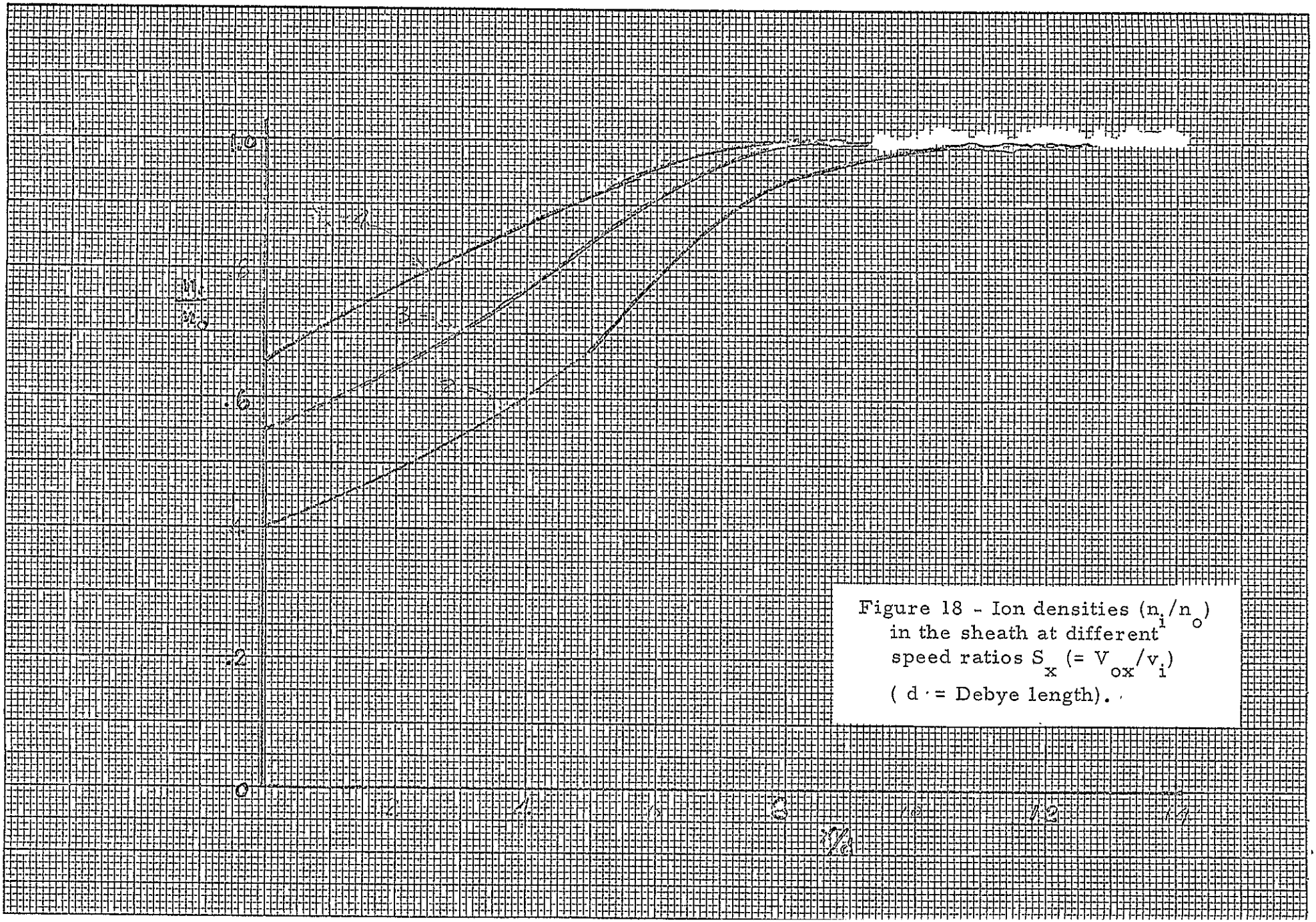

Figure 18 - Ion densities (n_i/n_o) in the sheath at different speed ratios S_x (= V_{ox}/v_i) (d = Debye length).

components and take into account the interference effect due to the proximity of the neighboring members in the ensemble. The details of these new self-consistent solutions for the distributions of charged particles and electric potentials in the wakes of cylinders and spheres are described in the Appendices B and C. We shall present here the computed results in Figures (19 - 72) for spheres and cylinders under various parameters of satellite environments and ambient conditions. Each solution is prescribed by four parameters: (1) R/d, (2) T_e/T_i, (3) V_o/v_i, and (4) ϕ_S. i.e. The ratio of body size (R) and Debye length (d), the ratio of electron and ion temperature, the ratio of free stream velocity and thermal ion velocity, and the surface potential (normalized by kT_i/e), respectively.

The common features of these solutions as shown in Figures (19 - 72) are as follows: (1) the mean free path of the ambient particles are many orders larger than the characteristic dimension (R) of the body which is, in turn, large compared with the Debye shielding length ($d = \sqrt{kT/4\pi e^2 n}$) of the ambient plasma; (2) the velocity of the moving body (V_o) is mesothermal, i.e. to say, it is much larger than the ionic thermal speed ($v_i = \sqrt{2kT_i/m_i}$) and yet much smaller than the electron thermal velocity ($v_e = \sqrt{2kT_e/m_e}$); (3) the surface potential is negative relative to the ambient plasma. The geomagnetic effect has been ignored. This is justifiable provided the ionic Larmor radius at the satellite altitude in question is large compared with the body size (R). The electron density is assumed

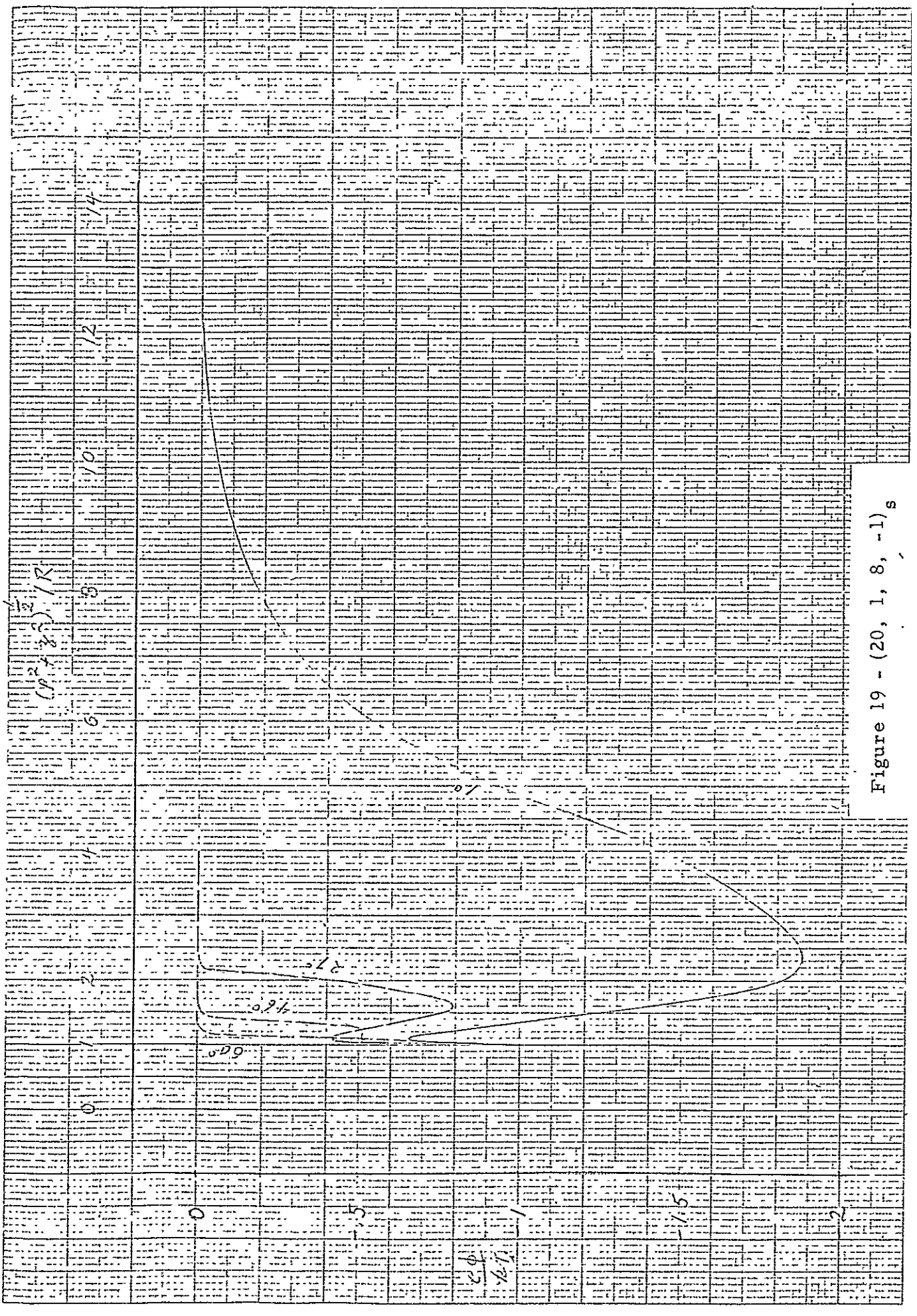

Figure 19 - $(20, 1, 8, -1)_s$

Figure 20 - $(20, 1, 8, -1)_s$

Figure 21 - $(20, 1, 8, -1)_s$

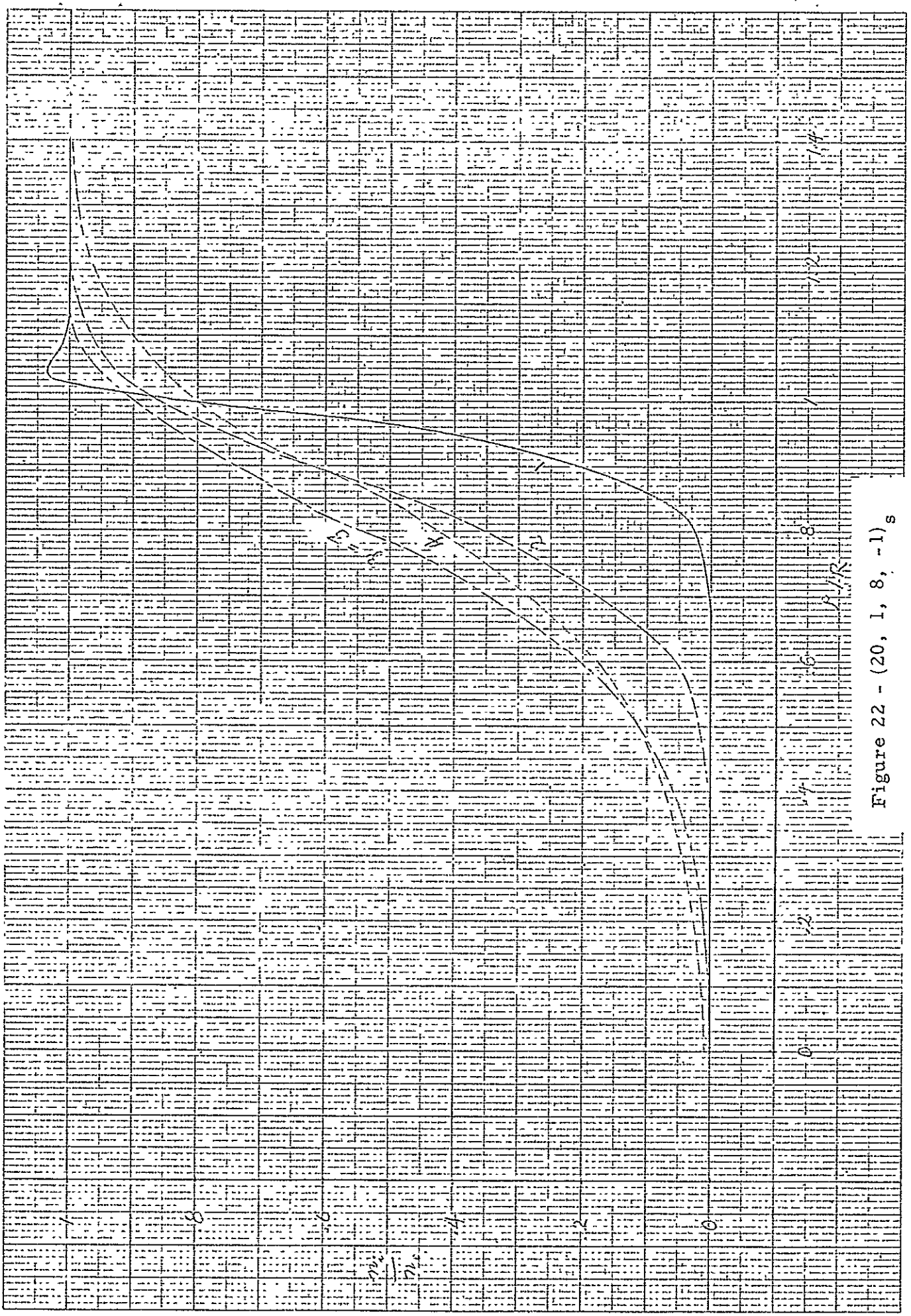

Figure 22 - (20, 1, 8, -1)$_s$

Figure 23 - $(1, 1, 8, -1)_s$

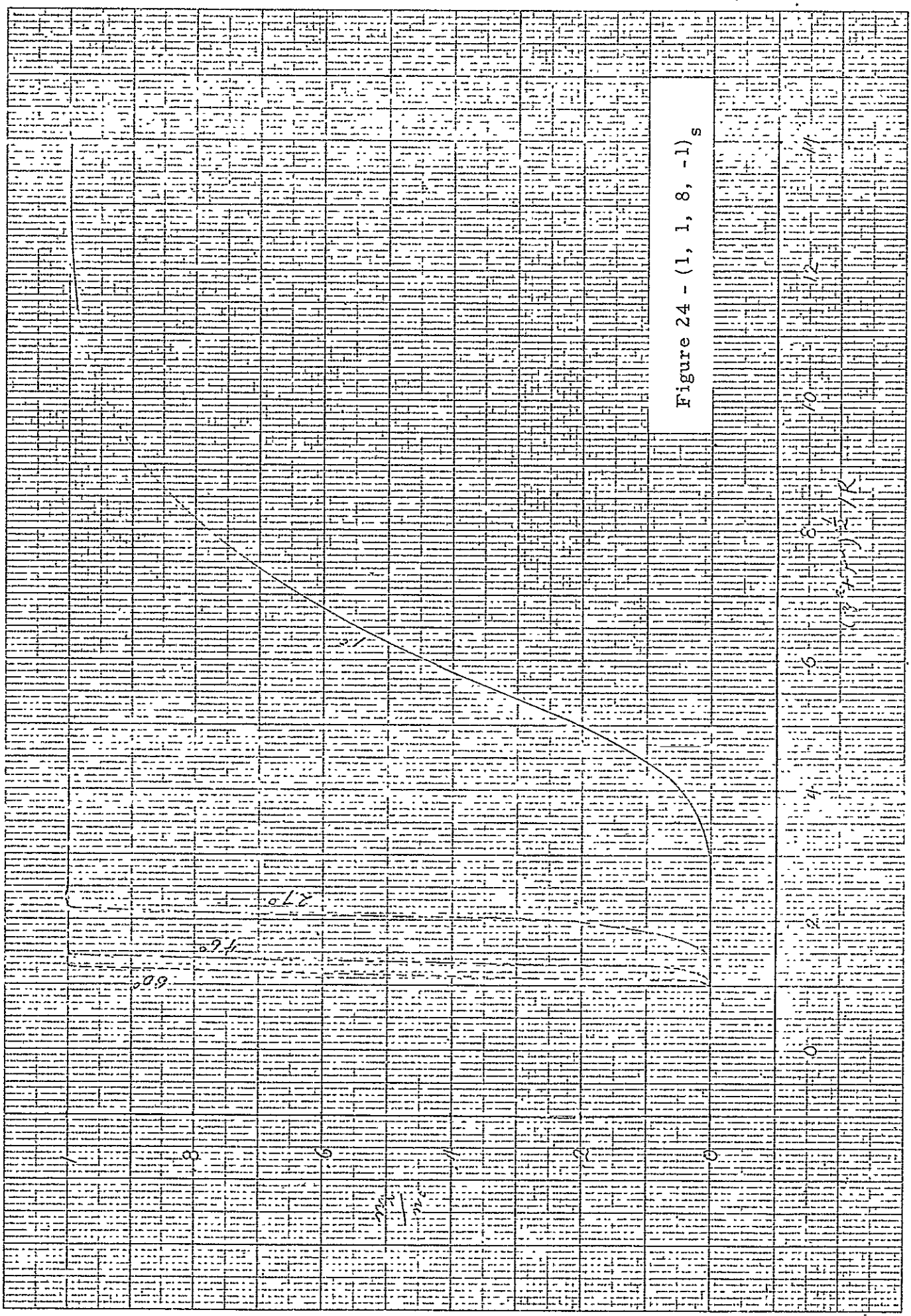

Figure 24 - $(1, 1, 8, -1)_s$

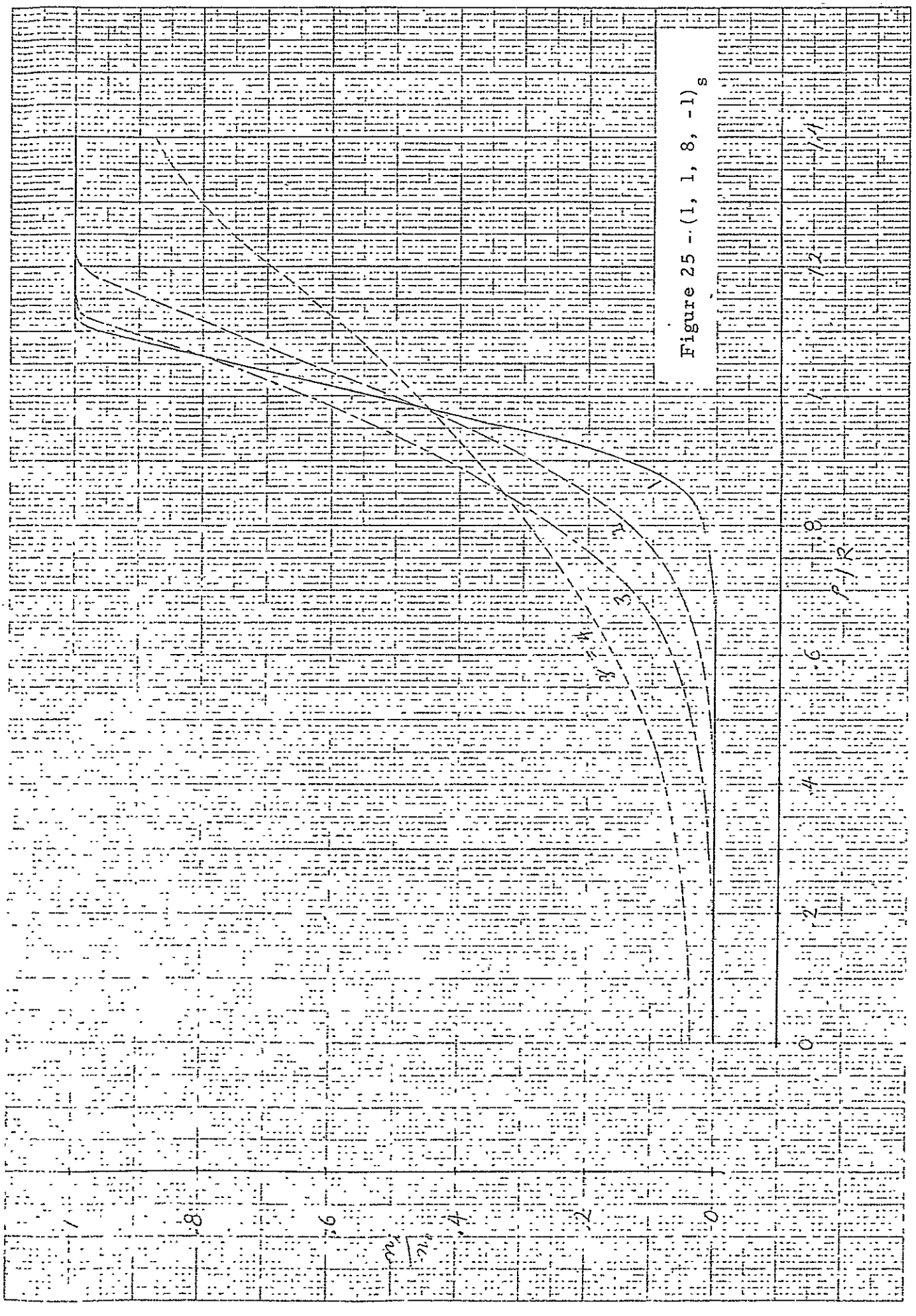

Figure 26 - $(1, 1, 8, -1)_s$

Figure 27 - $(5, 1, 8, -1)_s$

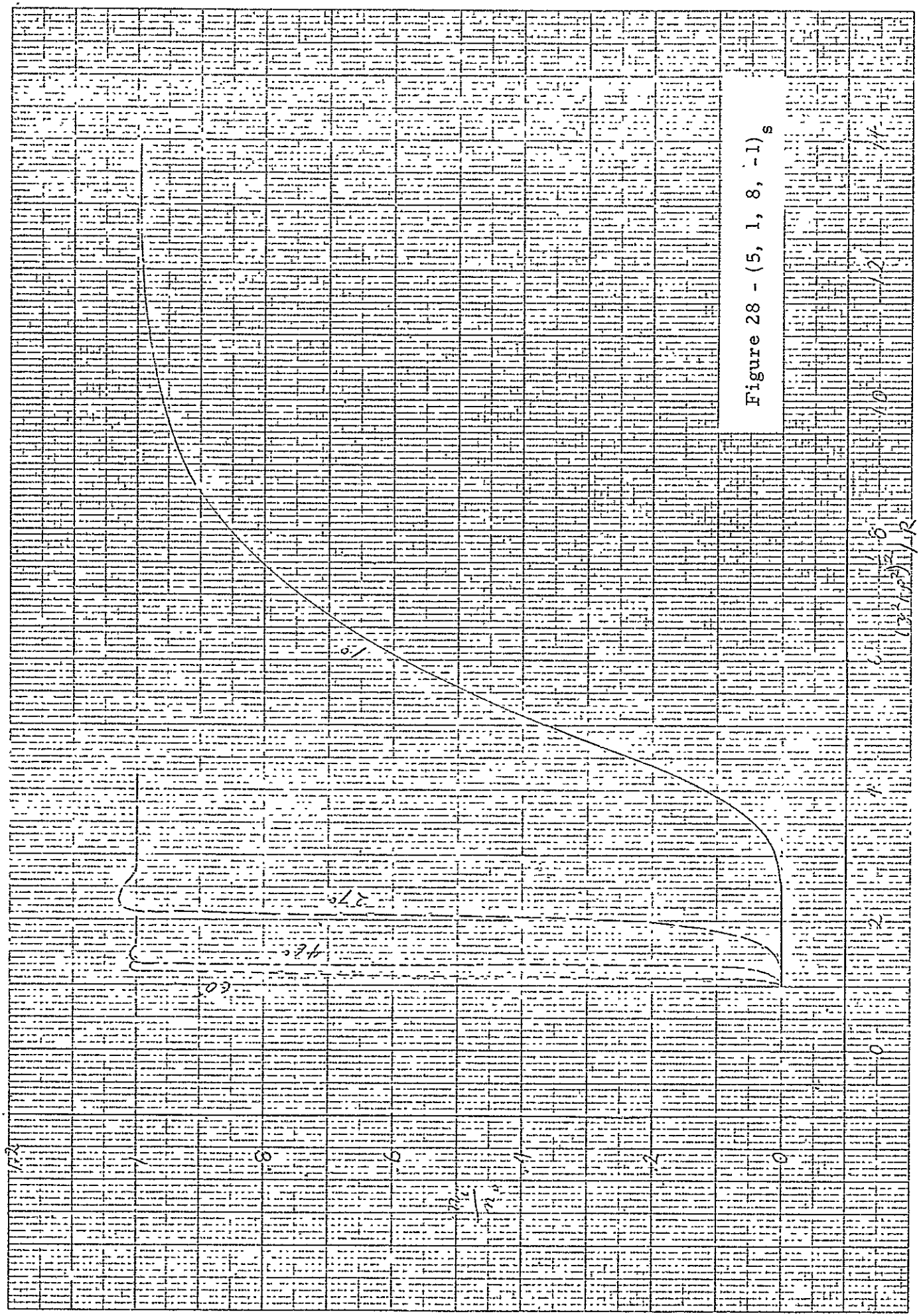

Figure 28 - $(5, 1, 8, -1)_s$

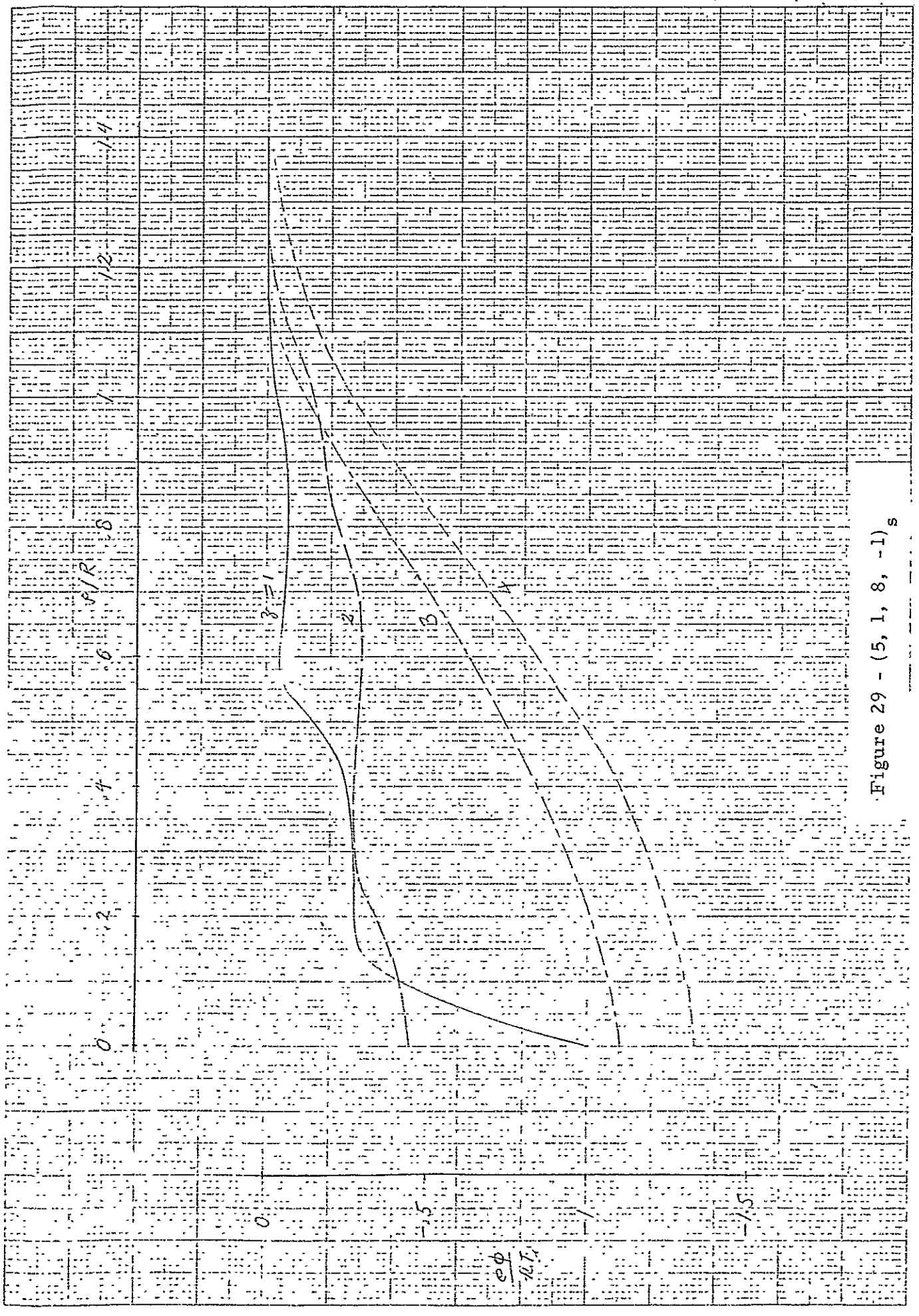

Figure 29 - $(5, 1, 8, -1)_s$

Figure 30 - (5, 1, 8, -1)s

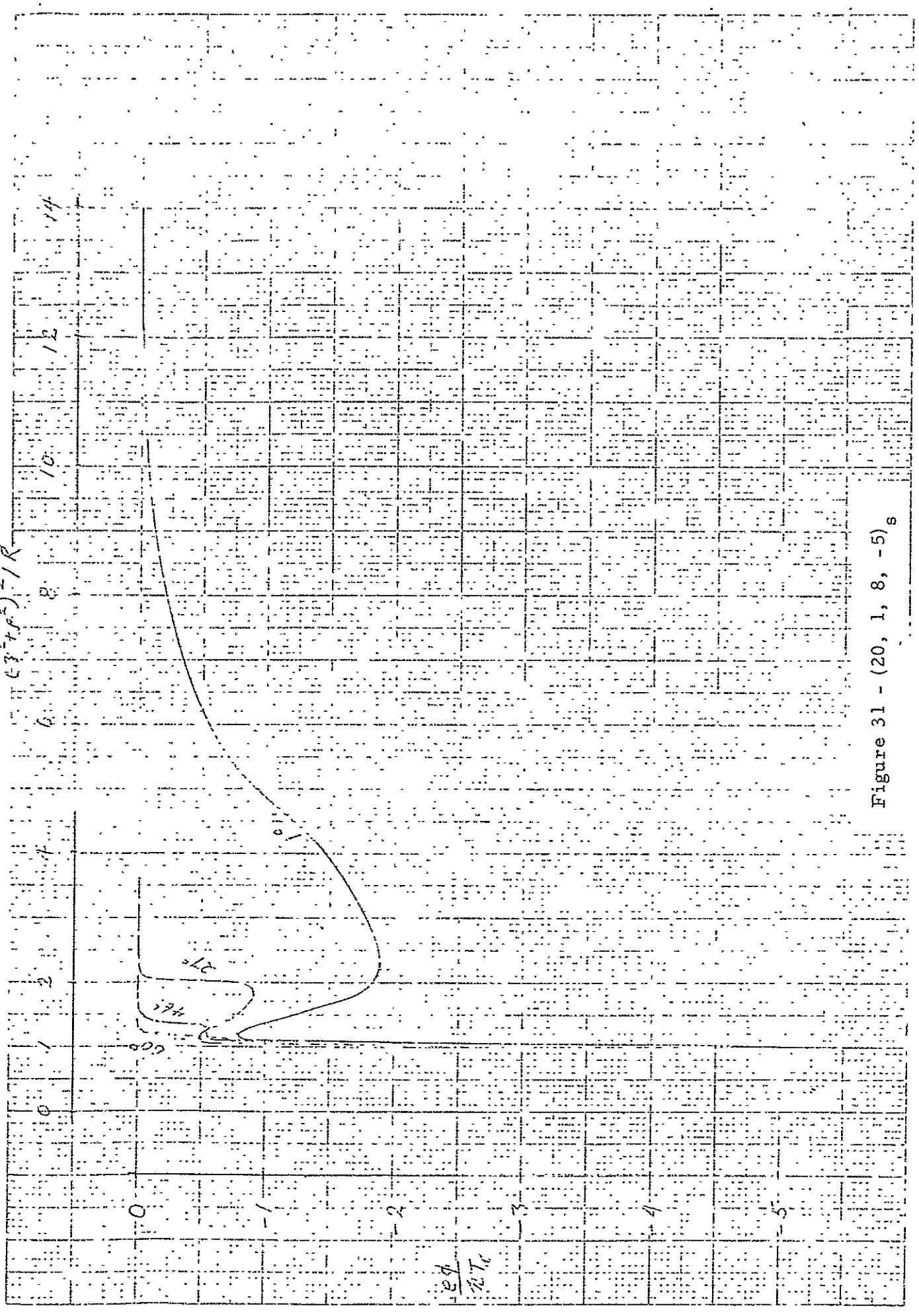

Figure 31 - (20, 1, 8, -5)$_s$

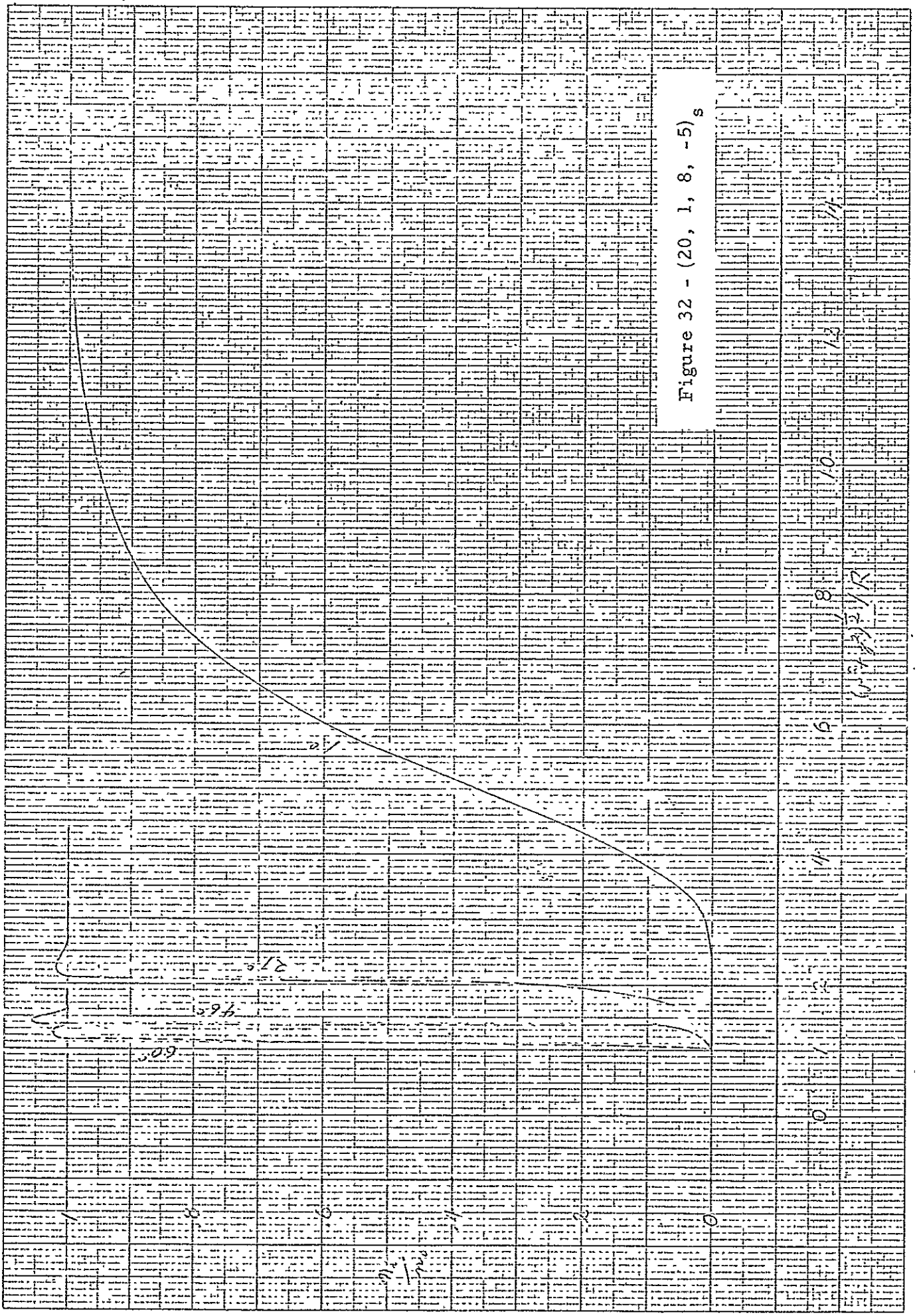

Figure 32 - $(20, 1, 8, -5)_s$

Figure 33 - $(20, 1, 8, -5)_s$

Figure 34 - $(20, 1, 8, -5)_s$

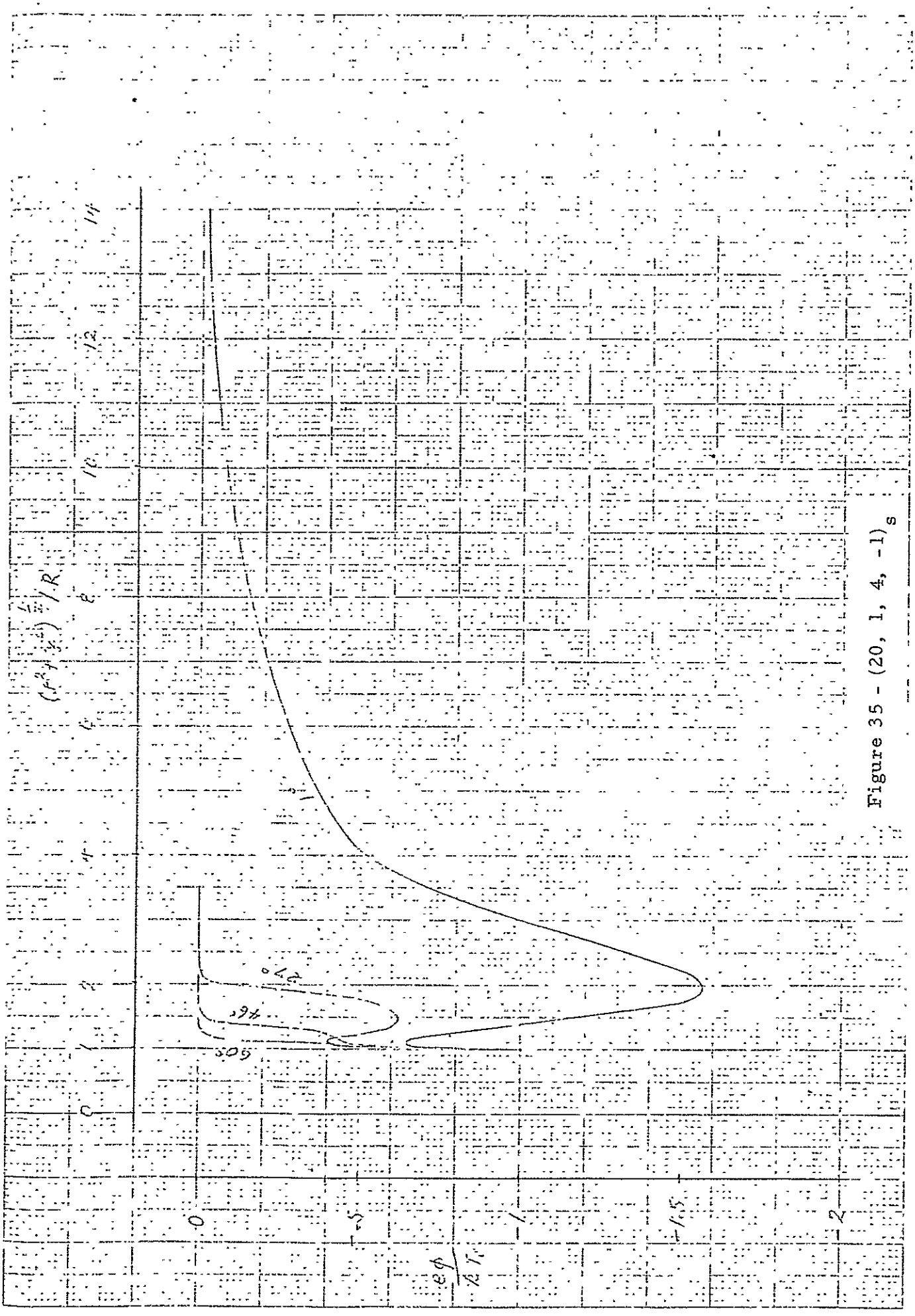

Figure 35 - $(20, 1, 4, -1)_s$

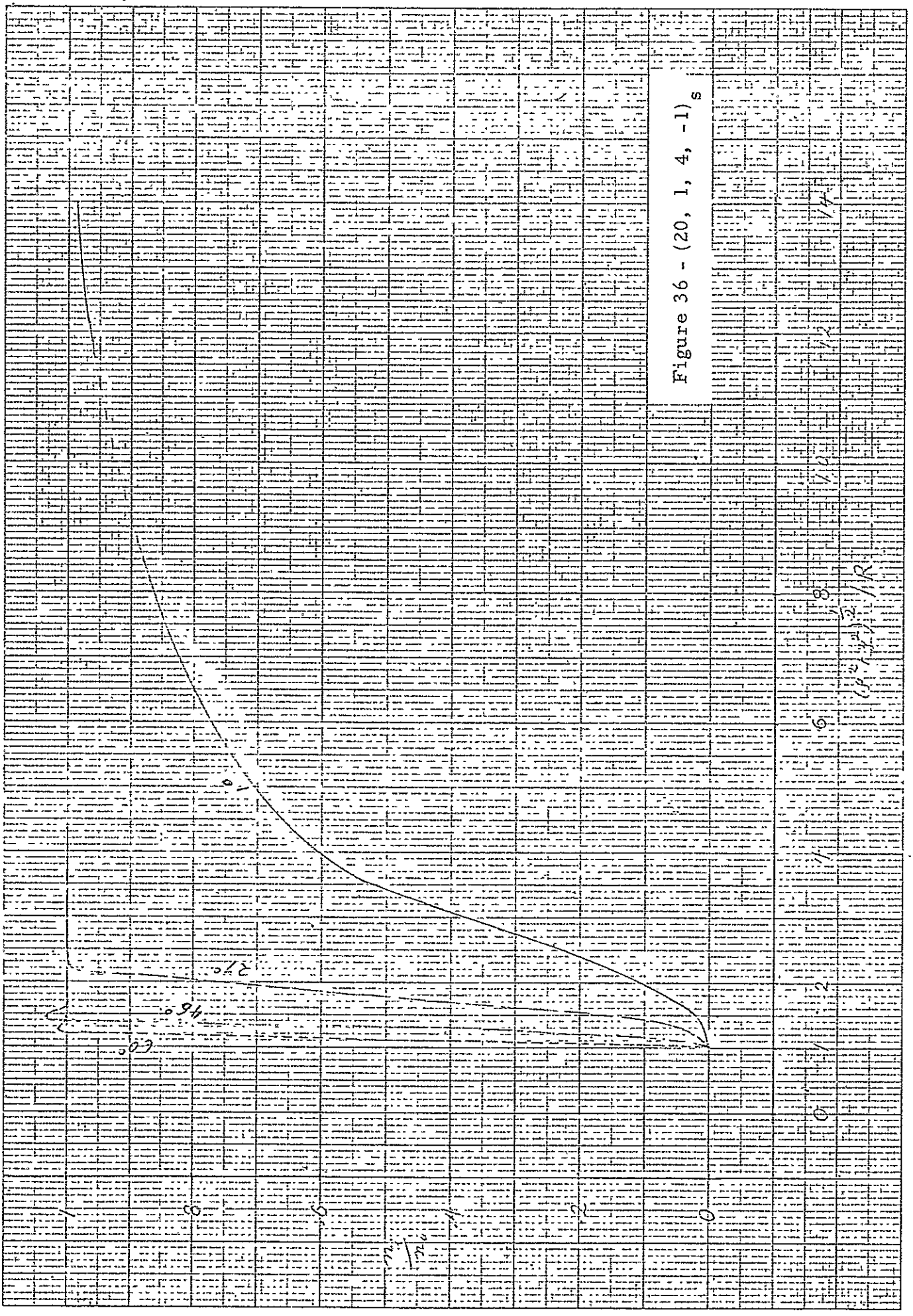

Figure 36 - $(20, 1, 4, -1)_s$

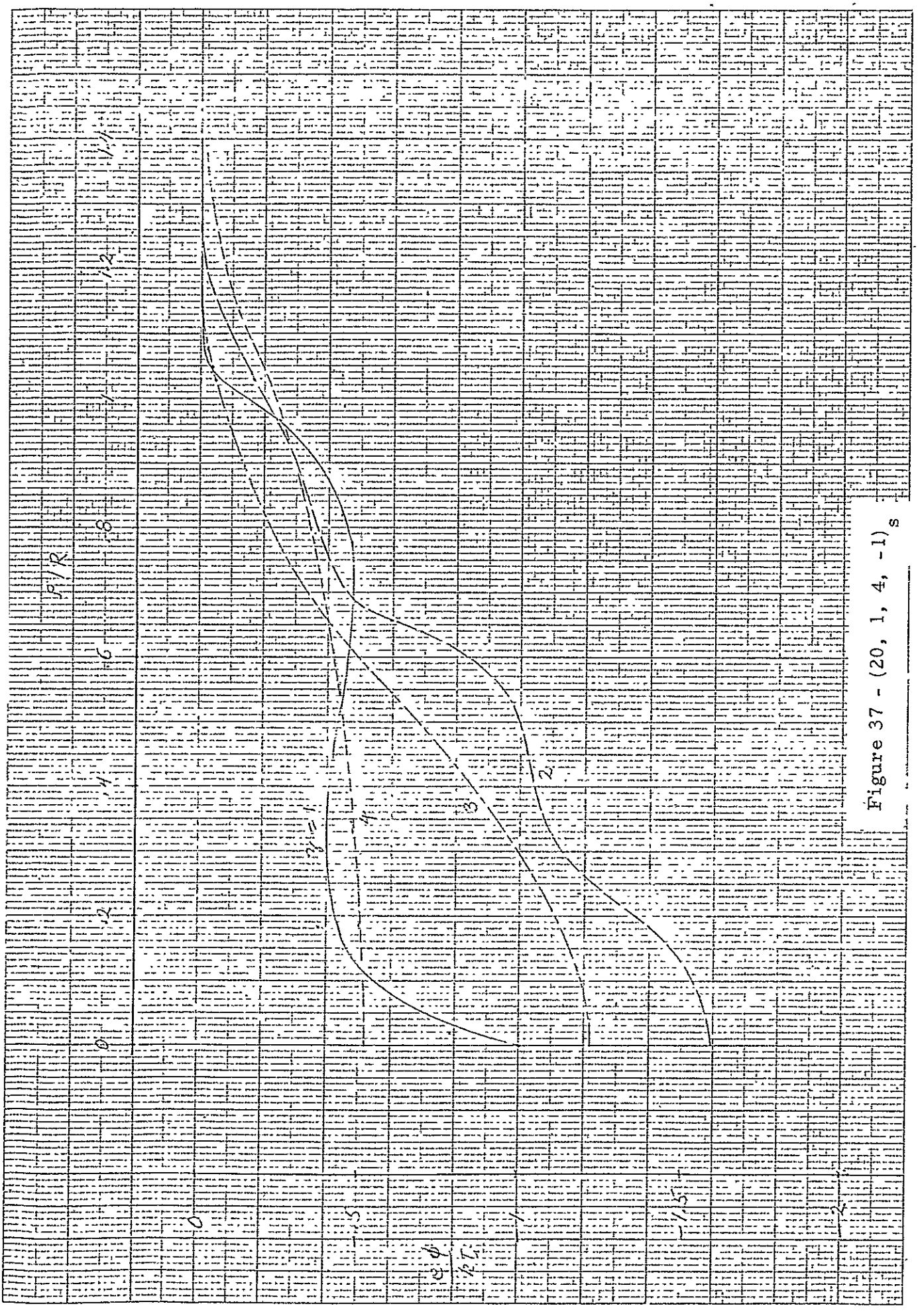

Figure 37 - $(20, 1, 4, -1)_s$

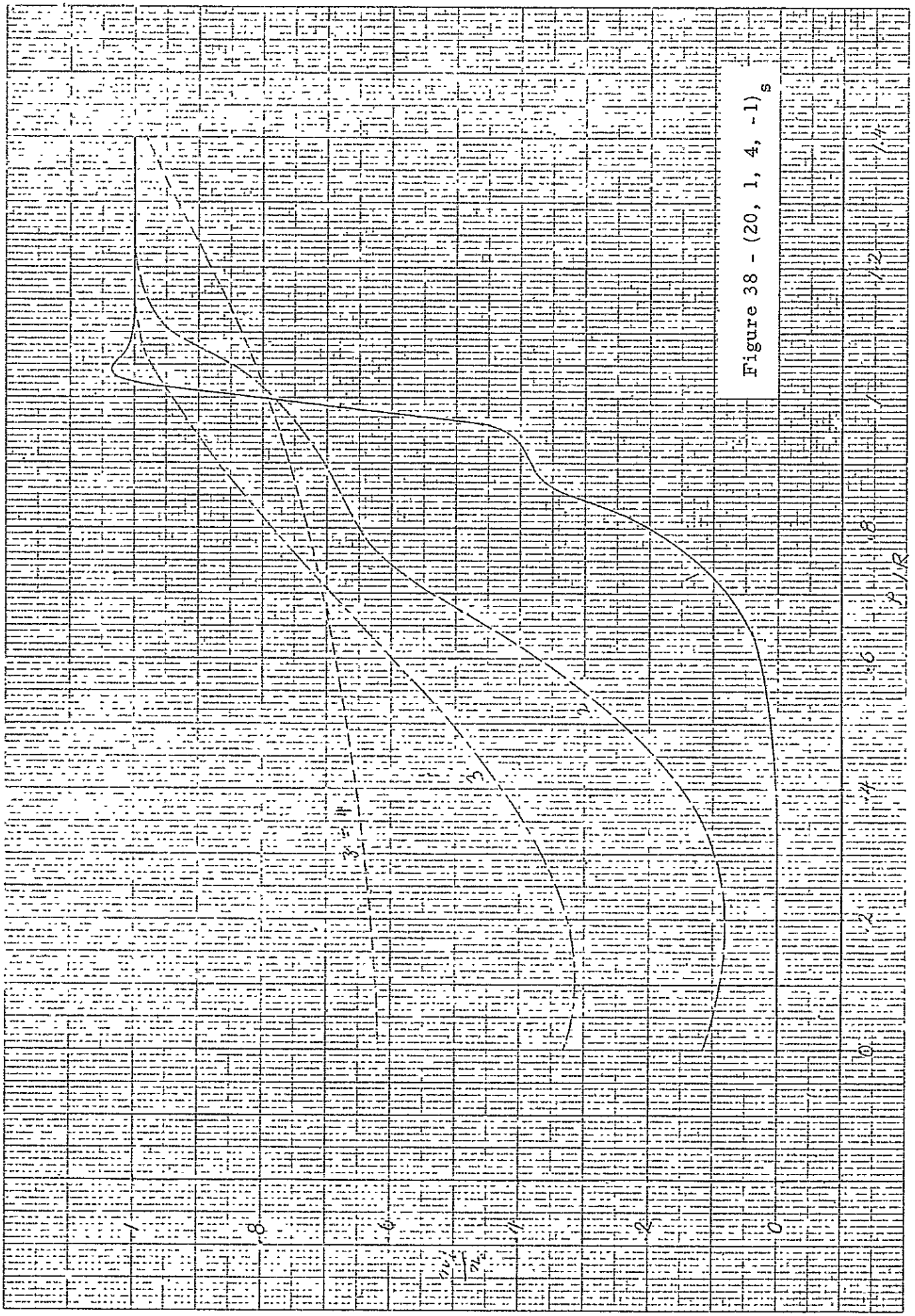

Figure 38 - $(20, 1, 4, -1)_s$

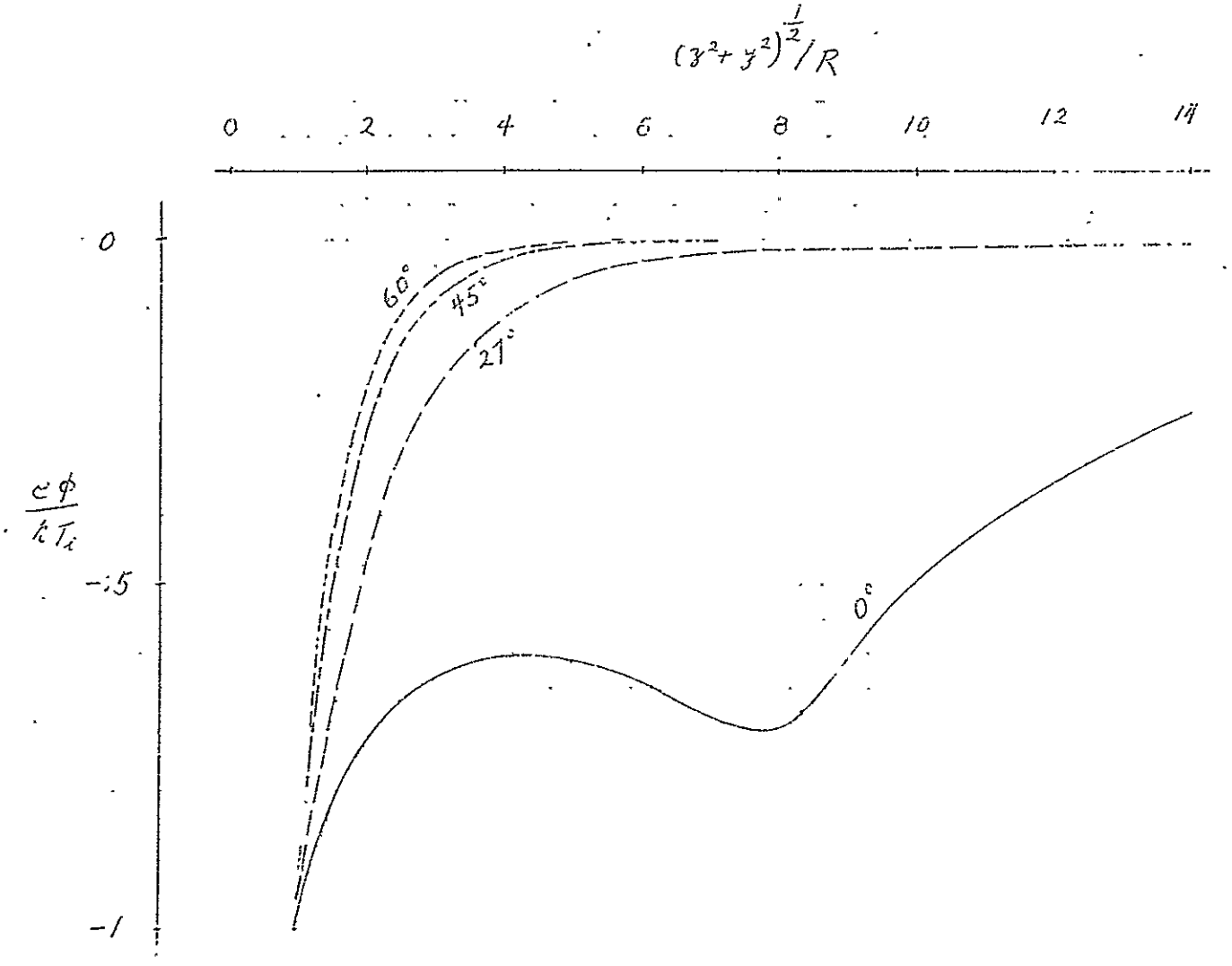

Figure 39 - $(1, 1, 8, -1)_c$

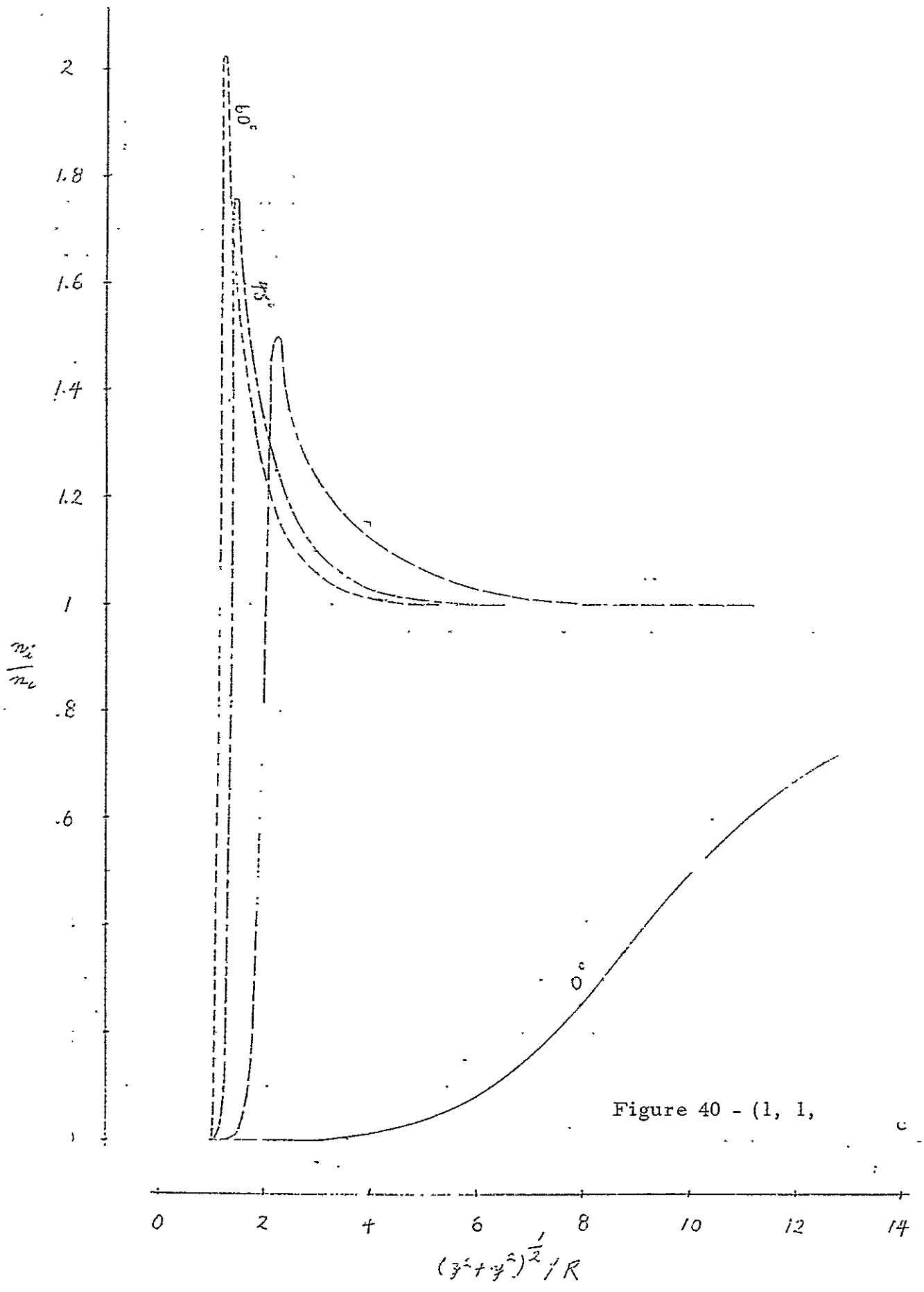

Figure 40 - (1, 1,

0
.4
.8
1.2
1.6
2
2.4
2.8
3.2
3.6
4
0
-.5
-1
$\frac{e\phi}{kT_i}$
1
2
3
4

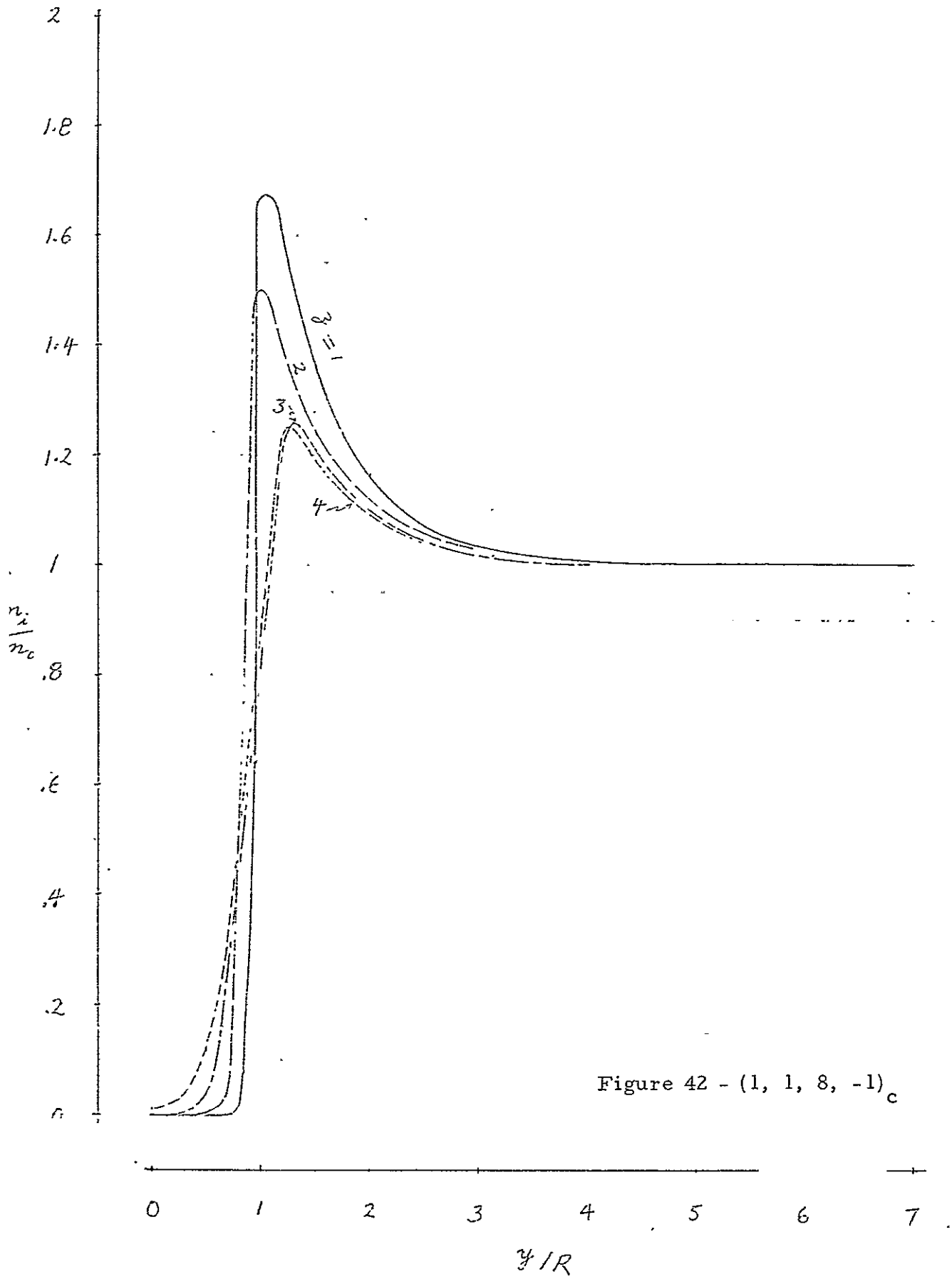

Figure 42 - $(1, 1, 8, -1)_c$

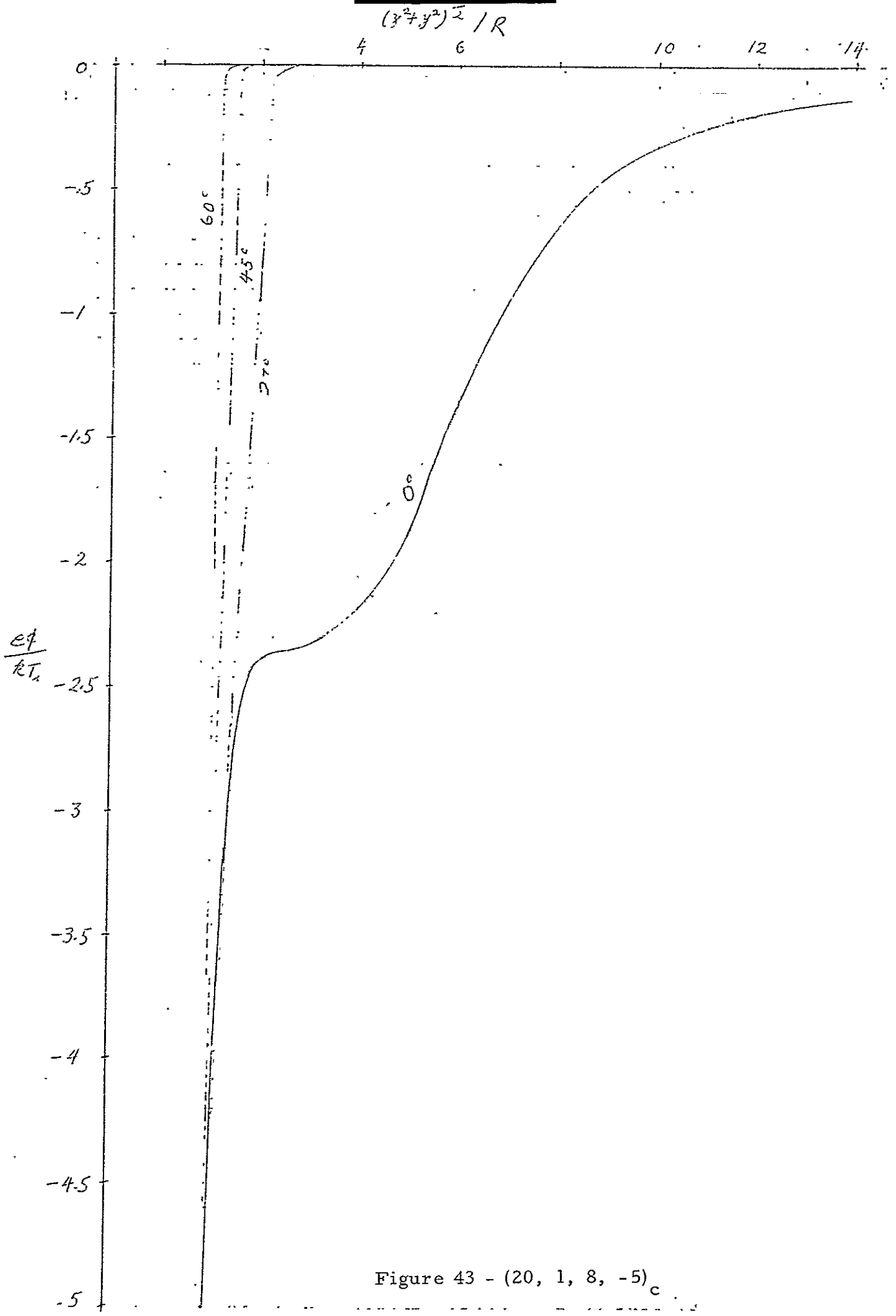

Figure 43 - $(20, 1, 8, -5)_c$

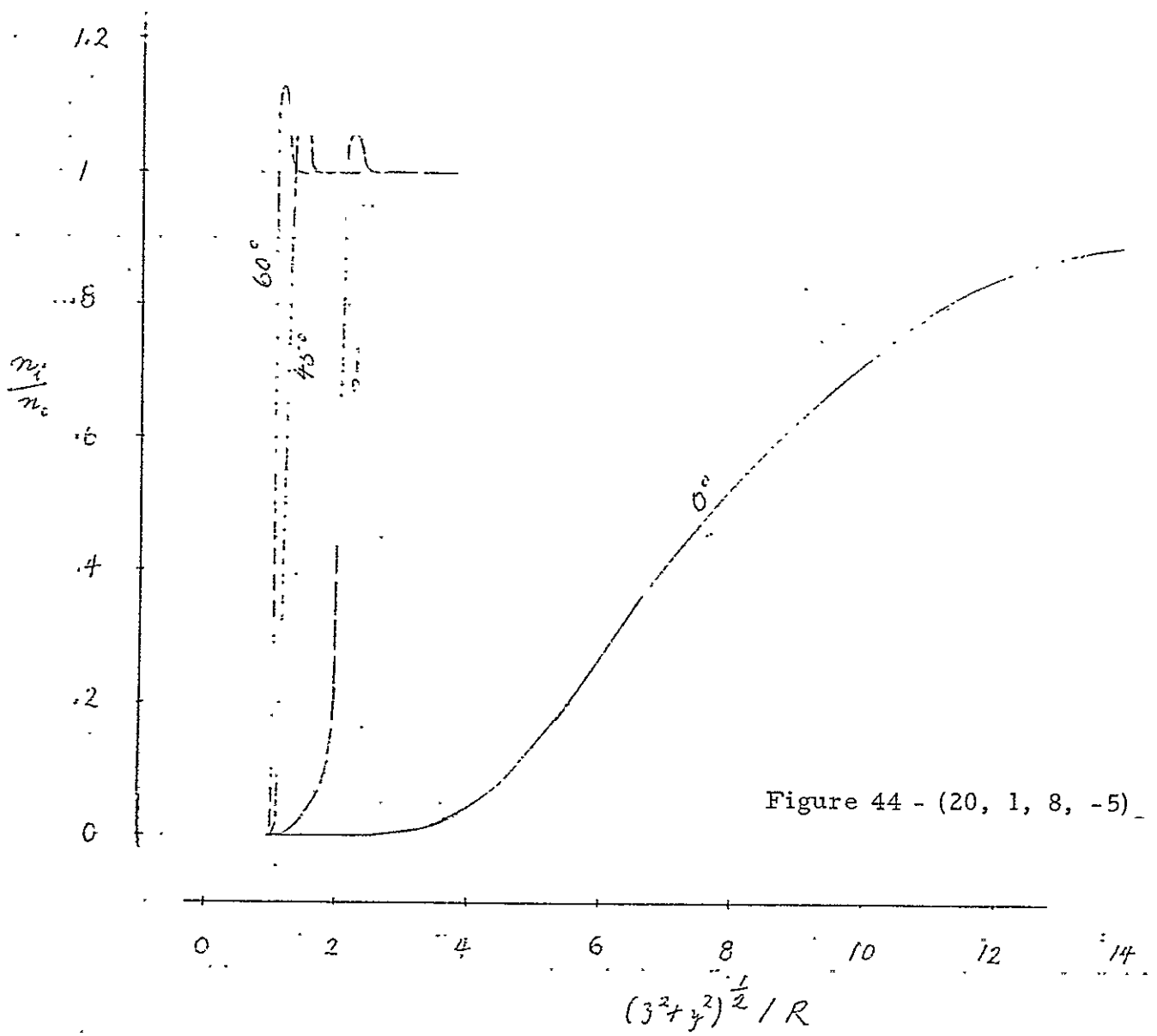

Figure 44 - (20, 1, 8, -5)

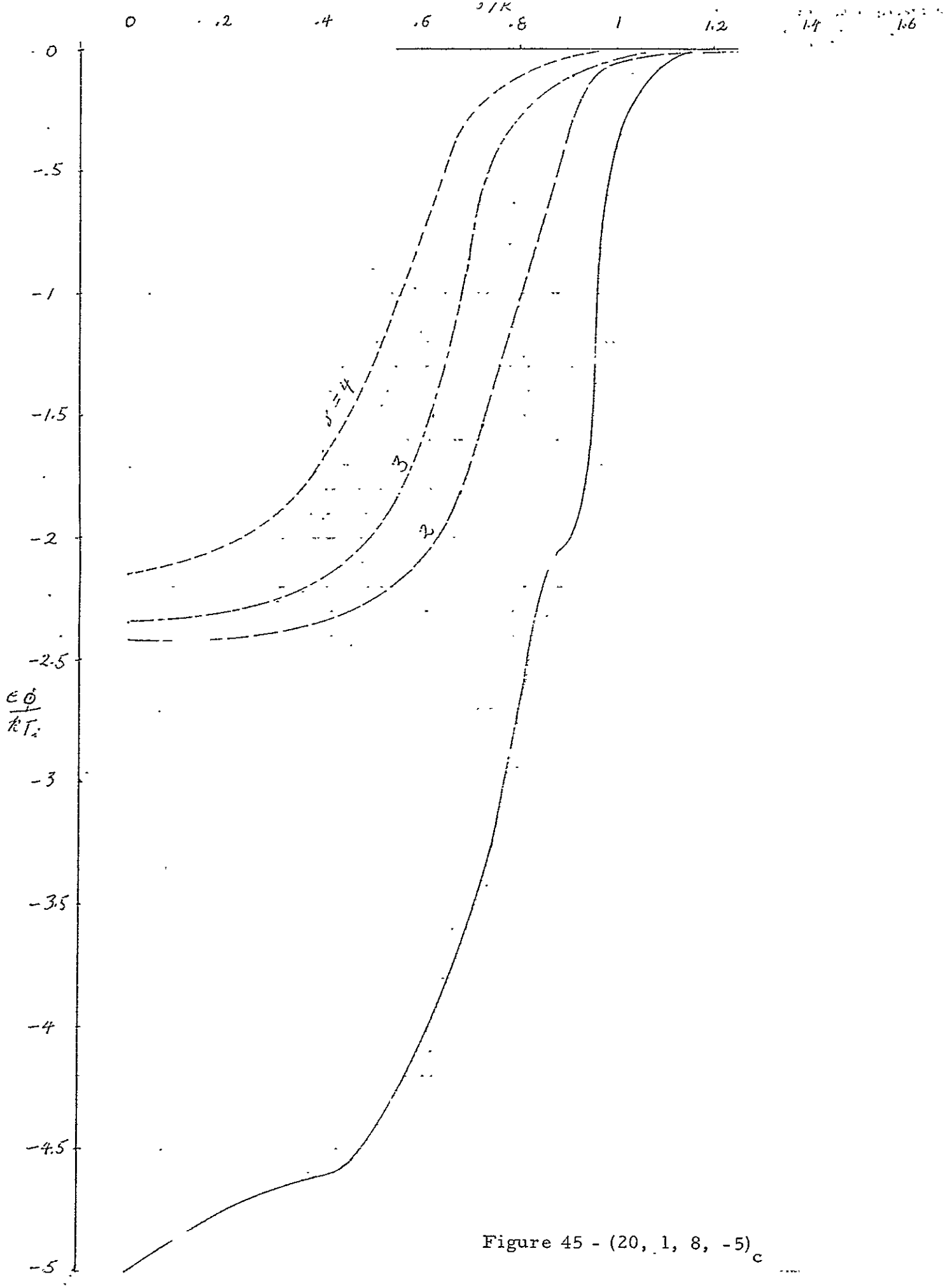

Figure 45 - $(20, 1, 8, -5)_c$

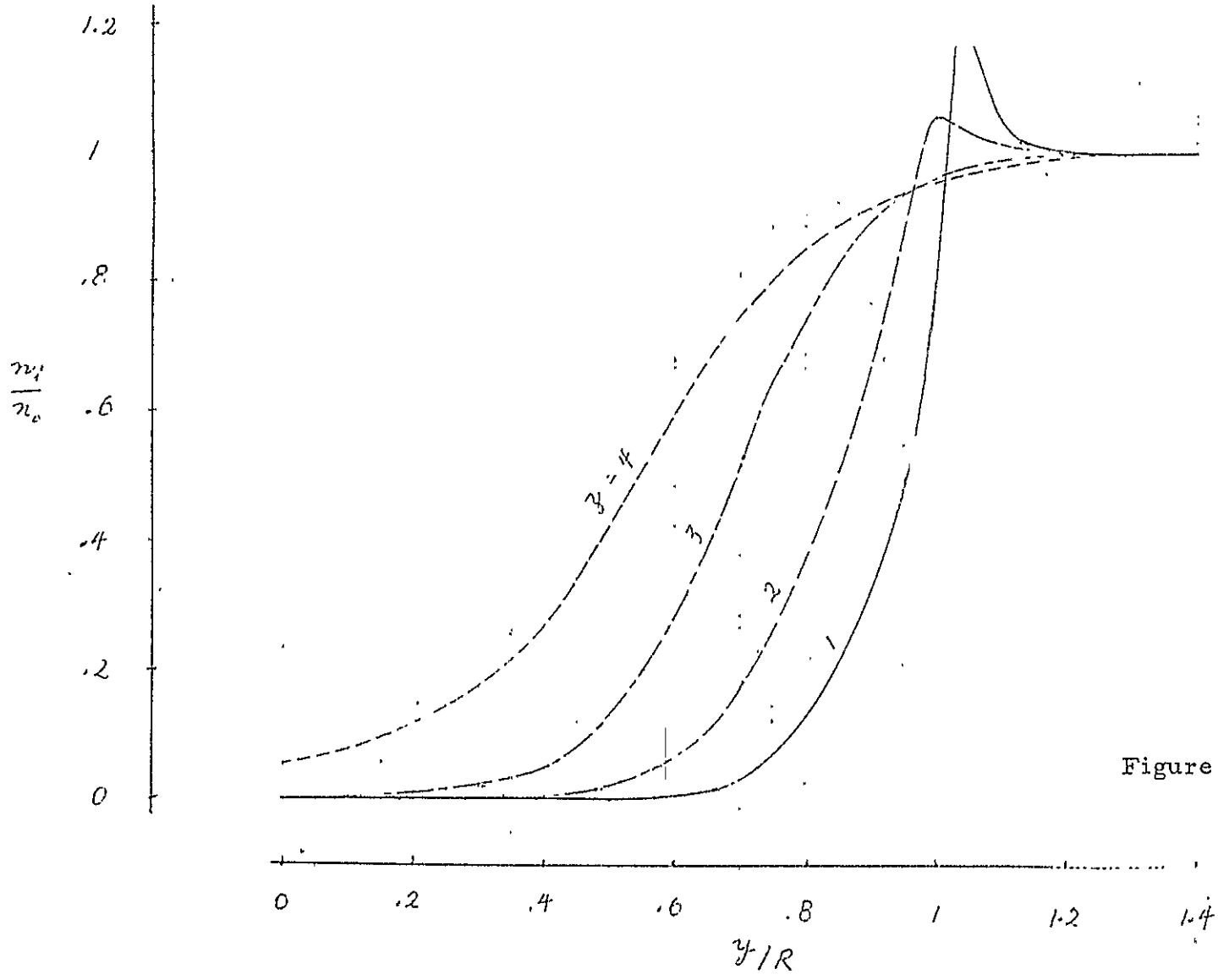

Figure 46 - $(20, 1, 8, -5)_c$

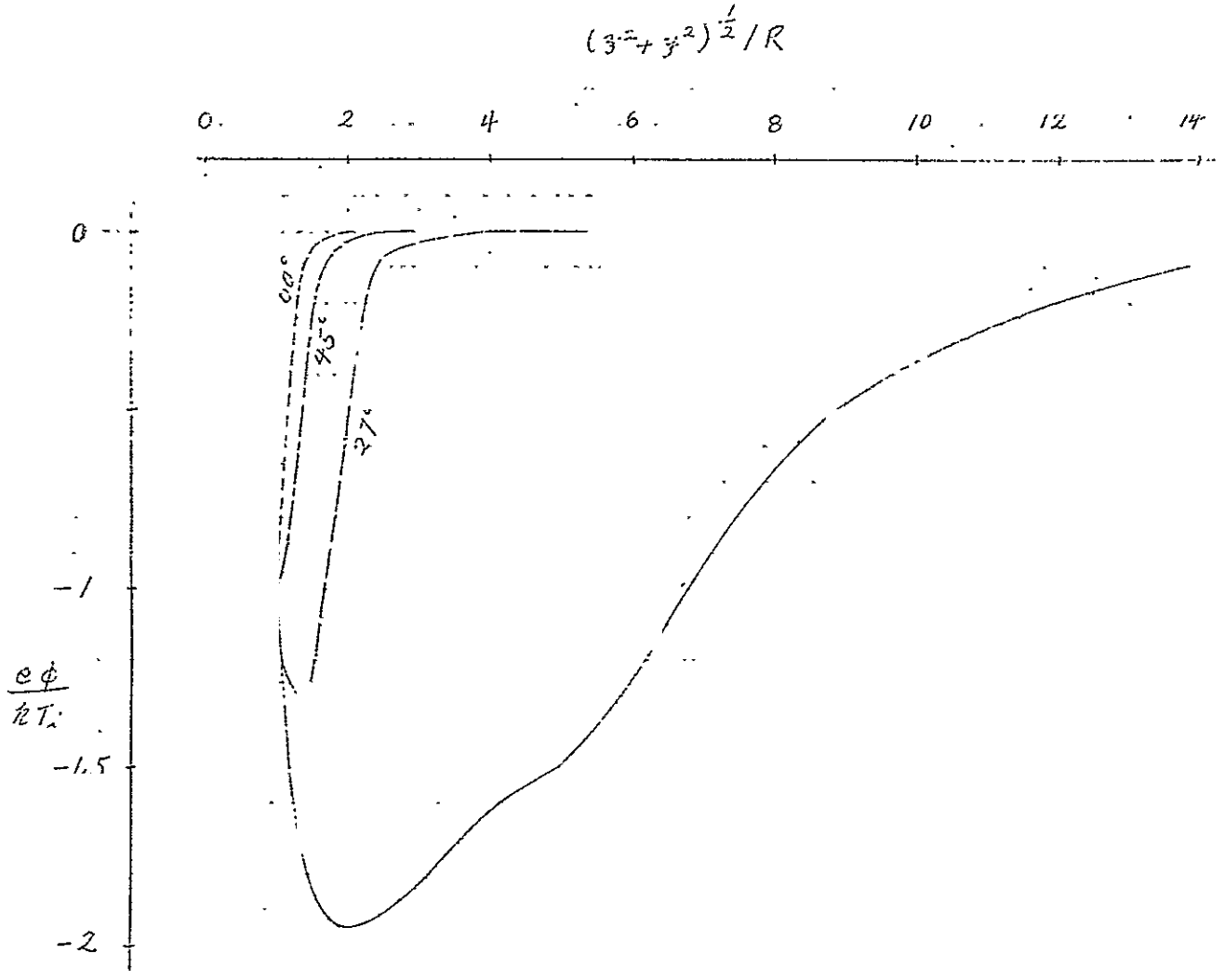

Figure 47 - (5, 1, 8, -1)$_c$

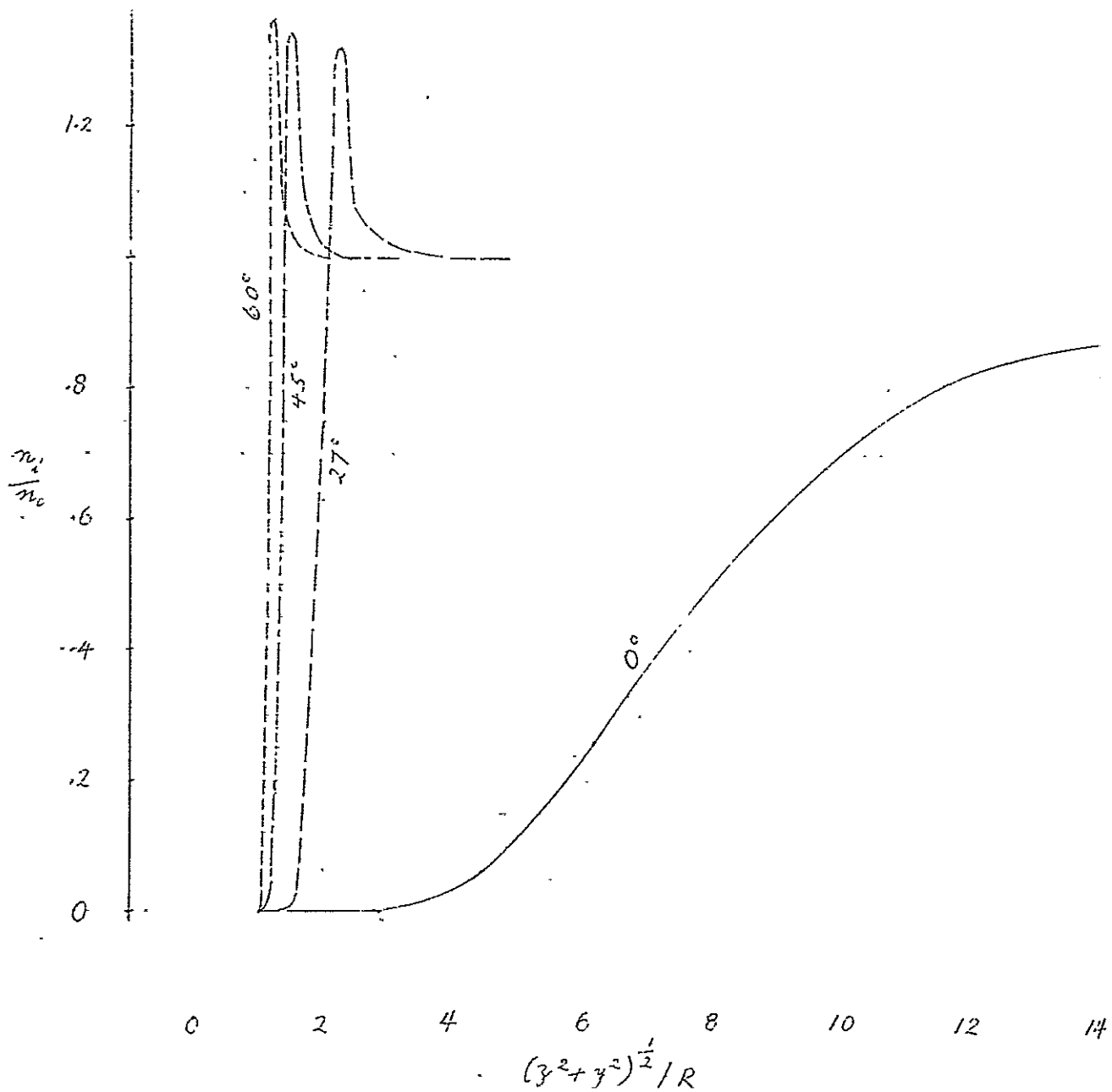

Figure 48 - (5, 1, 8, -1)$_c$

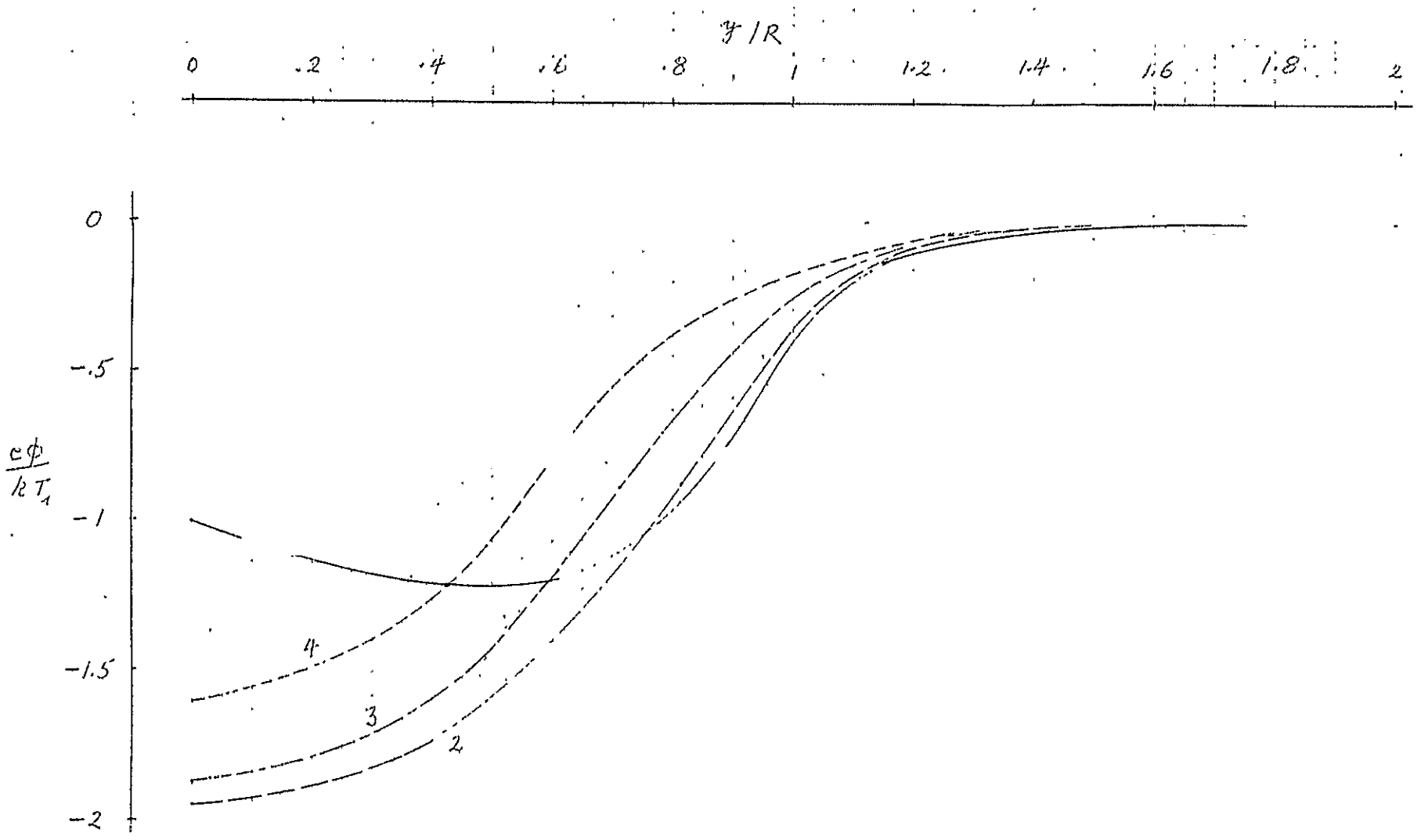
y/R
0
.2
.4
.6
.8
1
1.2
1.4
1.6
1.8
2
eφ/kT₁
0
-.5
-1
-1.5
-2
4
3
2

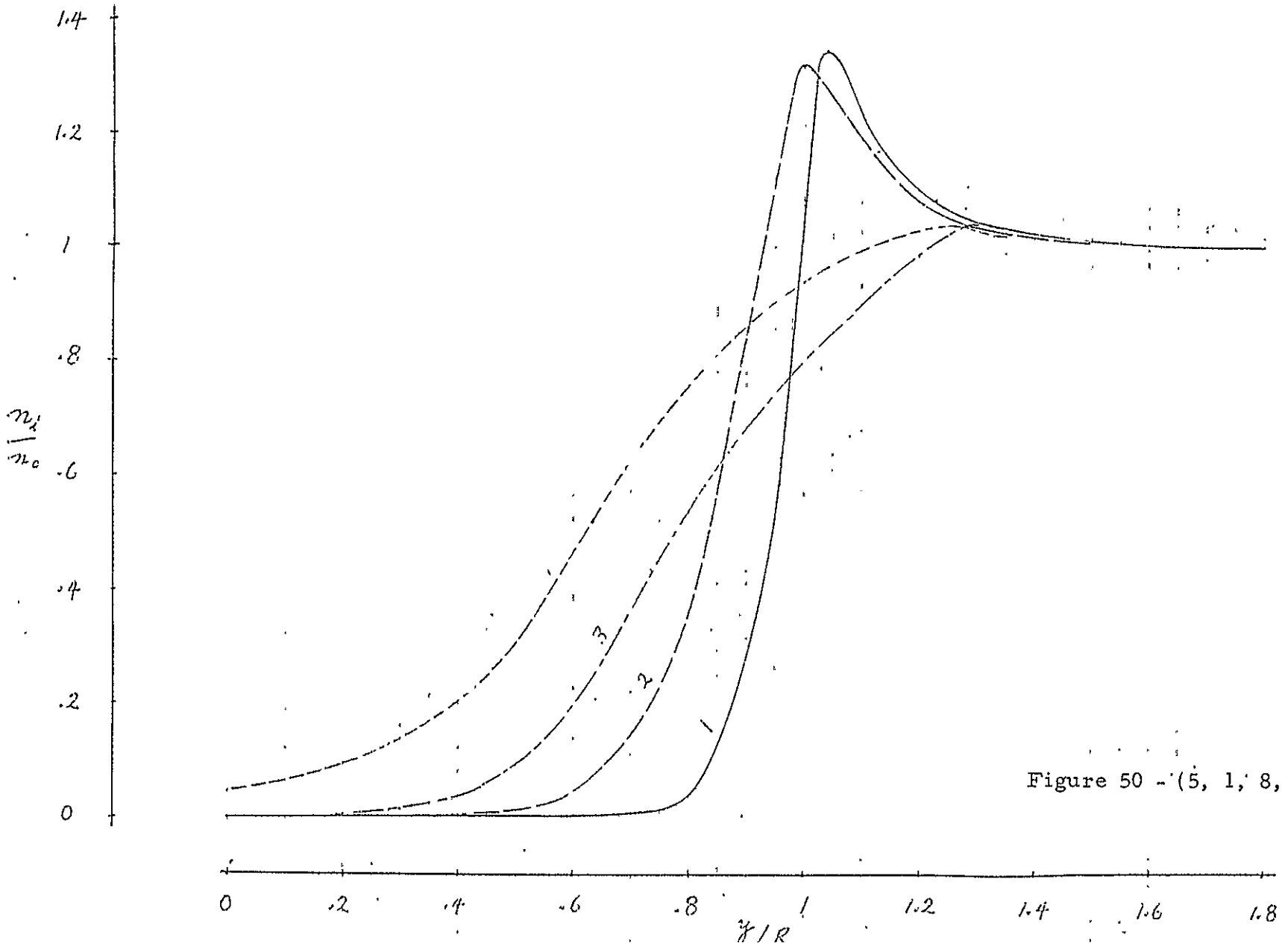

Figure 50 - $(5, 1, 8, -1)_c$

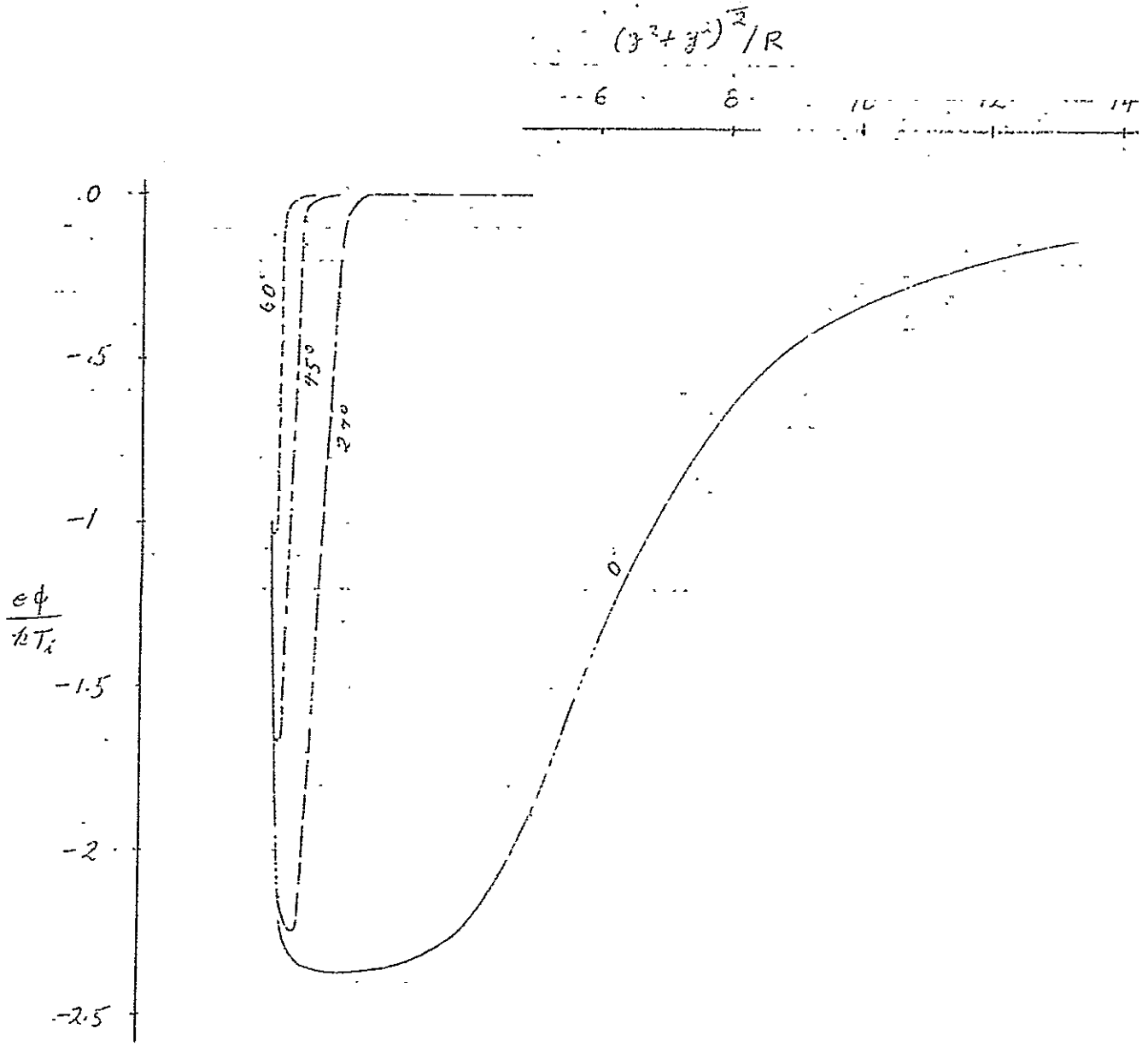

Figure 51 - (20, 1, 8, -1)$_c$

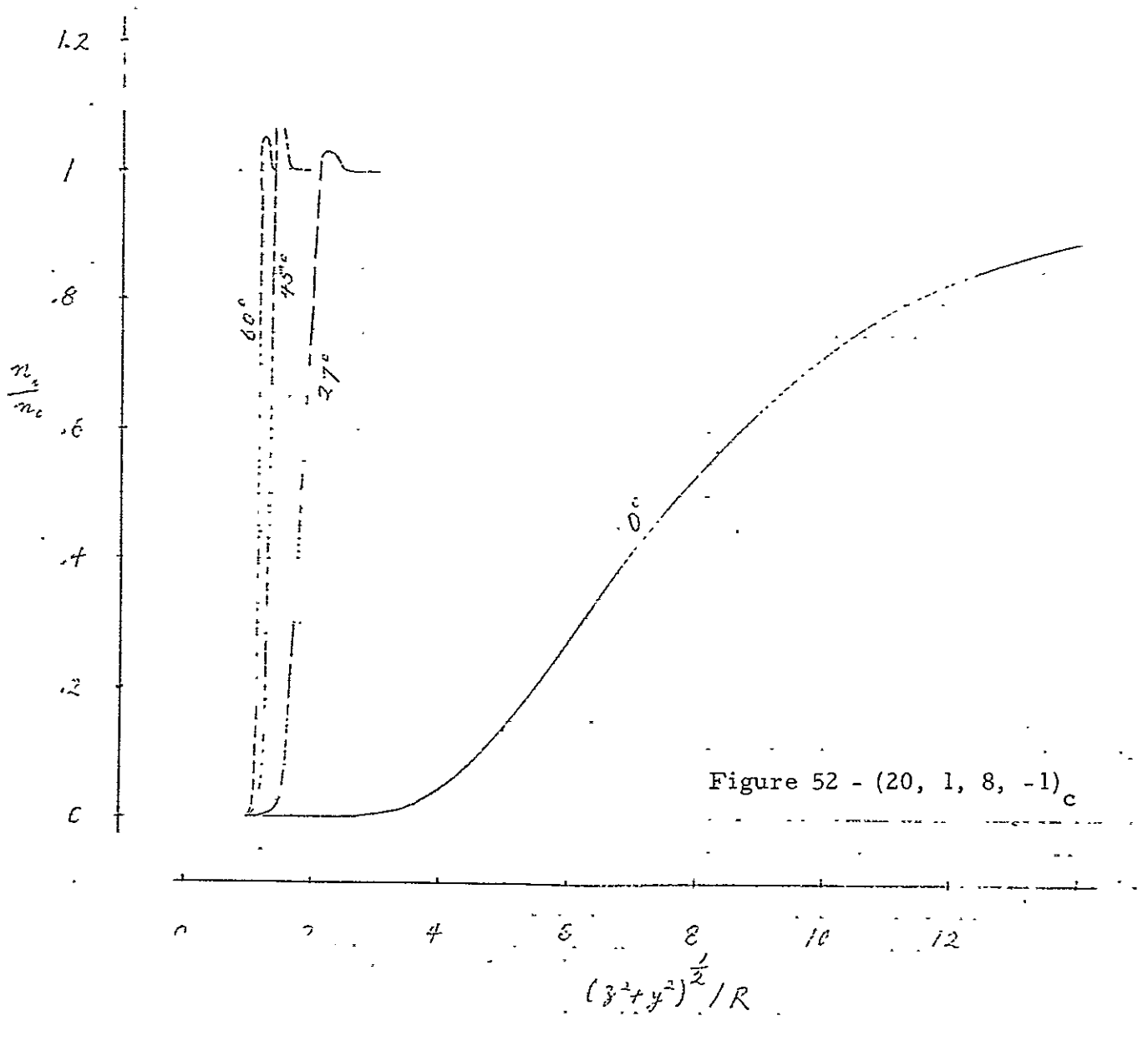

Figure 52 - $(20, 1, 8, -1)_c$

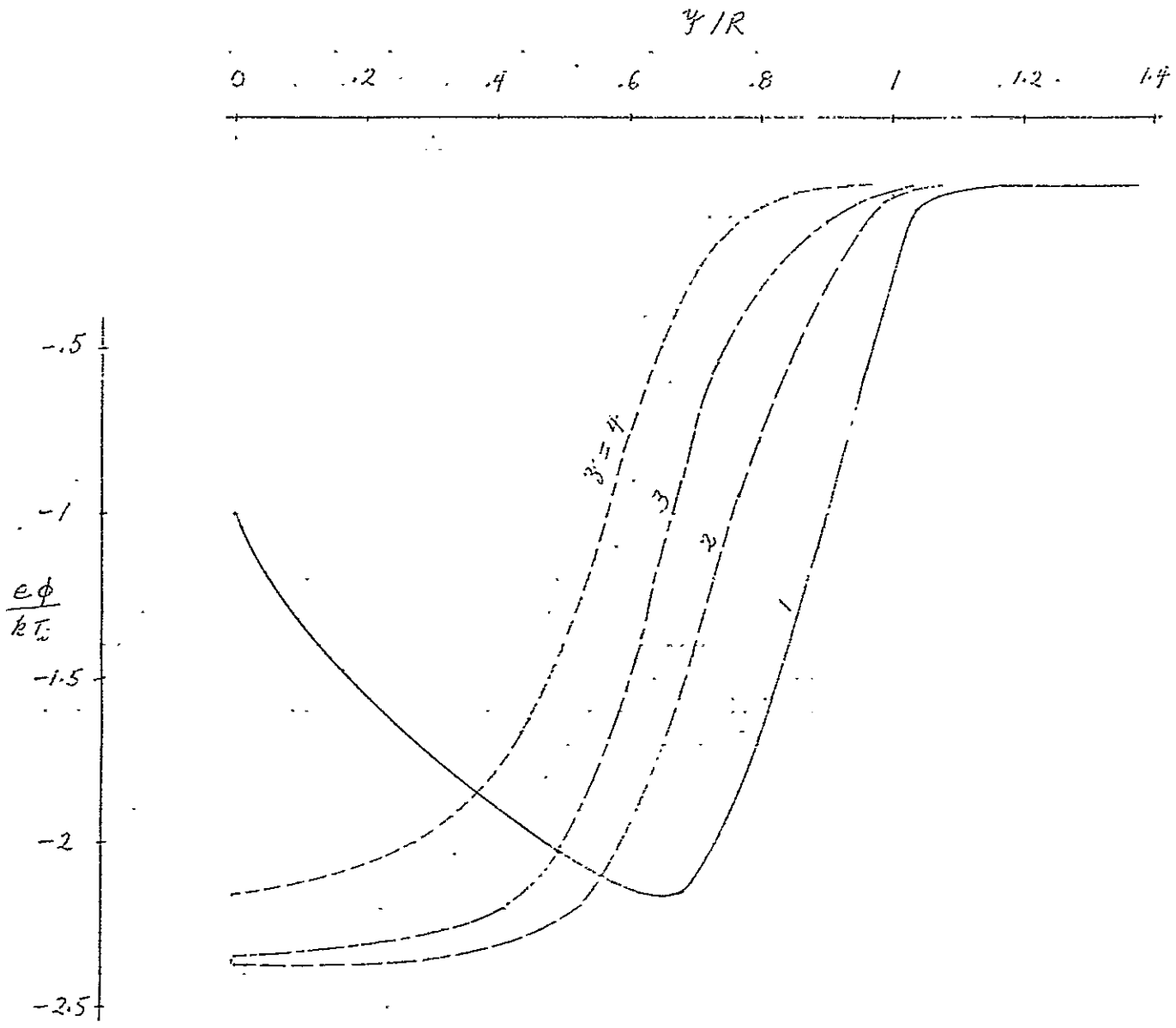

Figure 53 - $(20, 1, 8, -1)_c$

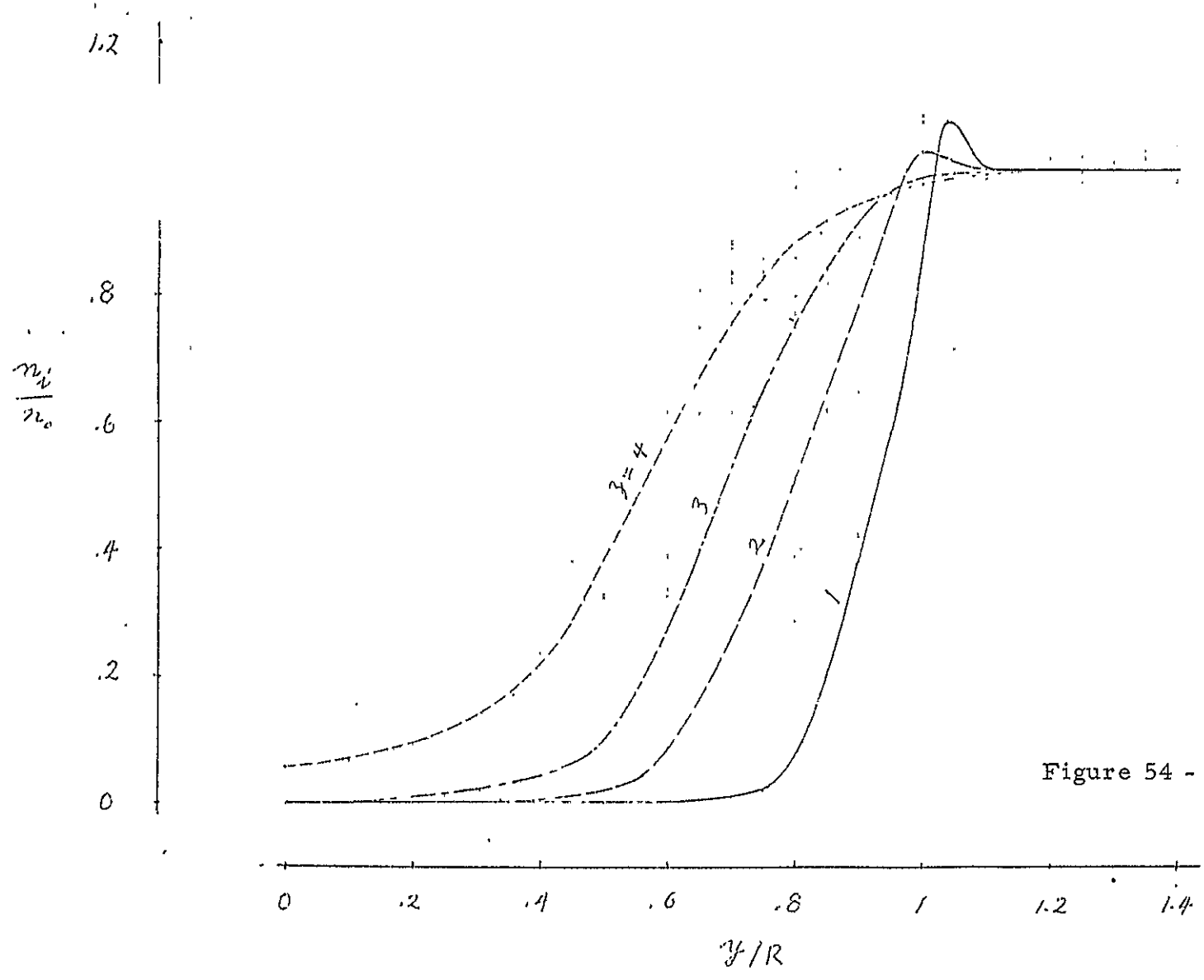

Figure 54 - $(20, 1, 8, -1)_c$

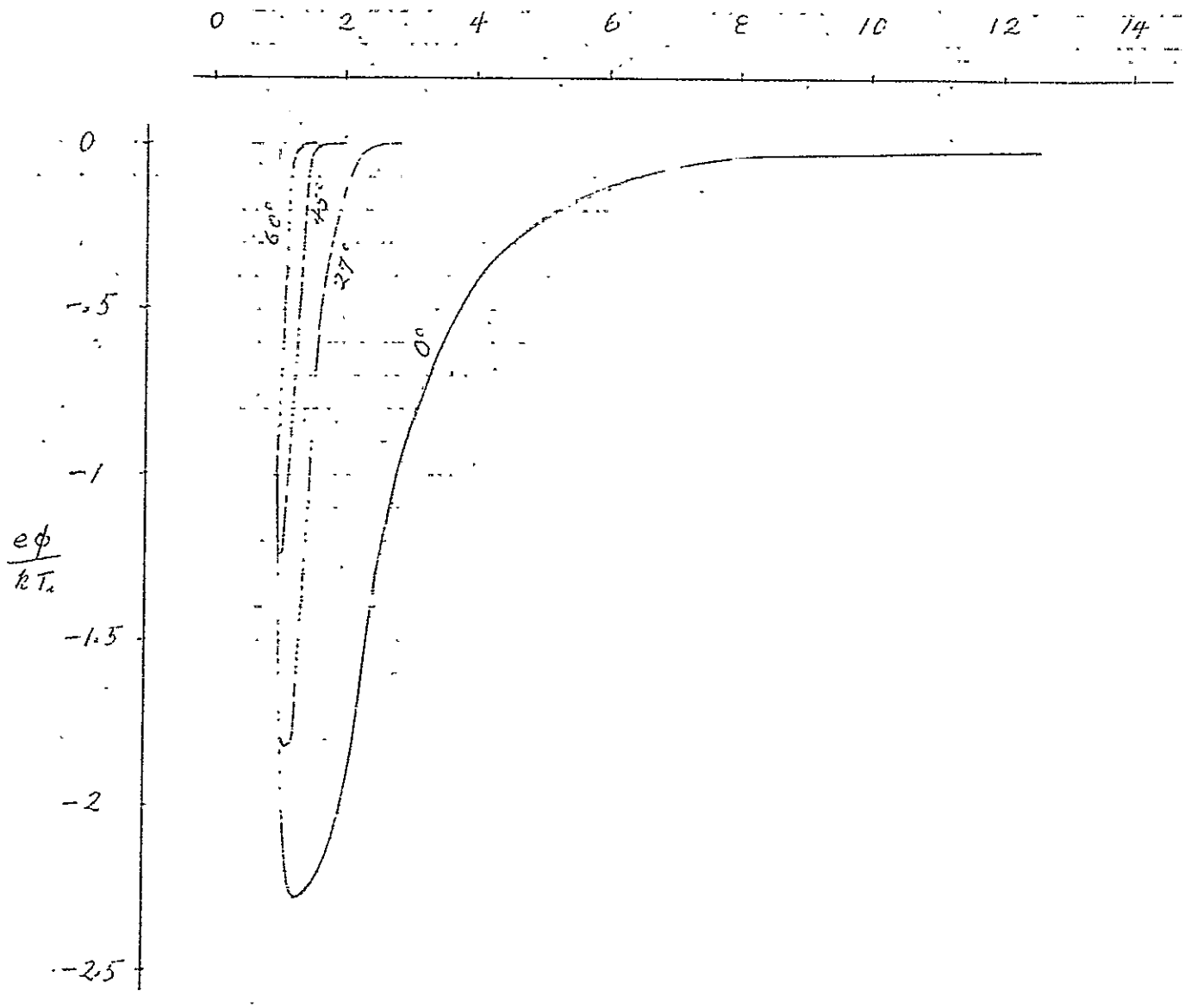

Figure 55 - $(20., 1, 4, -1)_c$

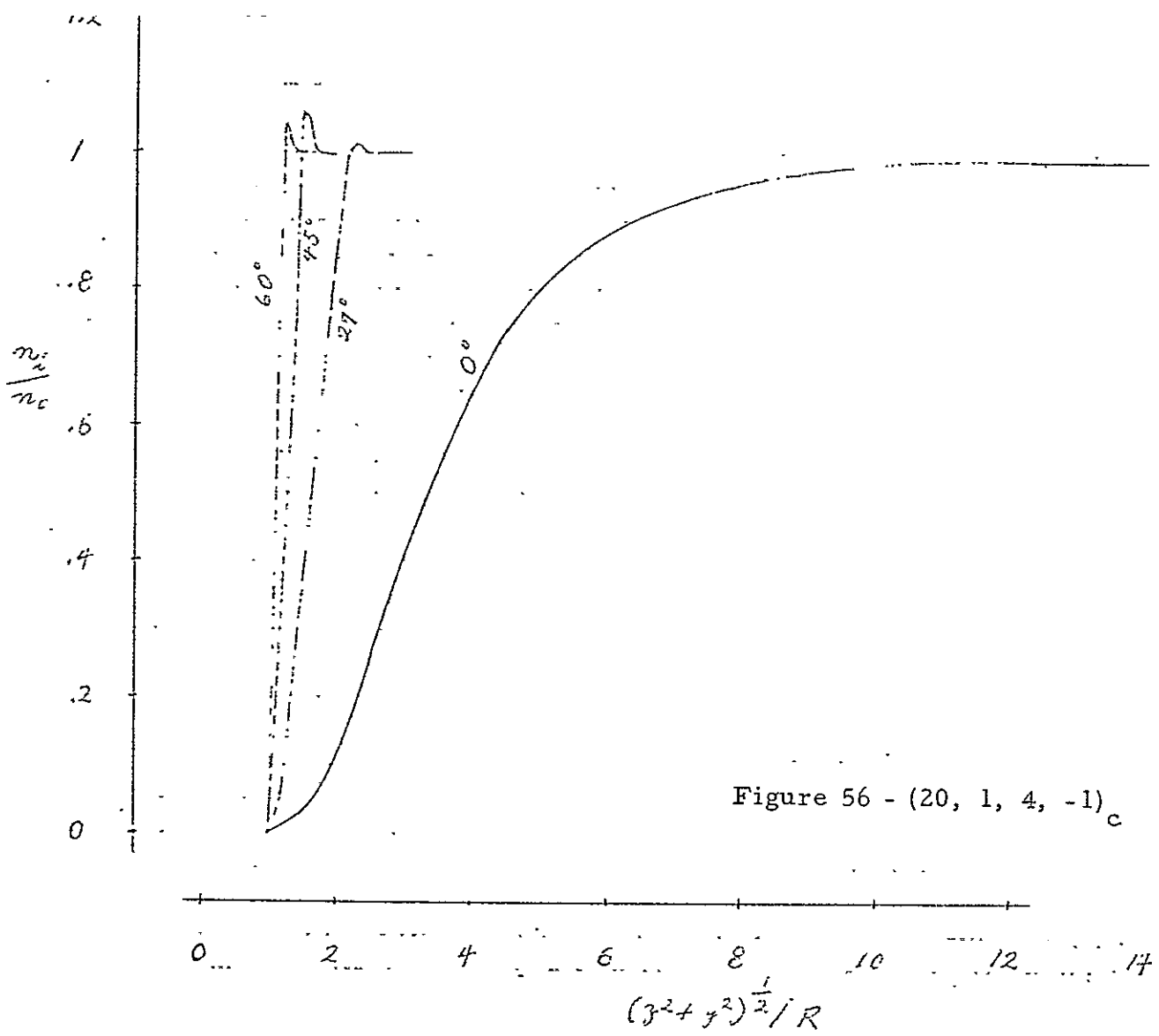

Figure 56 - $(20, 1, 4, -1)_c$

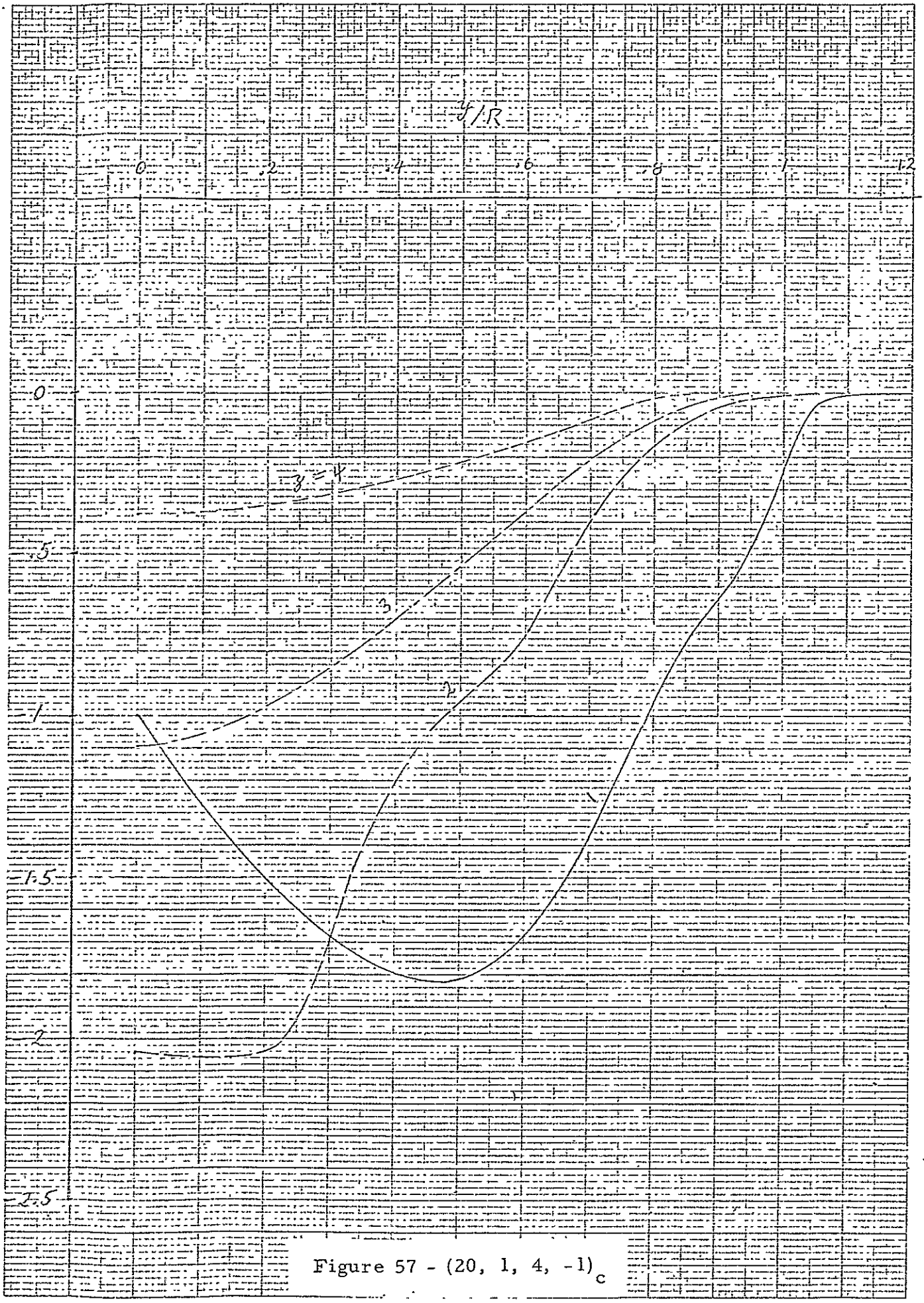

Figure 57 - $(20, 1, 4, -1)_c$

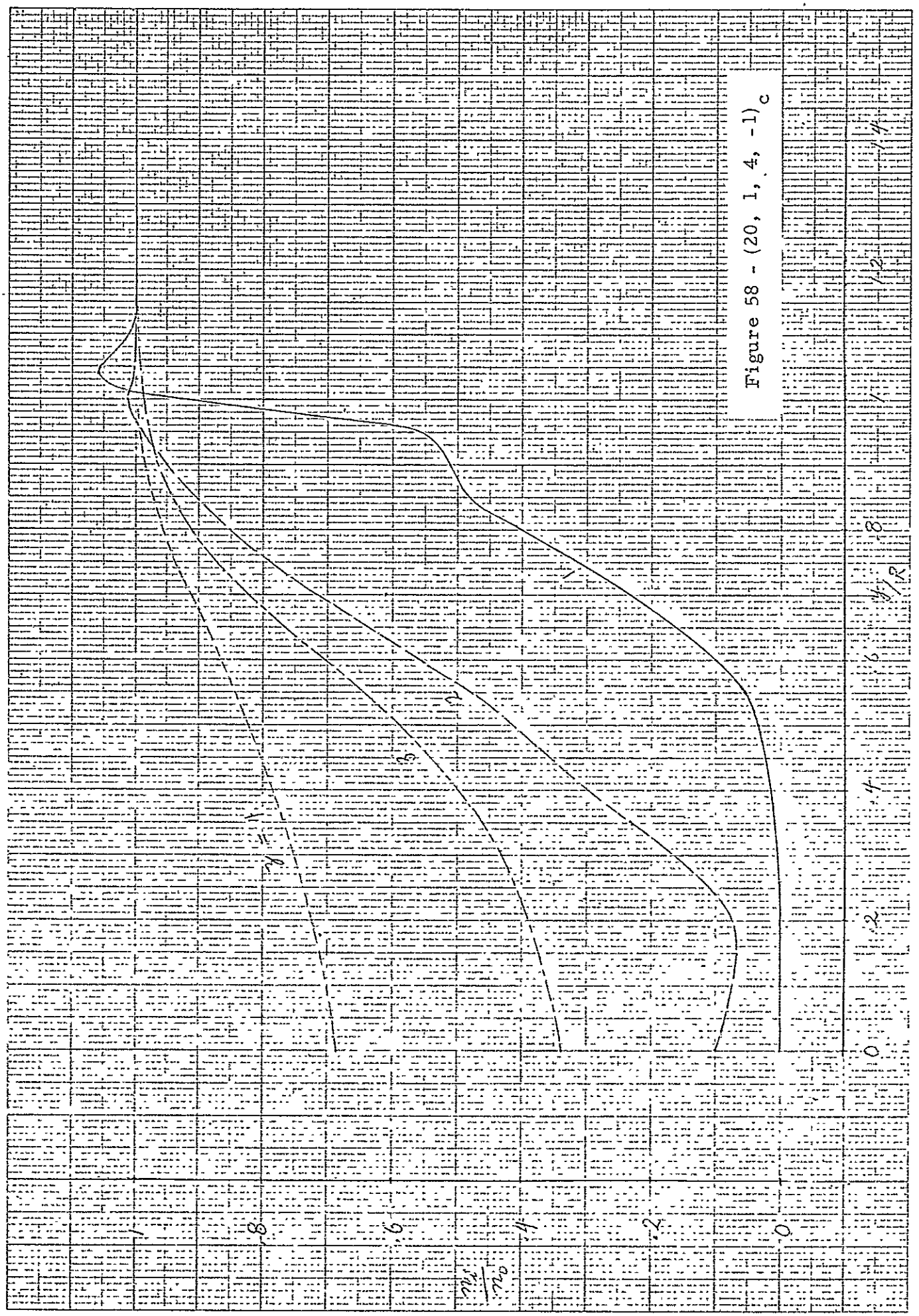

Figure 58 - $(20, 1, 4, -1)_c$

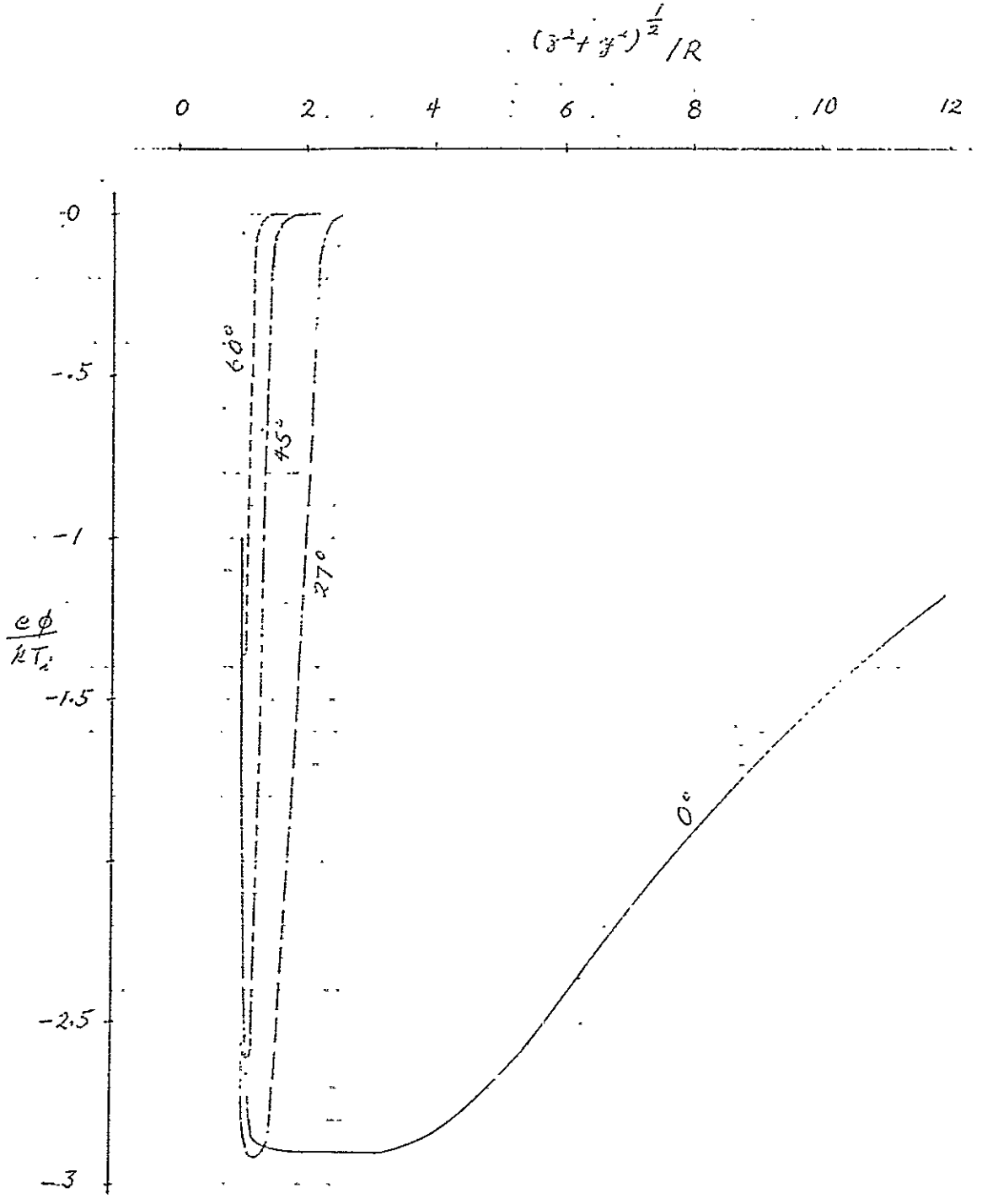

Figure 59 - $(20, 5, 8, -1)_c$

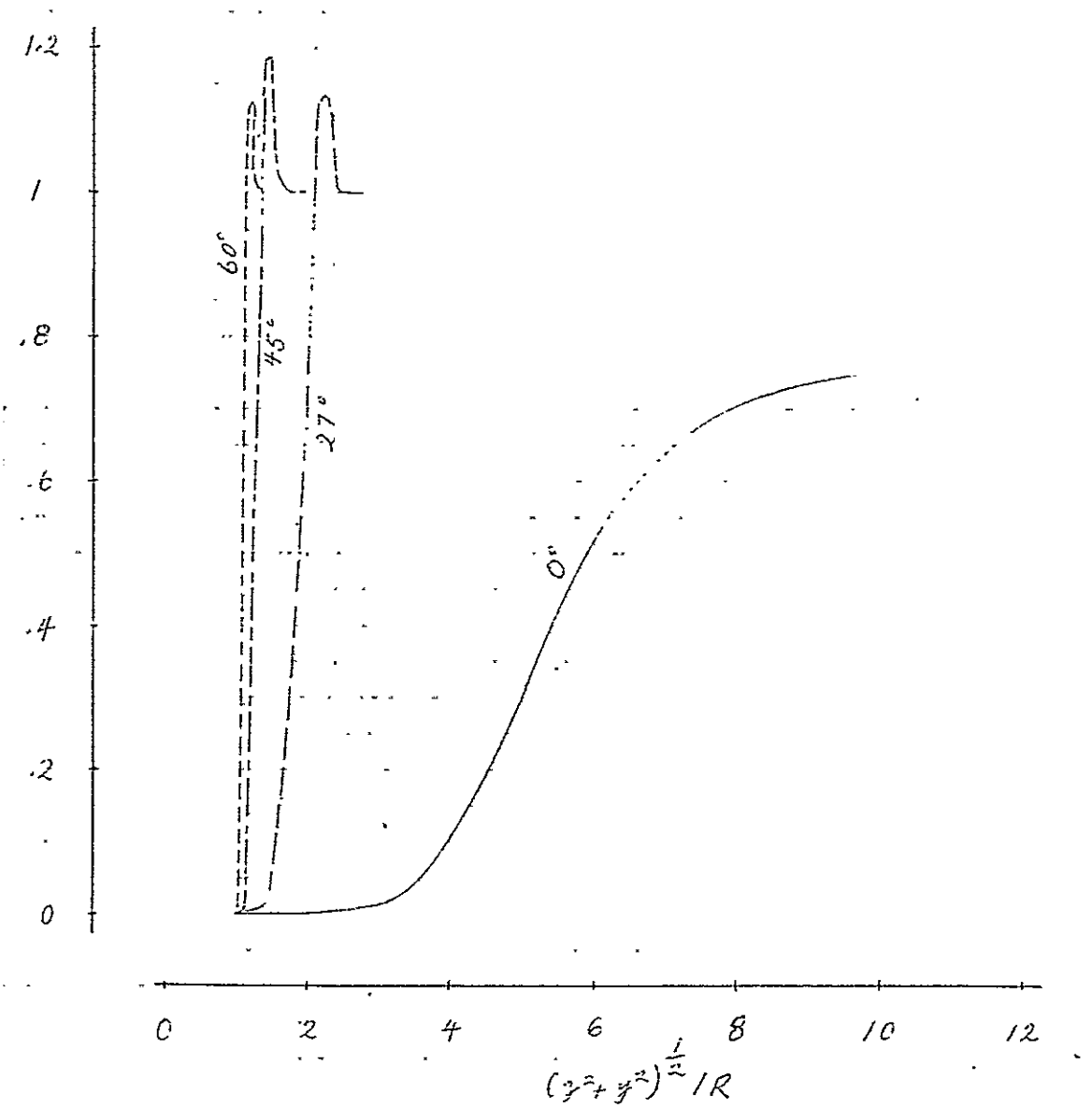

Figure 60 - $(20, 5, 8, -1)_c$.

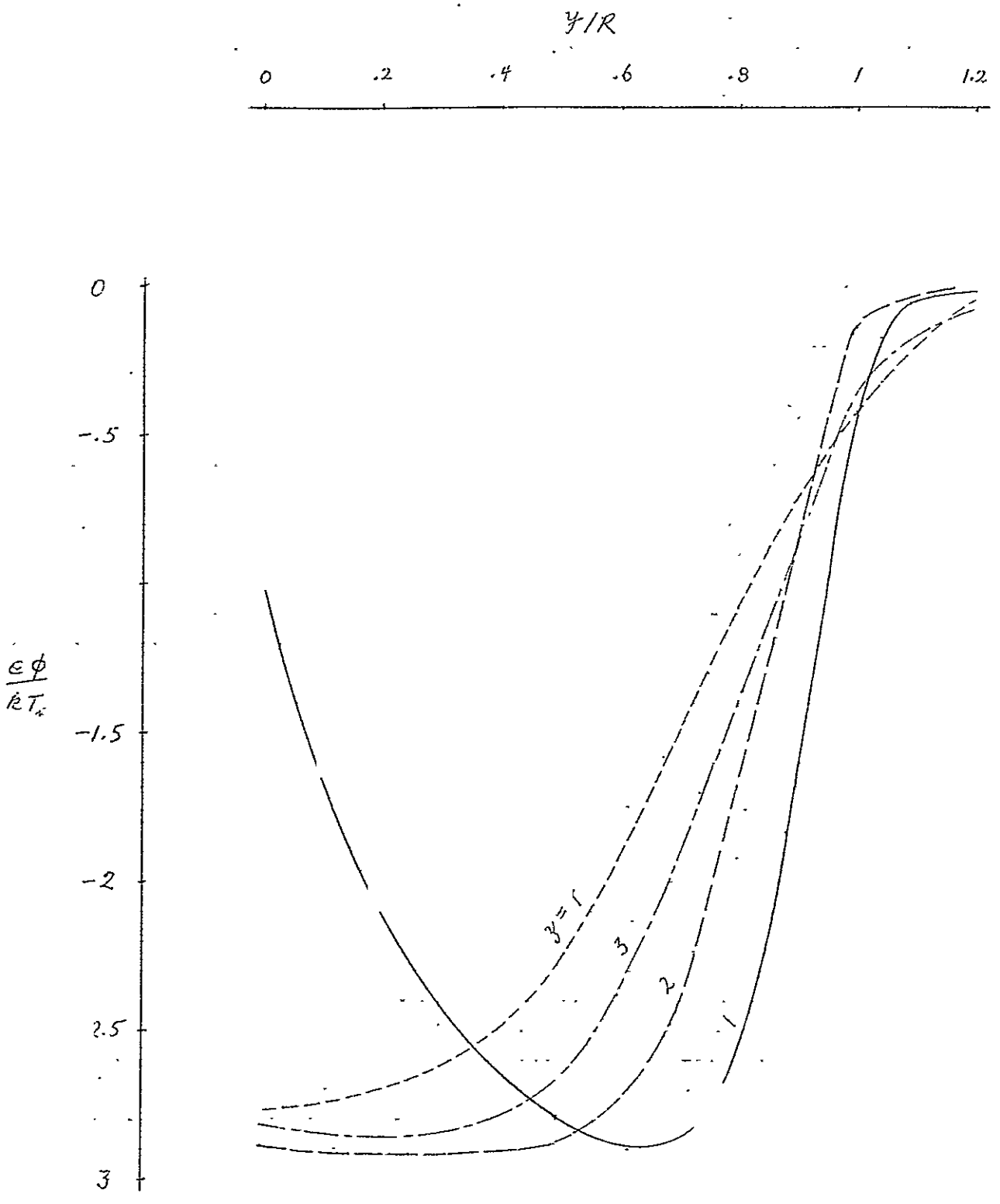

Figure 61 - $(20, 5, 8, -1)_c$

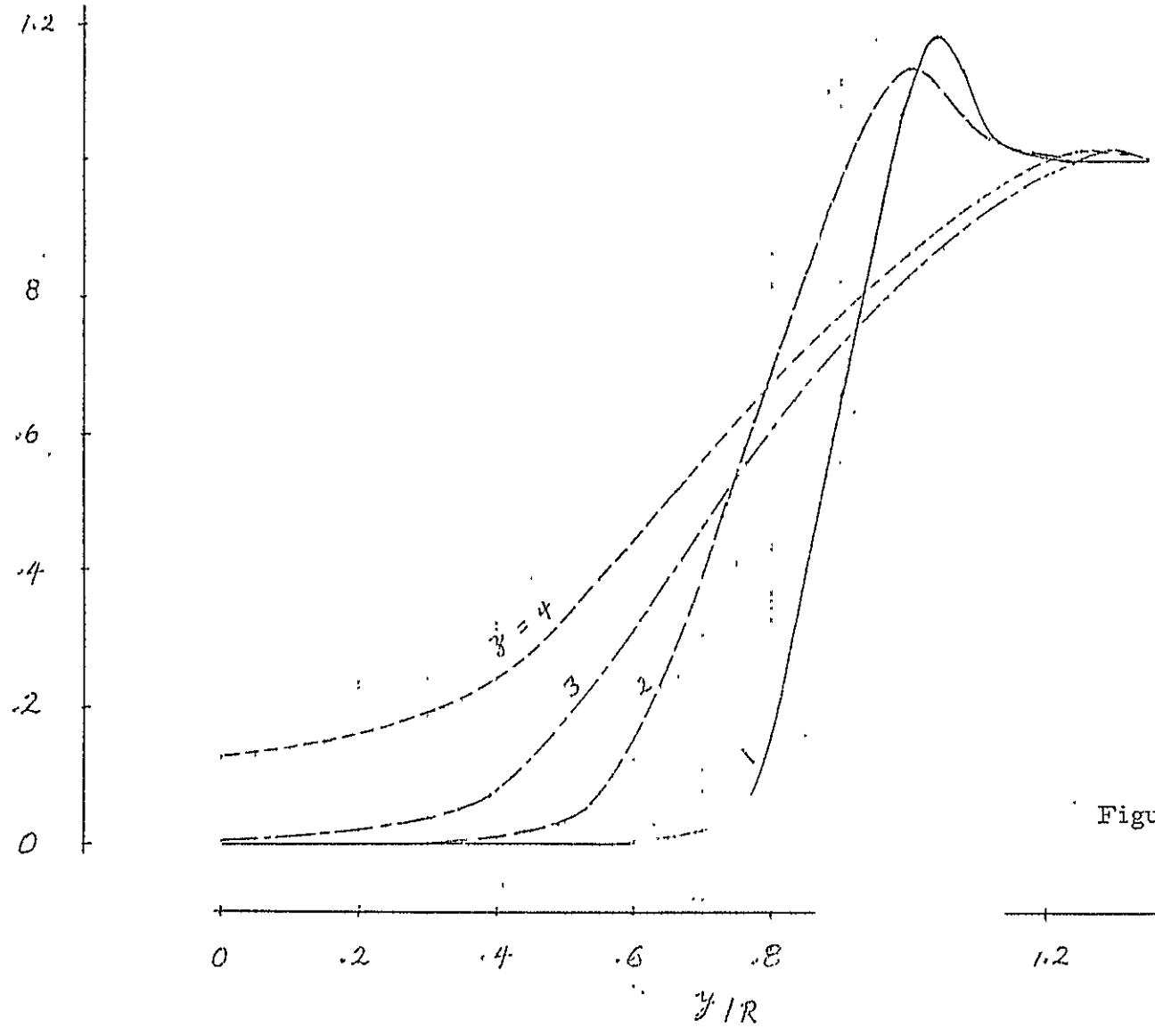

Figure 62 - $(20, 5, 8, -1)_c$

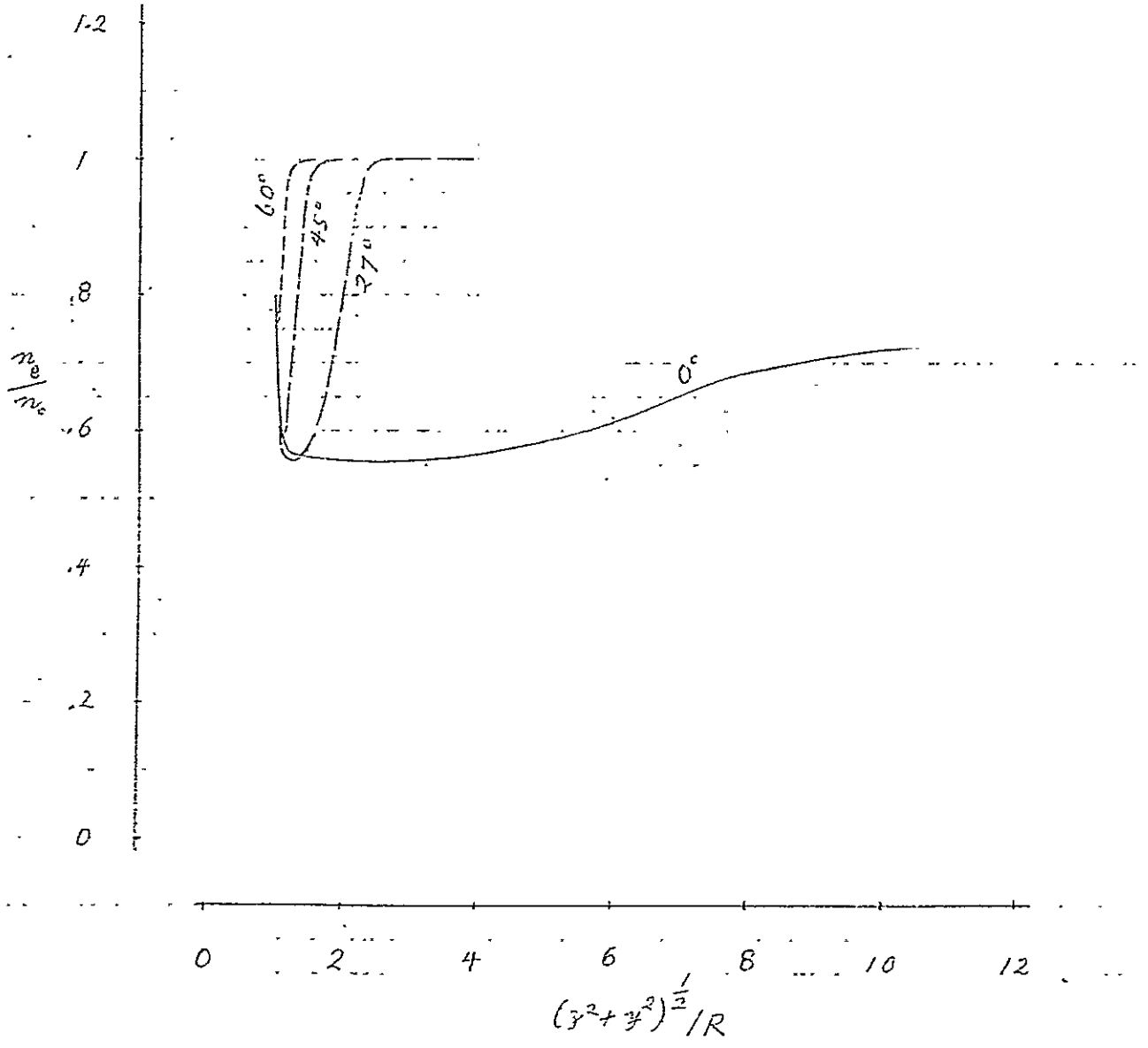

Figure 63 - electron density (n_e/n_o)
$(20, 5, 8, -1)_c$

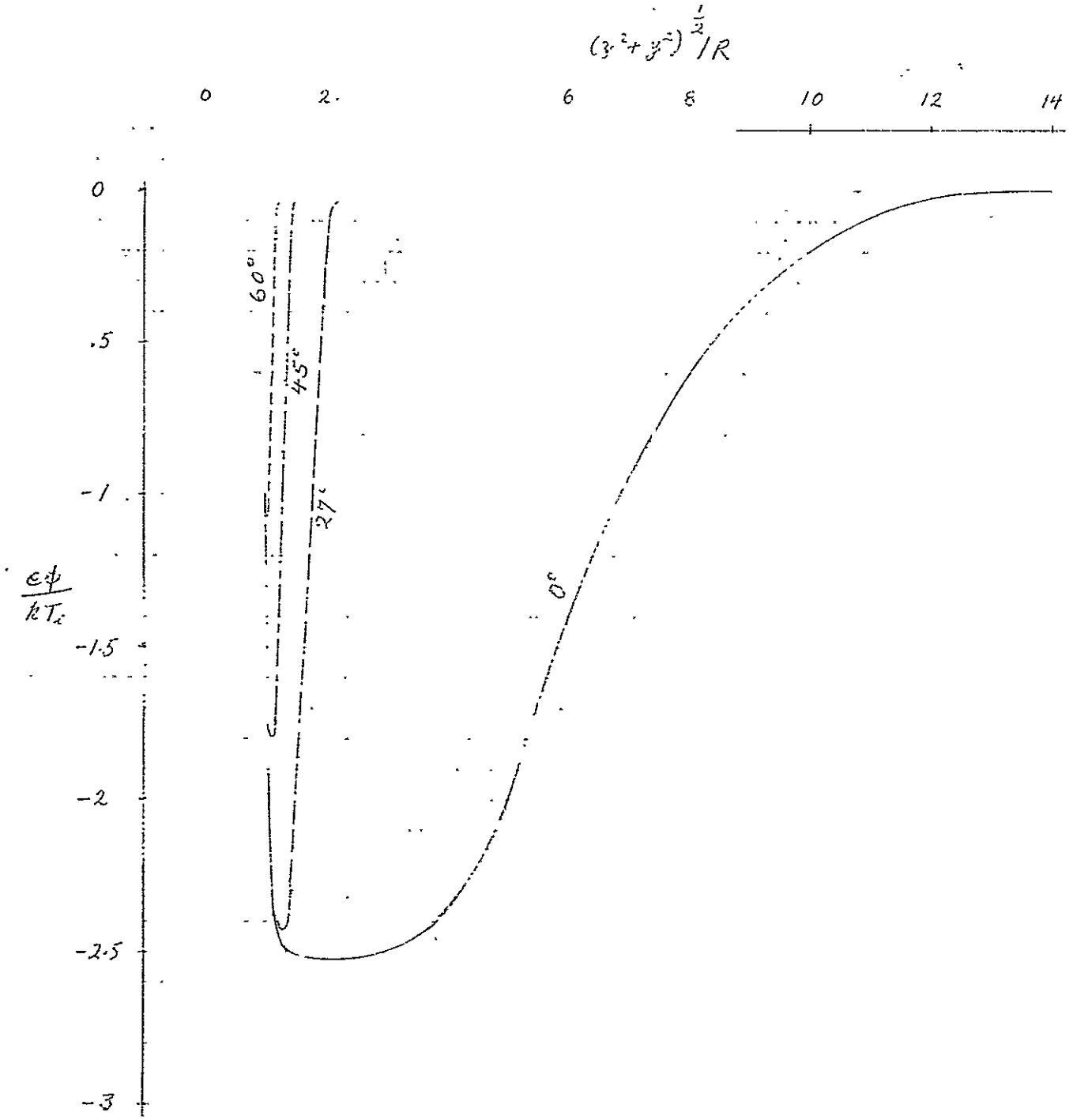

Figure 64 - $(20, 1.2, 8, -1)_c$

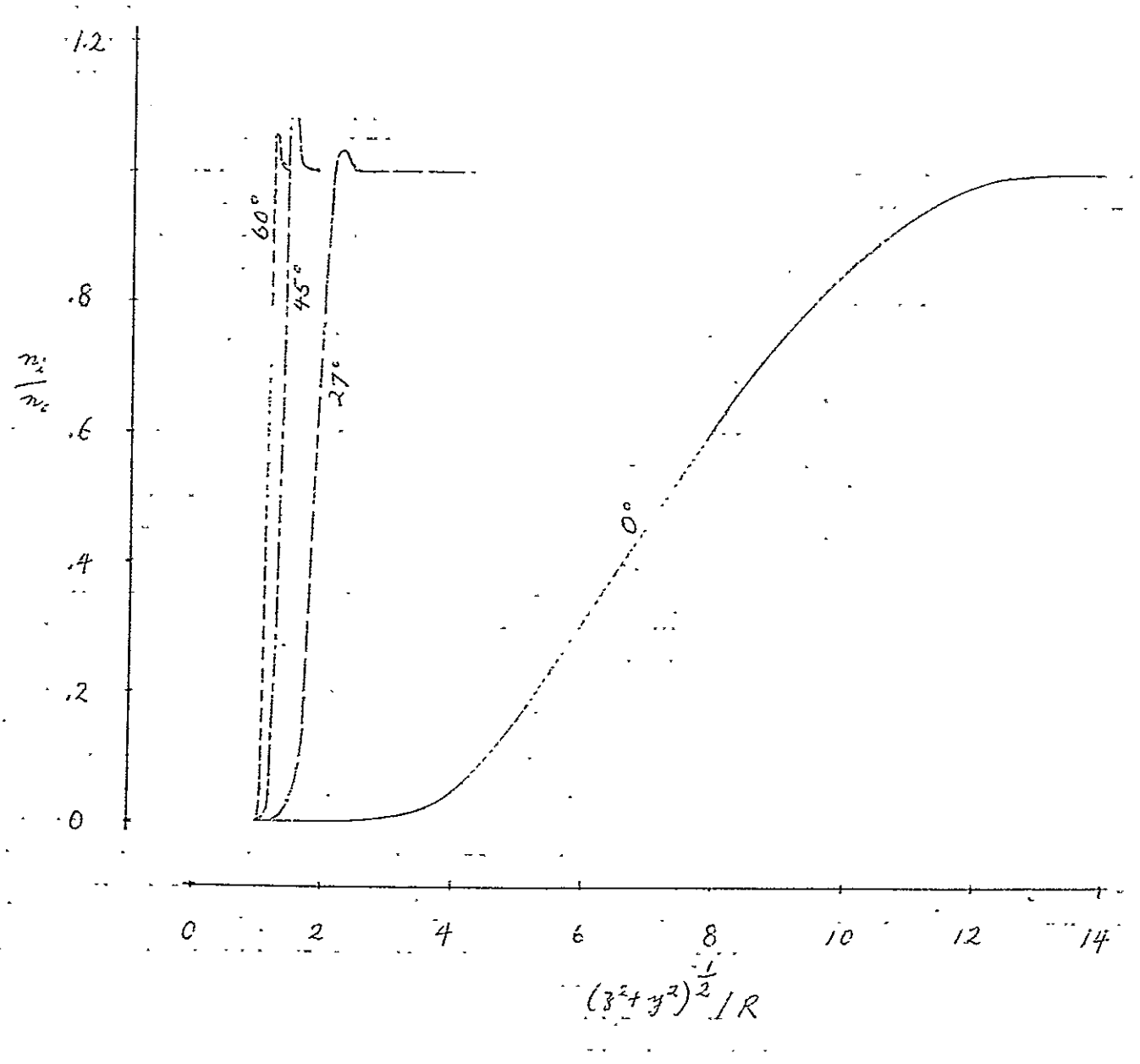

Figure 65 - (20, 1.2, 8, -1)

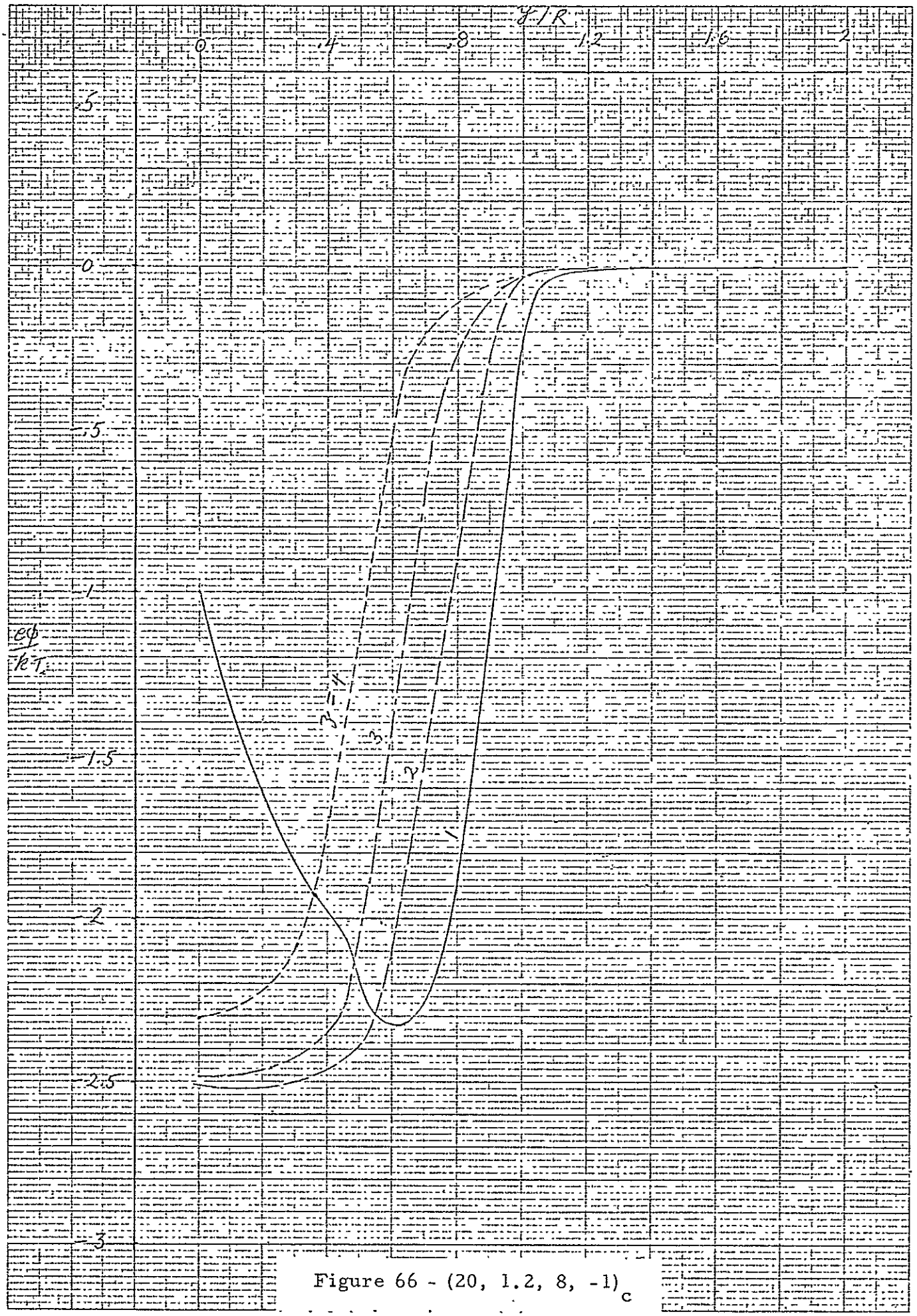

Figure 66 - $(20, 1.2, 8, -1)_c$

Figure 67 - $(20, 1.2, 8, -1)_c$

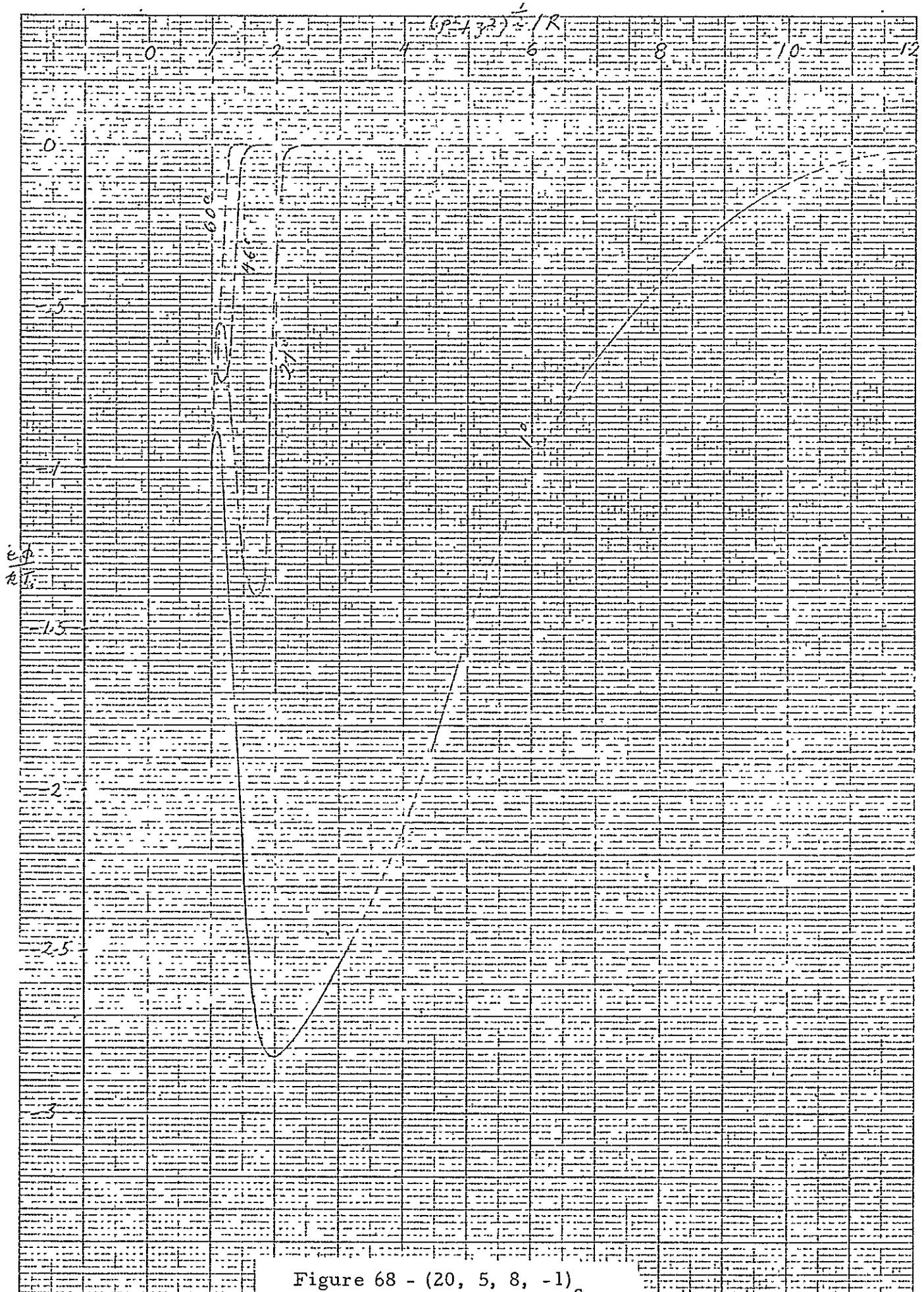

Figure 68 - $(20, 5, 8, -1)_s$

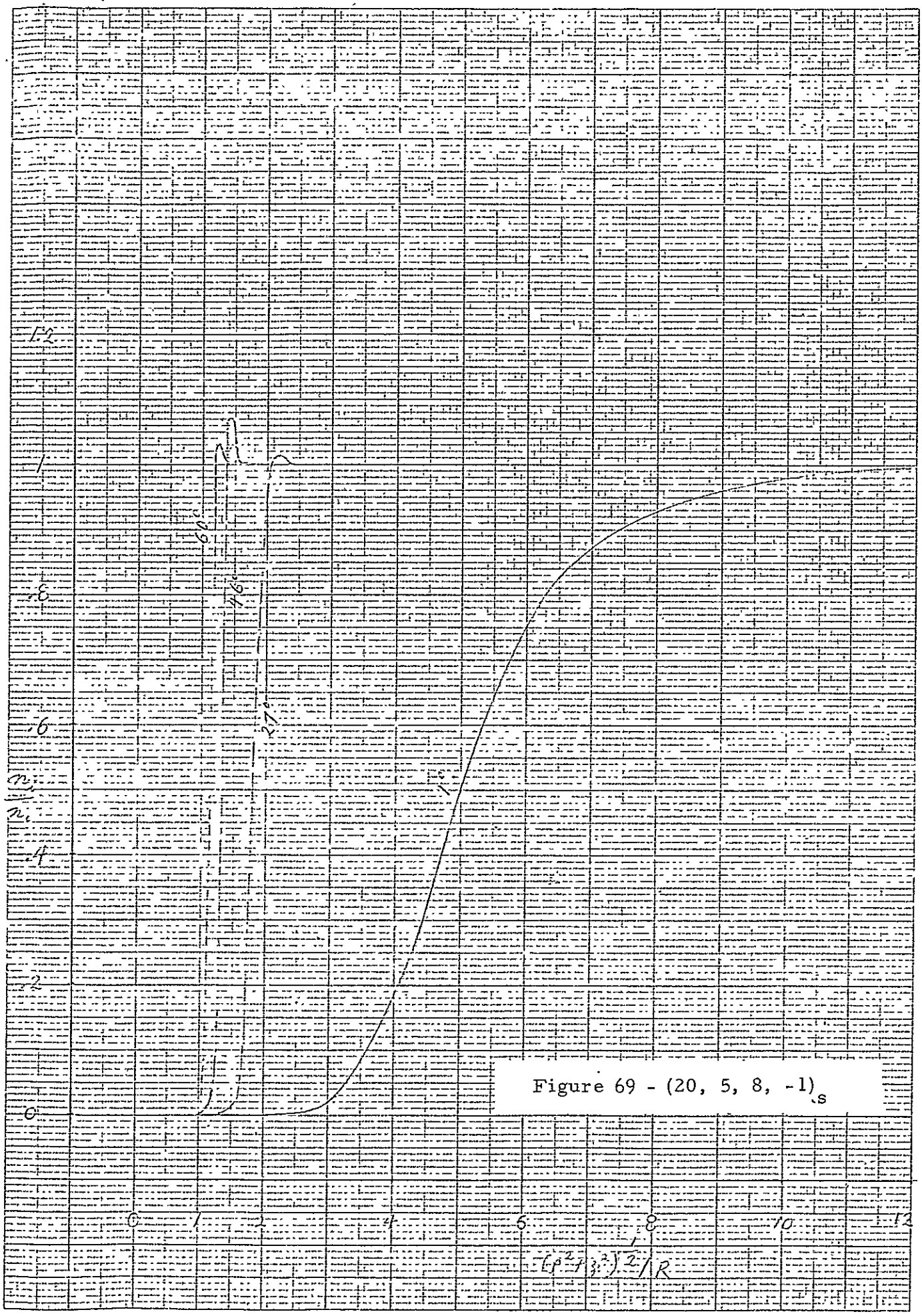

Figure 69 - $(20, 5, 8, -1)_s$

Figure 70 - $(20, 5, 8, -1)_s$

Figure 71 - $(20, 5, 8, -1)_s$

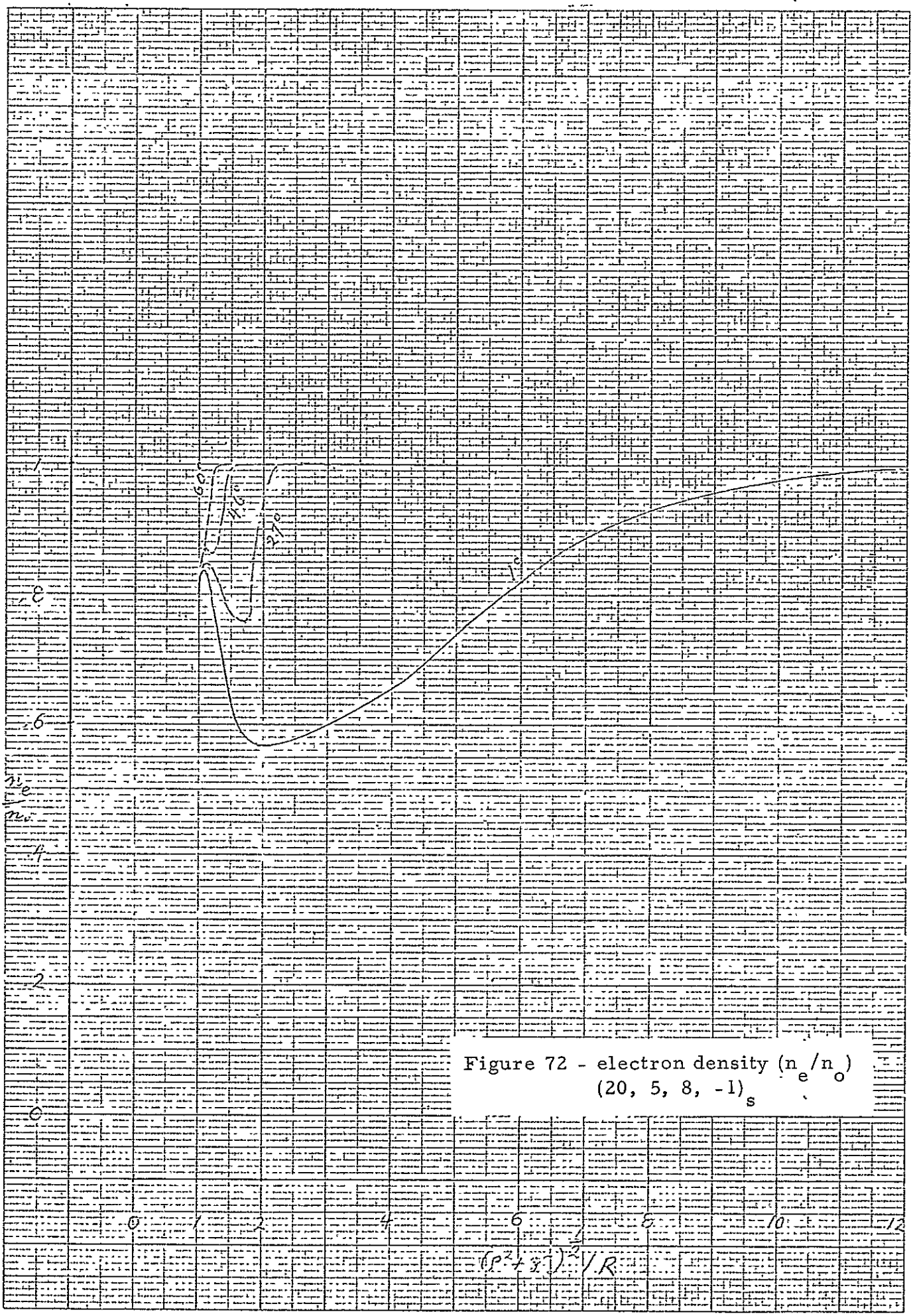

Figure 72 - electron density (n_e/n_o) $(20, 5, 8, -1)_s$

to follow Maxwell-Boltzmann distribution, namely, $n_e = n_o \exp(T_i \phi^*/T_e)$ where n_o denotes the ambient electron density; ϕ^*, the local electric potential (normalized); hence, n_e is not tabulated here.

It is of interest to describe some of the significant conclusions of the present calculations: (1) It is found that the distributions of both the particles (n_i and n_e) and the potential (ϕ^*) are insensitive to the change of R/d as long as $R/d \gg 1$; e.g. the difference in the solutions for $R/d = 20$ and $R/d = 100$ is negligible. (2) As long as $R/d \gg 1$, there is always a pronounced potential well of negative voltage present in the wake at a distance of $(1 - 2)R$ from the rear surface of the body. Even with $R/d = 1$, there is a potential well of mild intensity in the wake. The theoretical prediction of the presence of this potential well has led to the hypothesis of trapped particles in the wake which might explain the anomalous plasma oscillations in the wake. (For details see Appendix D.) ($\phi^* = e\phi/kT_i$)

V. Illustration of Applications

The procedure for the use of the present manual in prediciting the disturbances in distributions of particles and potential near a moving satellite can be illustrated by an example. Consider a satellite with a configuration as shown in Figure (72). It consists of two spheres A and C which are connected by a long cylindrical rod of radius R_3, all of which has a normalized surface potential of $\phi_S = -1\ (kT_i/e)$ volts.

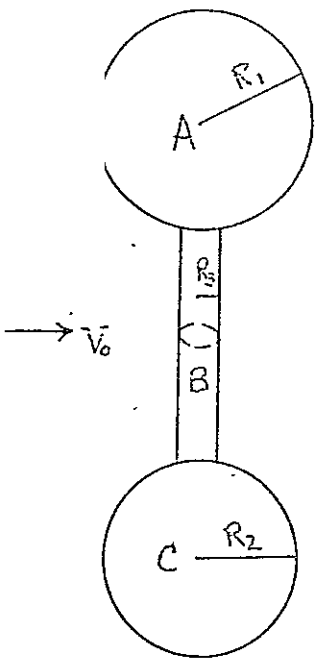

Figure 73

It is assumed that the satellite is orbiting at an altitude of 600 Km. It is of interest to know the distributions of charged and neutral particles and also the electric potential near the satellite.

The procedure to determine the quantities of interest can be stated as follows:

(a) neutral particle distribution - The configuration of Figure (73) is resolved into three components: spheres A and C, and cylinder B. It is noted from the figures of computed solutions of neutral particles Figures (5 - 16) that the parameter of primary interest is the free stream speed ratio V_o/v_{th}. The thermal speed (v_{th}) of the ambient particles is estimated, by using Table I, to be 1.5×10^5 cm/sec. Thus, V_o/v_{th} can be easily obtained. Knowing V_o/v_{th}, the particle distributions around the components A, B, and C can be determined by the use of formulas in Section II and Figures (5 - 16).

To combine the component distributions for the composite distribution pertinent to Figure (73), we take the mean value of the distributions in the overlapped regions. It is believed that with the satellite speed ratio which is in the order 10, the suggested means

of treating the mutual interference effect should be accurate within ±10%.

(b) charged particle distribution - To evaluate the ion and electron distribution and the electric potential around the satellite, Figure (73), by the use of Figures (19 - 58), we must first determine the following parameters:

(1) R/d where d, the Debye length is given in Table I, $d \approx 0.5$ cm, hence, the ratios of R/d for components A, B, and C are estimated to be in the order $R/d \approx 20$ if R = 10 cm. Since the results will not be sensitive to the values of R/d as long as $R/d \gg 1$, hence the order R/d = 20 is close enough.

(2) The temperature ratio T_e/T_i must be estimated for practical estimation, take $T_e/T_i = 1$, unless T_e/T_i is known to be much larger than 1. There is, however, only a limited case of calculations given for $T_e/T_i \neq 1$. See e.g. Figures(59 - 72).

(3) To determine the speed ratio V_o/v_i, we use Table I to obtain the ion thermal speed $v_i \approx v_{th}(\text{neutral}) \approx 1.5 \times 10^5$, then to estimate V_o/v_i from the given value for V_o, the satellite speed.

(4) The surface potential (ϕ_S^*), as well as the other electric potential ϕ^* given in the figures are all normalized by the quantity kT_i/e. Knowing T_i from Table I (usually it is assumed $T_i = T$, the kinetic temperature of neutral particles), the quantity kT_i/e can be calculated, e.g. with $T = 2000^{\circ}K$, $kT_i/e = 1.72$. $(\phi_S^* = e\phi_S/kT_i)$

With the four parameters $(R/d, T_e/T_i, V/v_i, \phi_S^*)$ prescribed as shown above, we can use Figures(19 - 58) to determine the ion

density n_i and potential ϕ^* behind the components A, B, and C, respectively. The corresponding electron density n_e can be calculated from the use of Maxwell-Boltzmann law, namely $n_e = n_o e^{\phi^*}$, where n_o is the ambient electron density which is shown in Table I.

To combine the component solutions for the composite configuration of Figure(73) we again take the mean value of corresponding quantities in the overlapped regions to reduce the mutual interference effects. It is believed that the results so obtained should be accurate within ±15% of the true solution with precisely prescribed parameters of R/d, T_e/T_i, V/v_i, and ϕ_S^* for the actual configuration.

The plasma sheath for the components A, B, and C can be determined by first segmenting the surfaces into small inclined planes and then using the Figures(17) and (18) for the ion density (n_i) and electric potential (ϕ^*). The electron density can be determined again by $n_e = n_o e^{\phi^*}$.

Legend of Figures 19 - 71

The cases of n_i- and ϕ-distribution in the wake of a sphere or a cylinder presented in Figures 19 - 71 are specified by four parameters (R/d, T_e/T_i, V_o/v_i, $e\phi_s/kT_i$) and a subscript "s" or "c" to denote "sphere" or "cylinder", respectively. The distributions are given in two different coordinate systems:

i) downstreams sections[see Figure I]: $z/R = 1, 2, 3, 4$ with

$(e\phi/kT_i)$ vs (ρ/R) or (n_i/n_o) vs (ρ/R) for sphere;

$(e\phi/kT_i)$ vs (y/R) or (n_i/n_o) vs (y/R) for cylinder.

ii) radial directions: $\theta = 1^o, 27^o, 46^o, 60^o$[see Figure I] with

$(e\theta/kT_i)$ vs $[(\rho^2 + z^2)^{\frac{1}{2}}/R]$ or (n_i/n_o) vs $[(\rho^2 + z^2)^{\frac{1}{2}}/R]$

for sphere; $\theta = 0^o, 27^o, 45^o, 60^o$ with $(e\phi/kT_i)$ vs $[(y^2 + z^2)^{\frac{1}{2}}/R]$

or (n_i/n_o) vs $[(y^2 + z^2)^{\frac{1}{2}}/R]$ for cylinder.

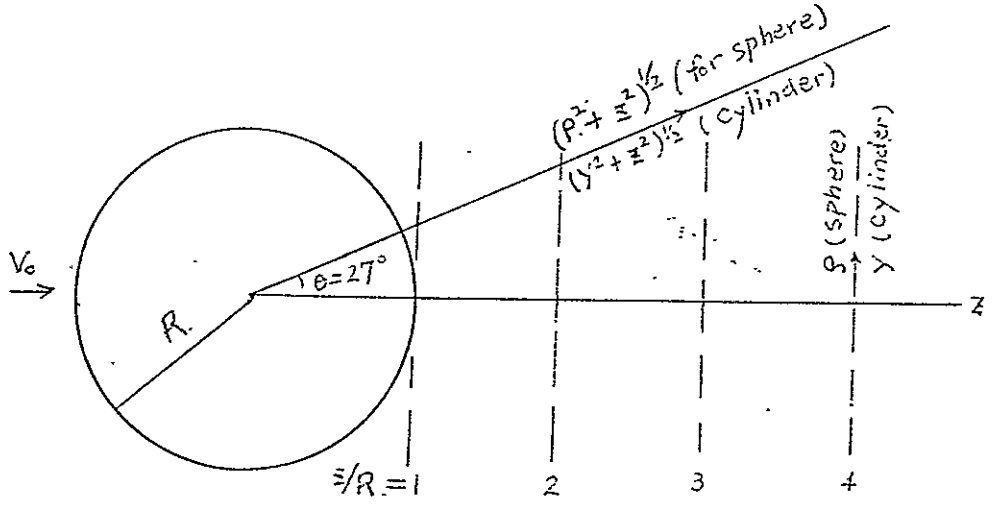

Figure I - Sphere or Cylinder

VI. References

1. Al'pert, Y. L., Gurevich, A. V., and Pitaevskii, L. P., Space Physics with Artificial Satellites, Consultant Bureau, 1965.

2. Bird, G. A.(Australian), Weapons Research Estab. TN HSA56, 1960.

3. Gustafson, W. A. and Kiel, R. E., Purdue Engineering Expt. Stat. Bull. 153.

4. Liu, V. C., Nature, vol. 208, 1965, p. 883.

5. Liu, V. C. and Jew, H., Rarefied Gas Dynamics 5th. Symposium, vol.2, 1967, p. 1703.

6. Liu, V. C. and Jew, H., A.I.A.A. Preprint No. 68-169, 1968.

7. Liu, V. C., Nature, vol. 215, 1967, p. 127.

8. Liu, V. C. and Hung, R. J., Planet & Space Sci.(to appear 1968).

Appendices

The reprints of published works under the present Research Grant (NsG-660) are compiled in the following pages. They are designated as follows:

Appendix A: Liu, V. C., Nature 208, 1965, pp. 883-884.

Appendix B: Liu, V. C. and Jew, H., Rarefied Gas Dynamics, 5th. Symposium, Vol. 2, 1967, pp. 1703-1715.

Appendix C: Liu, V. C. and Jew, H., A.I.A.A. Preprint No. 68-169, (A.I.A.A. 6th. Aerospace Sciences meeting, Jan. 1968).

Appendix D: Liu, V. C., Nature 215, 1967, pp. 127-128.

Appendix E: Liu, V. C. and Hung, R. J., "Double Scattering of the Plasma Streams in a Bi-Thermal Ionosphere," to appear in Plant. Space Sci., 1968.

Appendices B and C (Self-consistent solutions of charged particle- and potential-distribution in the near wake of a satellite).

The work reported in Appendix C ("Near Wake of the Rarefied Plasma Flows at Mesothermal Speeds," A.I.A.A. Preprint No. 68-169) is an improved version of that in Appendix B ("On the Electrodynamic Wake in a Rarefied Plasma," Rarefied Gas Dynamics, 5th. Symposium, vol. 2). The results presented in Figures (19 - 71) are based on a further improved version which will be described in detail in a forthcoming Ph.D. thesis (H. Jew, University of Michigan, 1968). The essential improvement over that in Appendix C includes a more rigorous expression for the third constant of motion (I_3) in the case of wake behind a sphere and the removal of a computational error in the case of wake behind a cylinder.